

https://dspace.org/

Manganese oxide- based gold catalysts for low temperature CO conversion

Padayachee, Diandree

2015
http://hdl.handle.net/10539/18804

Downloaded from a DSpace repository. https://dspace.org/

Manganese oxide- based gold catalysts for low temperature CO conversion

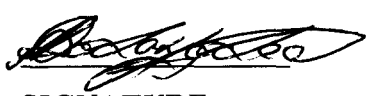
Diandree Padayachee

A dissertation submitted to the Faculty of Science, University of the Witwatersrand, in fulfilment of the requirements for the degree of Master of Science.

Johannesburg, 2003

DECLARATION

I, Diandree Padayachee, declare that this dissertation is my own, unaided work. It is being submitted for the degree of Master of Science at the University of the Witwatersrand, Johannesburg. It has not been submitted previously at this, or any other university, for any degree or examination.



SIGNATURE

30/12/2003

DATE

ABSTRACT

Initial investigations at Mintek, into the addition of gold to commercial hopcalite ($Cu_xMn_yO_z$), showed that it improved the activity of hopcalite. So this study was initially focused on investigating Au/hopcalite catalysts further. Also, since according to literature, Mn_xO_y has catalytic potential, the study of Au/Mn_xO_y catalysts was included.

Au/hopcalite and Au/Mn_xO_y catalysts were made by means of deposition-precipitation, colloidal gold deposition and co-precipitation. Only one catalyst-type was highly active at room temperature – the co-precipitated Au/Mn_xO_y catalysts. The optimised co-precipitated Au/Mn_xO_y catalysts were more active than all the other catalysts by at least an order of magnitude. So the study focus changed, to make the optimisation of Au/Mn_xO_y catalysts a priority.

Cerium is a well-known promoter on Mn_xO_y catalysts, and so was also added to the co-precipitated Au/Mn_xO_y catalysts. However, even small amounts of cerium had an adverse effect on the catalysts' activities.

The compaction and crushing of a co-precipitated Au/Mn_xO_y catalyst to obtain granules of larger particle size than the powders, was also carried out. The activities and surface areas of the catalysts were found to be comparable. This augers well for industrial purposes, since the use of powdered catalysts in industry is not viable.

This is dedicated to my parents for instilling in me the importance of a good education, while never letting me forget that "the end of education is character".

Acknowledgements

- My supervisor, Prof. Mike Scurrell, for all his input and assistance.
- Mintek, for funding my MSc.
- My boss, Elma van der Lingen, for providing me with the opportunity to study, and for all her support and encouragement.
- Iris Klingbiel, for the activity measurements.
- Bernard Joja, Iris Klingbiel and Daven Compton for carrying out SEM analysis.
- Chris van der Merwe for HRSEM analysis.
- Stefanie Taylor, Wilma Clark and Brian Mullinder for XRD analysis.
- My family for their encouragement and love.
- Rainer Süss, for his love and support (and food!) during those long days and weekends spent writing up.
- And most importantly, to God, for His infinite love and blessings.

TABLE OF CONTENTS

1. INTRODUCTION 1
2. LITERATURE REVIEW 3
2.1. Au particles 3
2.2. Catalyst support 3
2.3. Catalyst preparation methods 4
2.4. Gold-support interaction 6
2.5. Mechanism for CO oxidation 7
2.5.1. Hopcalite 7
2.5.2. Gold catalysts 7
2.6. Alkali metal promoters 8
2.7. Oxidation state of gold 9
3. CATALYST PREPARATION, ACTIVITY TESTS AND CHARACTERISATION TECHNIQUES 10
3.1. Catalyst preparation 10
3.2. Chemical analysis 10
3.3. Activity tests 10
3.4. SEM/HRSEM analysis 11
3.5. X-ray diffraction analysis 11
3.6. Zeta potential 12
3.7. Surface area 12
4. DEPOSITION-PRECIPITATION 13
4.1. Hopcalite 13
4.1.1. Experimental 13
Hop 0 15
Hop 9 16
4.1.2. Results and discussion 17
4.2. MnO_2 24
4.2.1. Experimental 24
4.2.2. Results and discussion 25
5. COLLOIDAL GOLD 33
5.1. Hopcalite 33

5.1.1. Experimental 33
5.1.2. Results and discussion 34
5.2. MnO_2 35
5.2.1. Experimental 35
5.2.2. Results and discussion 35
6. CO-PRECIPITATION 39
6.1. Mn_xO_y 39
6.1.1. Experimental 39
6.1.2. Results and discussion 43
6.1.3. Comparison of CPMn- catalysts with those of Hoflund *et al.*[5] 83
6.2. Hopcalite 84
6.2.1. Experimental 84
6.2.2. Results and discussion 87
7. CATALYST PARTICLE SIZE OPTIMISATION 96
8. CONCLUSION 97
9. REFERENCES 99

LIST OF FIGURES

Figure 1. Schematic flow diagram of CO rig. 11

Figure 2. Comparison of activities of Hop 0 – Hop 8; 0.5 g catalyst; 60 ml/min; room temperature 19

Figure 3. Activity of hopcalite (SG-2157);0.5 g catalyst, 60 ml/min, room temperature 20

Figure 4. Comparison of activities of catalysts (SG-2157) made with Mg citrate; 0.5 g catalyst, 60 ml/min, room temperature 21

Figure 5. Comparison of activities of N-140 (new hopcalite) and SG-2157 (old hopcalite); 0.5 g catalyst, 60 ml/min, room temperature 22

Figure 6. Activities of Hop 17 and NHop 1 catalysts; 0.5 g catalyst,60 ml/min, room temperature 23

Figure 7. XRD spectrum of MnO_2 received from Sigma-Aldrich 26

Figure 8. XRD spectrum of electrolytic MnO_2, Hydrometallurgy Division, Mintek 27

Figure 9. Activities of Mn 1, Mn 2 and Mn 3; 0.25 g catalyst, 60 ml/min; room temperature 28

Figure 10. Secondary electron image and backscattered electron image of Mn 1 29

Figure 11. Secondary electron image and backscattered electrom image of Mn 3 ... 29

Figure 12. Secondary electron images of NMn 1 30

Figure 13. Hydrolysed Au speciation as a function of log [Cl^-] and pH 31

Figure 14. Activity of NHop 2; 0.25 g catalyst,60 ml/min, room temperature 34

Figure 15. Backscattered electron image of NHop 2 35

Figure 16. Activity of Mn 4; 0.25 g catalyst,60 ml/min, room temperature 36

Figure 17. Backscattered electron image of Mn 4 37

Figure 18. Activity of Mn 5; 0.5 g catalyst,60 ml/min, room temperature 38

Figure 19. Backscattered electron image of Mn 5 38

Figure 20. Activities of CPMn 1-5, calcined at 200°C; 0.25 g catalyst (CPMn 1), 0.5 g catalyst (CPMn 2-5), 60 ml/min; room temperature 47

Figure 21. Activities of CPMn 2, 4 and 5, calcined at 400°C; 0.5 g catalyst, 60 ml/min; room temperature 49

Figure 22. Activity of CPMn6, calcined at 400°C; 0.5 g catalyst, 60 ml/min; room temperature 50
Figure 23. Activities of CPMn 5_rpt, 7-9, calcined at 400°C; 0.5 g catalyst, 60 ml/min; room temperature 51
Figure 24. Activities of CPMn 10-16,19, 20; calcined at 400°C; 0.5 g catalyst, 60 ml/min, room temperature 53
Figure 25. Activities of CPMn 21 and 23, calcined at 400°C; 0.5 g catalyst, 60 ml/min; room temperature 56
Figure 26. XRD spectra of CPMn 10 (top trace) and CPMn 23 (bottom trace)..... 57
Figure 27. Activities of CPMn 17 and 18, calcined at 400°C; 0.5 g catalyst, 60 ml/min; room temperature 58
Figure 28. Activities of CPMn 24- 28, calcined at 400°C; 0.5 g catalyst, 60 ml/min; room temperature 59
Figure 29. Comparison of co-precipitated catalysts made using different base concentrations; 10 minutes ageing, calcined at 400°C; 0.25 g catalyst, 400 ml/min; room temperature 61
Figure 30. Dependence of activity on Na_2CO_3 concentration 62
Figure 31. Comparison of activities of CPMn 24 and CPMn 26; 0.25 g catalyst, 400 ml/min; room temperature 63
Figure 32. Comparison of activities of CPMn 25 and CPMn 39; 0.25 g catalyst, 400 ml/min; room temperature 64
Figure 33. Comparison of activities of CPMn 30 and CPMn 31; 0.5 g catalyst, 60 ml/min; room temperature 65
Figure 34. Activity of CPMn 33; 0.5 g catalyst, 60 ml/min; room temperature 66
Figure 35. Activity of CPMn 34; 0.25 g catalyst, 60 ml/min; room temperature 67
Figure 36. (a) Proposed structure, leading to sintering on a Au/Al_2O_3 catalyst; (b) Displacement of Cl^- by OH^-, so that the complexation shown in (a) does not occur [43] 68
Figure 37. Effect of calcination temperature and citrate washing on the activity of CPMn 35; 0.25 g catalyst, 400 ml/min; room temperature 69
Figure 38. Comparison of activities of CPMn 25, CPMn 36 and CPMn 37; 0.25 g catalyst, 400 ml/min; room temperature 70
Figure 39. Secondary electron image of CPMn 5, 2000 X magnification 71
Figure 40. Secondary electron image of CPMn 5 (repeat), 2000 X magnification... 71

Figure 41. Secondary electron image of CPMn 10, 2000 X magnification 72
Figure 42. Secondary electron image of CPMn 24, 2000 X magnification 72
Figure 43. Backscattered electron images of (a) CPMn 5 and (b) CPMn 5_rpt..... 73
Figure 44. HRSEM image of CPMn 24 (secondary/backscattered combination)..... 75
Figure 45. XRD spectra of CPMn 24 (bottom trace) and CPMn 24_ used (top trace) (Background correction, Kα2 lines stripped, CPMn 24_used spectrum offset) 78
Figure 46. XRD spectra of CPMn 24 and CPMn 38 (Background correction, Kα lines stripped)..... 79
Figure 47. Secondary electron image and backscattered electron image of CPMn 10 80
Figure 48. HRSEM images of (a)CPMn 24 and (b)CPMn 27 secondary/ backscattered combination) 81
Figure 49. Secondary electron image of CPMn 27 81
Figure 50. Backscattered electron image of CPMn 24..... 82
Figure 51. Comparison of activities of CPHop 1-4; 0.50 g catalyst, 60 ml/min; room temperature 89
Figure 52. Secondary- electron image of CPHop 1 90
Figure 53. Secondary- and backscattered- electron images of CPHop 1 91
Figure 54. Secondary electron images of CPHop 2 (left) and CPHop 3 (right)..... 92
Figure 55. Backscattered electron images of CPHop 2 (left) and CPHop 3 (right) .. 92
Figure 56. Secondary electron image and backscattered electron image of CPHop 493
Figure 57. XRD spectra of CPHop 3 and CPHop 4 (Background correction, Kα lines stripped) 94
Figure 58. Comparison of activity of CPMn2_200 in powder and granular form; 0.5 g catalyst, 60 ml/min, room temperature 96

LIST OF TABLES

Table 1. Experimental conditions for Au/hopcalite catalysts 15

Table 2. Experimental conditions for Au/hopcalite catalysts prepared with Mg citrate 16

Table 3. Experimental conditions of catalysts made at pH 3 17

Table 4. Analysed wt % Au loading on hopcalite catalysts (deposition precipitation) 18

Table 5. Summary of HR SEM observations for Hop 0 – Hop 8 20

Table 6. Chemical compositions (wt %) of SG-2157 and N-140 23

Table 7. Changes to standard catalyst preparation method 24

Table 8. Analysed wt % Au loading on MnO_2 catalysts (deposition precipitation).. 25

Table 9. Calculated μmol CO/g Au/s for Au/hopcalite and Au/MnO_2 catalysts made by the deposition-precipitation method 32

Table 10. Au loading and calculated μmol CO/g Au/s of Mn 4 and Mn 5 36

Table 11. Experimental conditions of CPMn 1-39 40

Table 12. Au loadings on co-precipitated Au/Mn_xO_y catalysts 43

Table 13. Calculated μmol CO/g Au/s for co-precipitated Au/Mn_xO_y catalysts (CPMn 1-39, calcined at 400°C) 46

Table 14. Calculated μmol CO/g Au/s for co-precipitated Au/Mn_xO_y catalysts (CPMn 1-5, calcined at 200°C) 48

Table 15. Comparison of expected and actual Ce and Mn molar proportions 60

Table 16. Compositions of selected Au/Mn_xO_y catalysts as determined by HRSEM-EDS 74

Table 17. Calculated Mn/O ratios for possible manganese compounds 75

Table 18. Mn/O ratios on analysed sites of CPMn 10, 24, 27 and 28 76

Table 19. Comparison of CPMn- catalysts with co-precipitated catalysts of Hoflund et al.[5] 83

Table 20. Experimental conditions of CPHop 1-4 86

Table 21. Gold loadings on co-precipitated Au/hopcalite catalysts 87

Table 22. Cu/Mn molar ratios for co-precipitated Au/hopcalite catalysts 87

Table 23. Calculated μmol CO/g Au/s for co-precipitated Au/hopcalite catalysts; (CPHop 1-4, calcined at 400°C,) 88

1. INTRODUCTION

Manganese oxides (Mn_xO_y) have been shown to have good catalytic potential. Their efficiency relies mainly on their strong redox capabilities, i.e. their oxidation/reduction cycles[1]. Many studies have been carried out on the potential of Mn_xO_y catalysts for low-temperature CO-NO_x reactions. This is reportedly due to their labile oxygen atoms[2]. Their use as the main catalytic component or as a promoter[3] to base-metal catalysts often yields positive results.

However, base-metal catalysts cannot compete with precious metal catalysts for low temperature CO conversion in terms of activity, so combinations of both are often made[1]. Silver added to a Mn_2O_3 catalyst, showed good CO conversion capability[1]. The addition of manganese to a Pd/SiO_2 catalyst (Pd:Mn 65:35) lowered the 100 % CO and NO conversion temperature by 50°C [4]. So whereas precious metals are often used as the promoter - in this instance - manganese was actually shown to improve the activity of a precious-metal catalyst.

Gold was found to definitely enhance the activity of Mn_xO_y - the addition of 2 at. % gold increased its activity ten-fold[5]. These Au/Mn_xO_y catalysts were compared with Pt/SnO_x catalysts for low-temperature CO oxidation. Not only did the Au/Mn_xO_y catalysts perform better, but their activities were also found to increase with time, unlike the large activity decay found with the Pt/SnO_x catalysts. Au/Mn_xO_y was found to be superior to Au/Fe_2O_3[6,7] as well as Mn_xO_y, Pt/Mn_xO_y, Pd/Mn_xO_y, Ag/Mn_xO_y, Cu/Mn_xO_y, Ru/Mn_xO_y and Au/Ce_xO_y with respect to low temperature CO oxidation in a stoichiometric CO-O_2 gas mixture[7] (Au/ Ce_xO_y was the second most active of these catalysts). Ueda and Haruta[8] found an improvement in the reduction of NO over a Au/Al_2O_3 catalyst, when Mn_2O_3 was mechanically-mixed with the catalyst.

The Au-Mn_xO_y combination therefore appears to be promising for noxious gas removal. Since gold alone or Mn_xO_y alone cannot achieve the low-temperature CO oxidation, this implies that a synergistic interaction occurs between the 2 components to effect such high activity at low temperatures[5].

The mixed copper-manganese oxide ($Cu_xMn_yO_z$) catalyst, hopcalite, is used industrially in respiratory protection applications. However, its drawbacks are that it deactivates rapidly, and is therefore unsuitable for extended use[9]. Hopcalite is also not very active at ambient temperature and loses activity in the presence of moisture[10]. Despite these drawbacks; and the fact that gold catalysts have been shown by Haruta *et al.*[10] to be much more active and stable, even under humid conditions; it is still, however, the preferred catalyst in respiratory apparatus[11]. Due to industry's being comfortable with hopcalite, the addition of gold to commercial hopcalite was investigated at Mintek[12]. Initial investigations showed that not only did the addition of gold improve the activity of hopcalite, but it also increased its durability to deactivation under humid conditions.

The aim of this project was to continue the work started at Mintek, and to extend the studies into optimisation of the preparation of Au/hopcalite catalysts. It was decided to include the singular oxide of manganese as a catalyst support, since Au/Mn_xO_y catalysts have also shown promise[5]. Various preparation techniques were investigated, in order to determine the optimum preparation technique for the Au/Mn_xO_y and Au/hopcalite catalysts.

It was also decided to investigate the CO oxidation ability of cerium-promoted Au/Mn_xO_y catalysts. Cerium is a popular additive in exhaust catalysts due to its ability to store oxygen[13], and has often been added as a promoter on Mn_xO_y catalysts. It has been reported that the addition of cerium to manganese oxides causes an increased concentration of manganese oxides in higher oxidation states, as well as increased oxygen mobility[14]. Hence the manganese oxide becomes a more effective oxidant. Machida *et al.*[15] found good results in the oxidative adsorption of NO_x onto an equimolar Mn_xO_y-CeO_2 support. Chen *et al.*[3] found a Mn/Ce molar ratio of 6/4 to be optimum in the oxidation of phenol.

Although both Au/Mn_xO_y[5, 6, 16] and Au/CeO_2 catalysts have been made[7, 17] (and been shown to compare well with other noble metal/Mn_xO_y catalysts[7]), no research appears to have been carried out into the effect of cerium on a Au/Mn_xO_y catalyst. It was therefore decided to also investigate, whether, on the more promising Au/Mn_xO_y catalysts, cerium would have a promoting effect.

2. LITERATURE REVIEW

2.1. Au particles

The gold particle size and structure are dependent on the catalyst preparation method, the support used and on the catalyst pre-treatment[17]. Catalysts with gold particles of around 2-5 nm have been reported to have the highest activity, with effective gold catalysts requiring hemispherical gold particles.

Hemispherical particles give a stronger gold-support interaction. This is because the shape of the particles ensures the longest perimeter interface [18]. Another advantage of hemispherical particles being attached to the support at their flat planes, is that this makes them thermally more stable than spherical particles[18].

One reason that large gold particles have low activity is that they might have very small interfacial areas and also, mostly atoms of high coordination number[19]. Atoms of low coordination number (found in small gold particles) have much stronger chemisorption properties and hence better activities.

2.2. Catalyst support

It has been stated that although the nature of the gold-support interaction is not understood, it seems to be a unique characteristic that is dependent on the support material[6]. So it appears that the choice of support can 'make-or-break' a gold catalyst. The best gold catalyst supports appear to be oxides derived from the first row of the Transition Series elements, such as titanium, zinc, iron, manganese, etc.[19]

According to Schubert *et al.*[20], there are 2 types of catalyst supports – the inert metal oxides (e.g. Al_2O_3, MgO) and the active metal oxides, such as the ones from the first row of the transition elements. The latter are reducible metal oxides and are more active than the inert metal oxides by as much as an order of magnitude. They have also stated that the size of gold particles, while critical on inert metal oxide supports,

is not as important on active metal oxide supports. Gold particles up to 30 nm on a reducible metal oxide support exhibit comparable activity to inert supports with small gold particles. This is because the participation of the active support in the reaction compensates for the larger gold particles in activity.

A disordered support has been reported to be essential for good catalytic activity[19] as it appears to guarantee good dispersion of gold particles. Also, it may be easier to create anion vacancies into which oxygen molecules can chemisorb (see Section 2.5.2.), in the disordered areas of a support.

2.3. Catalyst preparation methods

Unlike with other noble metal catalysts, effective gold catalysts cannot be prepared via the impregnation route. With impregnation, spherical gold particles are obtained, which don't give a strong enough metal-support interaction[21]. The successful techniques for producing supported gold catalysts are briefly described here.

a) **Deposition-precipitation** - This involves the precipitation of gold onto a support material, at a required pH. Deposition precipitation can be broken down into 2 processes[22]:

   1) Precipitation (of gold) from bulk solution
   2) Interaction with the support surface.

   Deposition-precipitation was preferred by Haruta *et al.*[23] as they claimed it produced gold particles with a narrow particle size distribution, and also prevented gold cluster formation (which was often observed on co-precipitated samples).

b) **Co-precipitation** – The gold and support precursors are precipitated out of solution with base, usually as a hydroxide and/or carbonate species. This can be carried out either by adding a mixed metal salt solution into the base (conventional co-precipitation), or by adding the base into a solution of the mixed metal salts (inverse co-precipitation).

The support is then converted to an oxide during calcination. The calcination step is very important in co-precipitation as it enables access to gold particles buried deep within the support, by means of loss of water, thus creating a more porous support structure[19].

c) **Chemical vapour deposition** - An organic gold compound is vapourised onto a metal oxide support and thereafter heat-treated in air to obtain small, well-dispersed gold particles. The advantage of this method is that there is no chloride contamination, since it is not present in the precursors[16].

d) **Co-sputtering** - This involves the simultaneous sputter-deposition of gold and metal oxide onto a metal substrate, in an oxygen atmosphere. This method is not very commonly used.

e) **Au-phosphine** - In this method, a $AuPPh_3NO_3$ complex is first formed, which is then deposited on the catalyst support. Better catalysts were obtained by depositing the gold-phosphine complex onto freshly-precipitated metal hydroxides, as opposed to the conventional metal-oxide supports[24]. It is reasoned that the gold is able to deposit into the pores and/or surface defects of the hydroxides, which thus prevents agglomeration, keeping the gold particles small. During calcination, the gold-phosphine complex decomposes and the support undergoes a phase change. It is this simultaneous change in gold complex and support which leads to a better gold-support interaction, and hence to more active gold catalysts[17].

f) **Colloidal Au** - This involves making a colloidal gold solution and then depositing the nanometer-size gold colloids onto a metal oxide support. Calcination thereafter, promotes the formation of the hemispherical gold particles, leading to better gold-support interaction.

Not all these preparation conditions are suitable for any type of support. Some preparation methods are suitable for only certain supports, e.g. deposition precipitation is the most suitable method for loading gold onto TiO_2[23].

2.4. Gold-support interaction

The most important role of the support has been reported to be stabilisation of the gold[25]. Thus the gold-support interaction is a very important factor, which is made stronger by calcination. Calcination at higher temperatures lead to the small gold particles melting (gold particles of 2 nm melt at 300°C[23]). Since gold melts have a strained structure and are thermodynamically unstable, the gold would rearrange its structure to form a stronger interaction with the support[16].

Studies on a colloidal Au/TiO_2 mixture showed that the gold-support interaction is more important than the gold particle size[16]. Although increasing calcination temperature increased the average gold particle size, it also increased the activity. In order to further substantiate this theory, the effect of SO_2 on the activity of a Au/TiO_2 catalyst was investigated. It was found that SO_2 suppressed CO oxidation on Au/TiO_2, but hardly affected a Pt/TiO_2 catalyst. Because a gold surface is more unreactive to SO_2 than platinum, it was reasoned that the reaction must be proceeding on the perimeter interface of the gold and metal oxide support; and the lower activity resulted from SO_2 blocking that interface.

The interfacial theory is also corroborated by the fact that large unsupported gold particles, (most) metal oxides by themselves, and impregnated gold catalysts, have little or no activity at ambient conditions[19]. As has been mentioned previously, impregnated gold catalysts have poor gold-support interaction due to their spherical gold particles. Catalysts made by methods such as deposition-precipitation have good gold-support interaction and good activities. Hence the implication that the active site of supported gold catalysts is at the interface of gold and metal oxide support.

2.5. Mechanism for CO oxidation

2.5.1. Hopcalite

The mechanism for CO oxidation by hopcalite[#], is reported by Vepřek *et al.*[26] to be as follows:

$$CO + Mn^{4+} \rightarrow CO^{+}_{ads} + Mn^{3+} \quad (1)$$

$$\tfrac{1}{2} O_2 + Cu^{+} \rightarrow Cu^{2+} + O^{-}_{ads} \quad (2)$$

$$O^{-}_{ads} + CO^{+}_{ads} \rightarrow CO_2 \quad (3)$$

$$Cu^{2+} + Mn^{3+} \rightleftharpoons Cu^{+} + Mn^{4+} \quad (4)$$

The active redox couple in hopcalite catalysts is therefore the Cu^{+} — Mn^{4+} couple, with the CO being adsorbed onto the Mn^{4+}, thus reducing it to Mn^{3+} (1), and the Cu^{+} being oxidised to Cu^{2+} by O_2 (2). After the oxidation of CO to CO_2 (3), the catalyst is regenerated (4).

No mechanism of Au/hopcalite catalysts has been reported in the literature to date.

2.5.2. Gold catalysts

A general mechanism for gold catalysts has been suggested by Bond and Thompson[19]. The authors have stated that the mechanism is probably not the same for different gold catalyst systems and variations will exist.

[#] The mechanism was first formulated by Schwab and Kanungo (ref. 11 of the paper by Vepřek *et al*[26])

$$Au^0 + CO \rightarrow Au^0\text{---}CO \quad (5)$$

$$Au^{3+} + OH_s^- \rightarrow Au^{2+}\text{---}OH \quad (6)$$

$$Au^0\text{---}CO + Au^{2+}\text{---}OH \rightarrow Au^{2+}\text{---}COOH + Au^0 \quad (7)$$

$$O_2 + \square_s^- \rightarrow O_2^- + \square_s \quad (8)$$

$$Au^{2+}\text{---}COOH + O_2^-\text{---}\square_s \rightarrow Au^{2+} + CO_2 + HO_2^-\text{---}\square_s \quad (9)$$

$$Au^{2+}\text{---}COOH + HO_2^-\text{---}\square_s \rightarrow Au^{2+} + CO_2 + 2OH_s^- + \square_s \quad (10)$$

$$Au^{2+} + \square_s \rightarrow Au^{3+} + \square_s^- \quad (11)$$

In this mechanism, CO is adsorbed onto Au^0 (5). The Au^0-CO bond is broken up by an OH^- group attached to a Au^{2+} ion (formed in 6), forming a $COOH^-$ group (7). O_2 adsorbs onto the support – if possible, into the anion vacancies ($\square_s$) (8). The vacancies were created by the removal of OH_s^- in Step 6. The O-O bond is then broken up by the adsorbed CO molecule and CO_2 is formed (9), (10). Au^{3+} and $\square_s^-$ are then regenerated (11).

To obtain the net reaction of $2\ CO + O_2 \rightarrow 2\ CO_2$, equations 5, 6 and 7 are doubled, then all the stages are summed.

2.6. Alkali metal promoters

It has been reported that sodium ions promote the catalytic reaction[19]. This is fortunate since in deposition- or co-precipitation, it is not easy to avoid using a base such as Na_2CO_3 for pH control. Au/Mn_xO_y catalysts made using Li_2CO_3 as the base, were found to perform better than those made with Na_2CO_3 or K_2CO_3[5].

However, studies into the mechanism of deactivation of hopcalite catalysts, show that potassium segregation at the surface is responsible for deactivation of the hopcalite catalyst[26]. This was also confirmed in a separate study[27], where it was seen that the more active catalysts had less sodium on the surface. Thus, it appears as if the presence of alkali metals in catalysts is not always advantageous, but rather depends on the individual systems.

2.7. Oxidation state of gold

There have been numerous debates on whether the catalytically active species of gold is ionic gold; usually reported to be Au(I); or metallic Au(0). Whilst some investigators have reported exclusively ionic gold as the active species[6, 28], others have found metallic gold to be the active species in their catalysts[17, 23, 25]. It has also been reported that the active state of gold might differ depending on the support used[16], e.g. Mössbauer analysis carried out on $Au/Mg(OH)_2$ and Au/TiO_2 catalysts showed that the active species in the former was Au^+, while metallic gold was the active species in Au/TiO_2.

However, Bond and Thompson[19] have postulated that both Au^{x+} *and* Au^0 are necessary for an active catalyst , with the gold ions forming the 'chemical glue' which binds the gold atoms to the support. The ratio of Au^{x+} to Au^0 is not fixed and can change during, e.g. calcination, reduction, etc. Complete reduction of Au^{x+} is not desired, as it will result in sintering of Au^0, resulting in loss of activity. On the other hand, having no Au^0 present is also detrimental to the catalyst's activity as Au^0 provides a site for CO adsorption (see Section 2.5.2., eq. 5).

Bond and Thompson[19] have also stated that using techniques such as XRD and XPS to deduce the oxidation state of gold - as many researchers do - may not always be a wise choice. Irradiation of the catalysts can cause physical and chemical changes, such as reduction of Au^{x+} to Au^0, to occur. Researchers then base their decisions on inaccurate results, which were actually caused by the characterisation technique being used. This poses a dilemma as it casts doubt on the results obtained by these techniques – but then, if these techniques are not used, it limits resources available for catalyst characterisation.

3. CATALYST PREPARATION, ACTIVITY TESTS AND CHARACTERISATION TECHNIQUES

3.1. Catalyst preparation

All catalysts were made in a Mettler Toledo LabMax® automatic lab reactor. Stirring of all solutions/slurries in the LabMax, was carried out at a speed of 450 rpm. Deionised water (< 1 μS/cm) was used in all catalyst preparation and washing stages. Chloroauric acid ($HAuCl_4$) was prepared using the method described by O'Reilly *et al.*[29]

3.2. Chemical analysis

The % gold loading on each catalyst was determined by means of inductively coupled plasma - atomic emission spectroscopy (ICP-AES). Filtrate and water-wash samples were analysed by means of atomic absorption spectroscopy (AAS).

3.3. Activity tests

Catalysts were tested for room-temperature activity in a fixed-bed reactor. The catalyst being tested was placed into a teflon chamber. The test gas (1% CO in air) was then passed through the catalyst bed. CO and CO_2 concentrations were measured by means of gas chromatography. A schematic diagram of the CO rig is shown in Figure 1.

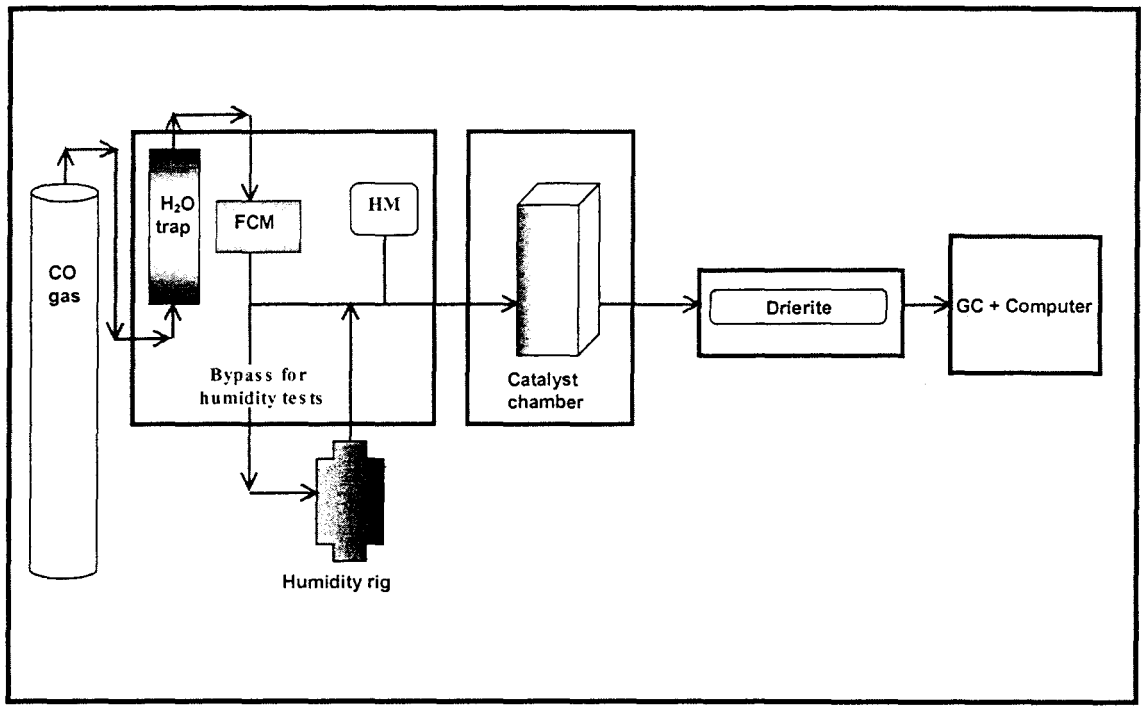


Figure 1. Schematic flow diagram of CO rig.
***FCM** – Flow control meter; **HM** – Hygrometer*

3.4. SEM/HRSEM analysis

A JEOL 640 scanning electron microscope was used for SEM analysis. Higher-magnification imaging was done using a high-resolution JEOL JSM-6000L instrument. Secondary electron images and backscattered electron images of the catalysts were taken.

3.5. X-ray diffraction analysis

X-ray diffraction measurements were carried out on two instruments.

a) A Siemens D500 utilising Cu Kα radiation. A step size of 0.02°2θ and a counting rate of 1 second per step were used. The samples were scanned from 5 to 80°2θ.

b) A Siemens D500 diffractometer utilising Mo Kα1 radiation. The samples were scanned from 10 to 55° 2θ, using a step size of 0.05° 2θ and a counting rate of 3 seconds per step.

3.6. Zeta potential

A Malvern Zeta Sizer 4 was used for zeta potential analysis. Analysis was done on 1 g of finely powdered sample dispersed in 100 g H_2O. pH adjustment was carried out using NaOH and HCl.

3.7. Surface area

The BET surface areas were determined using a Micromeritics ASAP 2010 analyser. The samples were degassed before analysis at 120°C for approximately 3h, and evacuated until the pressure in the sample chamber was less than 20 μm Hg. The analysis was then carried out with N_2 at < 10 μm Hg.

4. DEPOSITION-PRECIPITATION

4.1. Hopcalite

4.1.1. Experimental

Commercial hopcalite, SG-2157 was provided by Süd-Chemie as pellets. The pellets were milled in a Zieb mill, followed by milling in a microniser. The fraction less than 106 μm was screened out for use in the catalyst preparation.

The catalysts were prepared as follows:

Step 1: A slurry of 5 g hopcalite and 500 ml water, stirring at 450 rpm, was heated to 70°C over 30 minutes.

Step 2: The pH was adjusted over the next 10 minutes with 0.1 M HNO_3 and 0.2 M Na_2CO_3.

Step 3: *Alternative 1*: The required amount of $HAuCl_4$ was pumped in at a flowrate of 0.55 ml/min (i.e. dropwise addition), with simultaneous adjustment of the pH to the required value.

Alternative 2: $HAuCl_4$ solution was poured into the slurry and a 0.01 M solution[30] of magnesium citrate (molar ratio of Mg:Au = 2.5 [31]) was pumped in over 30 min, at a flowrate of 2.1 ml/min. pH was simultaneously adjusted to the required value.

Alternative 3: $HAuCl_4$ solution was poured into the slurry and solid magnesium citrate (molar ratio of Mg:Au = 2.5 [31]) was then added in, together with addition of acid/base to maintain the pH at the set value.

Step 4: Catalyst stirred at 70°C for 1 h*.

Step 5: Catalyst aged for the required time, while cooling down to room temperature. The stirring rate was reduced to 300 rpm during ageing.

---

* The Au/hopcalite catalysts initially made at Mintek[12] had this step of 'stirring at 70°C for 1 h' before 'ageing' the catalyst. Since this project started as a follow-on of that work, this was still done initially.

After ageing, the slurry was filtered and the catalyst was washed with hot water under vacuum to remove any ions still present. A conductivity meter was used to confirm the removal of ions. The washed catalyst was dried at 80°C for 4 h and thereafter calcined at 100°C for 4 h. Previous work[12] showed the optimum heat-treatment temperature for Au/hopcalite catalysts, to be 100°C.

The method reported above is the standard method that was used in the making of these catalysts. Any deviations to the standard method, during investigations of the different preparation parameters, are reported in the relevant sections.

Preparation parameters were investigated in stages, with the preparation conditions of the most active catalyst, being carried through to the subsequent stage.

Activity tests were carried out on 0.5 g catalyst (flowrate = 60 ml/min; SV = 7200 $ml/g_{cat}/h$).

A) Effect of pH and ageing times

In order to determine the optimum preparation conditions for Au/hopcalite catalysts with a low gold loading, a series of catalysts were prepared at different pH's and with varying ageing times. The matrix that was constructed is illustrated in Table 1.

Table 1. Experimental conditions for Au/hopcalite catalysts

Catalyst	pH	Ageing time, *h*
Hop 0	7.0	1
Hop 1	7.0	3
Hop 2	7.0	12
Hop 3	8.5	1
Hop 4	8.5	3
Hop 5	8.5	12
Hop 6	6.0	1
Hop 7	6.0	3
Hop 8	6.0	12

pH's were not tested over a wider range, since pH's of 5, 7 and 10 were tested in earlier work carried out at Mintek[12], and the best conversion was obtained with the use of pH 7. So it was decided to concentrate efforts around that pH. Ageing times of 0 h, 1 h and 24 h were also tested previously[12], the optimum ageing time found to be 1 h. Since no ageing times between 1 h and 24 h had been tested, ageing times of 3 h and 12 h were included. Reaction temperatures were not varied, as these were tested previously[12], with the best temperature being 70°C.

In the preparation of Hop 0 – Hop 8, *Alternative 1* of Step 3 was used for all the catalysts.

B) Addition of magnesium citrate

The effect of magnesium citrate was tested on a few of the catalysts. Kung *et al.*[31] have stated that way in which the citrate works is that it competes for sites on the support and chelates the gold species, thus preventing the formation of large gold clusters on the support. Haruta *et al.*[30] added magnesium citrate into a slurry of metal-oxide support and $HAuCl_4$ to reduce the gold onto the metal-oxide supports. They also stated that small gold particles were obtained using this method. Thus after

addition of the $HAuCl_4$ solution to the hopcalite, magnesium citrate solution was pumped in (Alternative 2 of Step 3).

For Hop 9-11, magnesium citrate was added in as a solid at different stages of the catalyst preparation (i.e. *Alternative 3* of Step 3, and deviations) to determine the optimum addition stage. Table 2 lists the deviations to *Alternative 3*, as well as the temperatures at which the catalysts were heat-treated.

Table 2. Experimental conditions for Au/hopcalite catalysts prepared with Mg citrate

Catalyst	Deviations to *Alternative 3*	Calcination temp. (^oC)
Hop 9	Mg citrate added at start of ageing	100, 400
Hop 10	None	400
Hop 11	Mg citrate added at start of experiment	400, 500

Although the optimum heat-treatment temperature was found to be 100°C previously[12], higher temperatures were investigated in this study. This is because there was concern about the catalyst being poisoned by carbon residues from the citrate if heat-treated at lower temperatures.

C) Zeta potential

At this stage of the research, a new batch of hopcalite (N-140) was received from Süd-Chemie. It differed from the hopcalite (SG-2157) used in the previous experiments. The technical data sheets for both SG-2157 and N-140 are shown in Appendix A. Of relevance in these data sheets is the difference in surface area of the different hopcalite batches. N-140 has a surface area of $200m^2/g$ and SG-2157 a surface area of $80\text{-}130m^2/g$. This implied that N-140 would have better activity than SG-2157. Activity tests were carried out to confirm this. The hopcalite samples were also analysed to determine any difference in chemical composition.

Key to hopcalite catalyst supports:

Hop = SG-2157

NHop = N-140

Unlike the previous hopcalite catalysts, Hop 17 and NHop 1 were made at pH 3. The point of zero charge of hopcalite was tested and found to be at around pH 3.5. Below this pH the hopcalite support would be positively-charged. Hop 17 and NHop 1 were therefore made at pH 3 to encourage the negatively-charged gold particles to adsorb *separately* (i.e. without clustering) onto the positively-charged hopcalite. Additional information on the experimental conditions of these catalysts, is shown in Table 3.

Table 3. Experimental conditions of catalysts made at pH 3

Catalyst	Deviation from standard method	Calcination temp. (^oC)
Hop 17	None	100, 400
NHop 1	Left out Step 4	100,300

Both catalysts were made using *Alternative 2* of Step 3.

4.1.2. Results and discussion

Results of the wet chemical analysis of the catalysts are shown in Table 4.

Table 4. Analysed wt % Au loading on hopcalite catalysts (deposition precipitation)

Catalyst	wt % Au
Hop 0	1.1
Hop 1	1.0
Hop 2	1.0
Hop 3	1.0
Hop 4	1.0
Hop 5	1.0
Hop 6	1.0
Hop 7	1.0
Hop 8	1.1
Hop 9	1.0
Hop 10	1.0
Hop 11	0.9
Hop 17	1.1
NHop 1	1.1

These results show that the gold loadings are very reproducible. Analysis of filtrate and wash-water samples showed no gold present in any of the solutions. This implies that all the gold was deposited on the support.

The wt % determinations for copper and manganese were carried out on hopcalite alone, as well as on a 1 wt % Au/hopcalite sample. In both instances, a Cu/Mn molar ratio of 1/1.5 was obtained. Thus the molecular formula of the hopcalite provided by Süd-Chemie appears to be $CuMn_{1.5}O_4$. This implies a +4 oxidation state of manganese, and not the +3 oxidation state, as was initially assumed. This assumption was based on references in papers[11, 32], to hopcalite having the formula $CuMn_2O_4$. However, studies by Xia *et al.*[33], have shown that Mn^{4+} gives better catalytic activity for CO oxidation than either Mn^{3+} or Mn^{2+}.

A) Effect of pH and ageing times

A comparison of catalyst activity is shown in Figure 2.

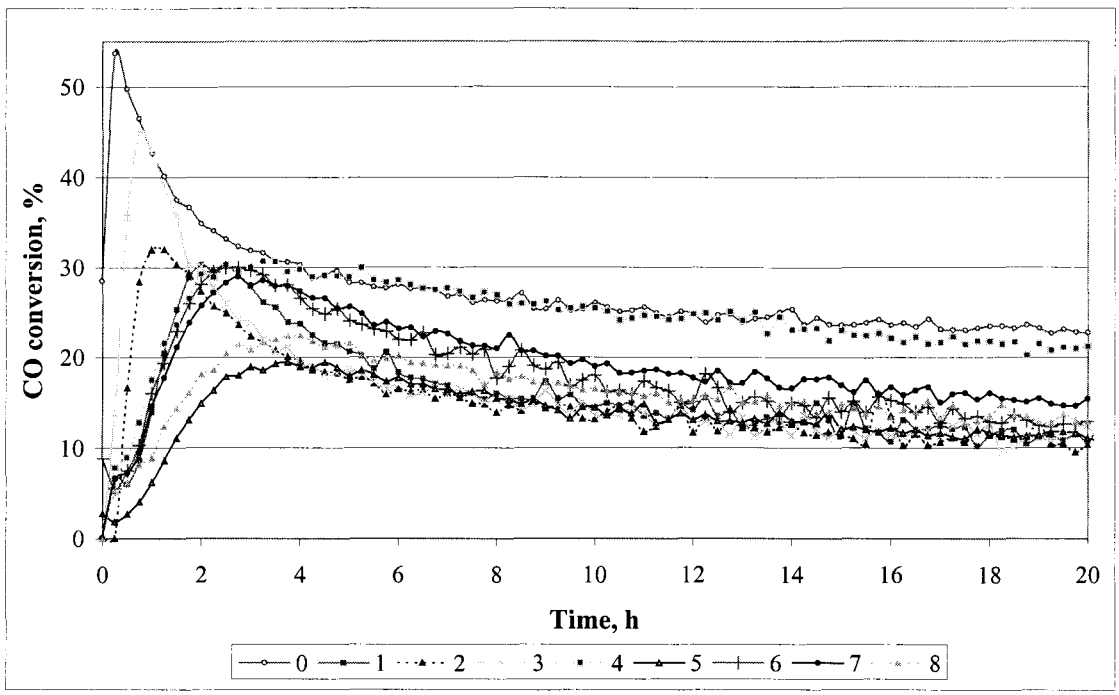


Figure 2. Comparison of activities of Hop 0 – Hop 8; 0.5 g catalyst; 60 ml/min; room temperature

The activities of all the catalysts decreased slowly over time. The best-performing catalysts were Hop 0 (pH 7.0, 1 h ageing time) and Hop 4 (pH 8.5, 3 h ageing time), with activities after 20 hours, of 22.7 % and 21.2 % CO conversion, respectively. The remainder of the catalysts had activities below 16 %.

However, even the Au/hopcalite catalysts that performed badly, had better activities than hopcalite alone (Figure 3).

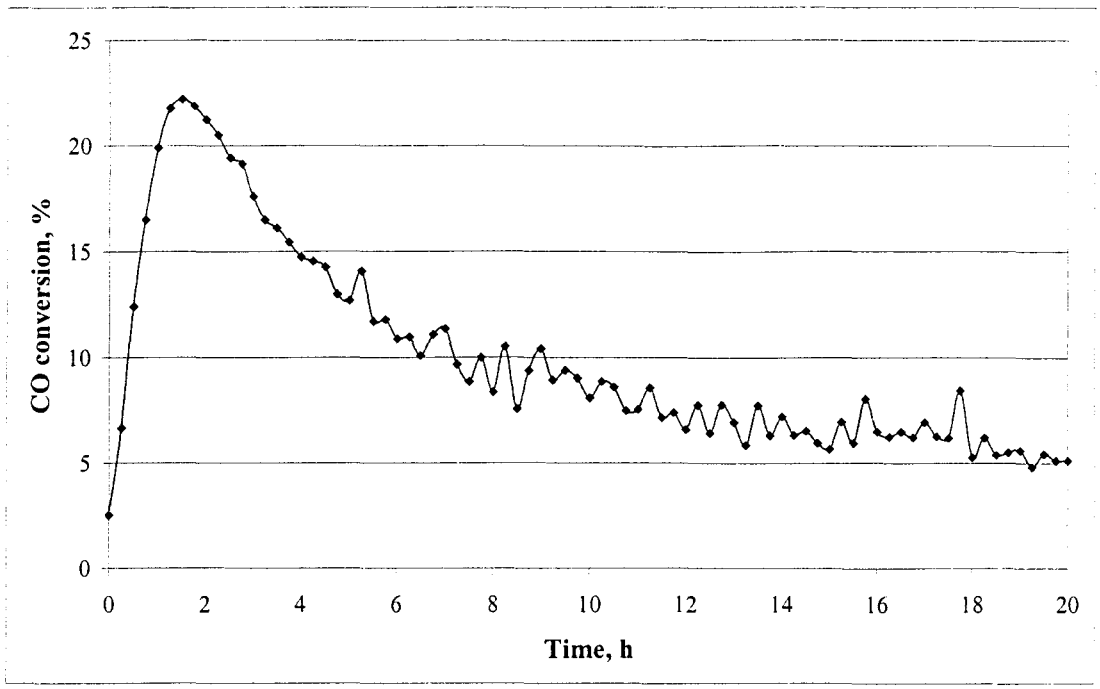


Figure 3. Activity of hopcalite (SG-2157);
0.5 g catalyst, 60 ml/min, room temperature

Gold particles on the catalysts were large. There was also a large particle size distribution of gold. Descriptions of gold particle size distribution for each catalyst are tabulated below (Table 5). The HRSEM secondary- and backscattered- electron images of a few of these catalysts are shown in Appendix B.

Table 5. Summary of HR SEM observations for Hop 0 – Hop 8

Catalyst	Au particle size distribution (nm)
Hop 0	50-200
Hop 1	200-500
Hop 2	100-500
Hop 3	100-500
Hop 4	50-500
Hop 5	100-500
Hop 6	250-1000
Hop 7	100-500 mainly. Few up to 2000
Hop 8	100-500 mainly. Few up to 2000

The best performing catalysts, Hop 0 and Hop 4, both had smaller gold particles, relatively well dispersed on the support. The remainder of the catalysts had larger clusters of gold particles.

B) Addition of Mg citrate

Since Hop 0 was the best-performing catalyst, its preparation conditions of pH 7 and 1 h ageing were used for these catalysts.

The activities of the catalysts made with Mg citrate are compared in Figure 4.

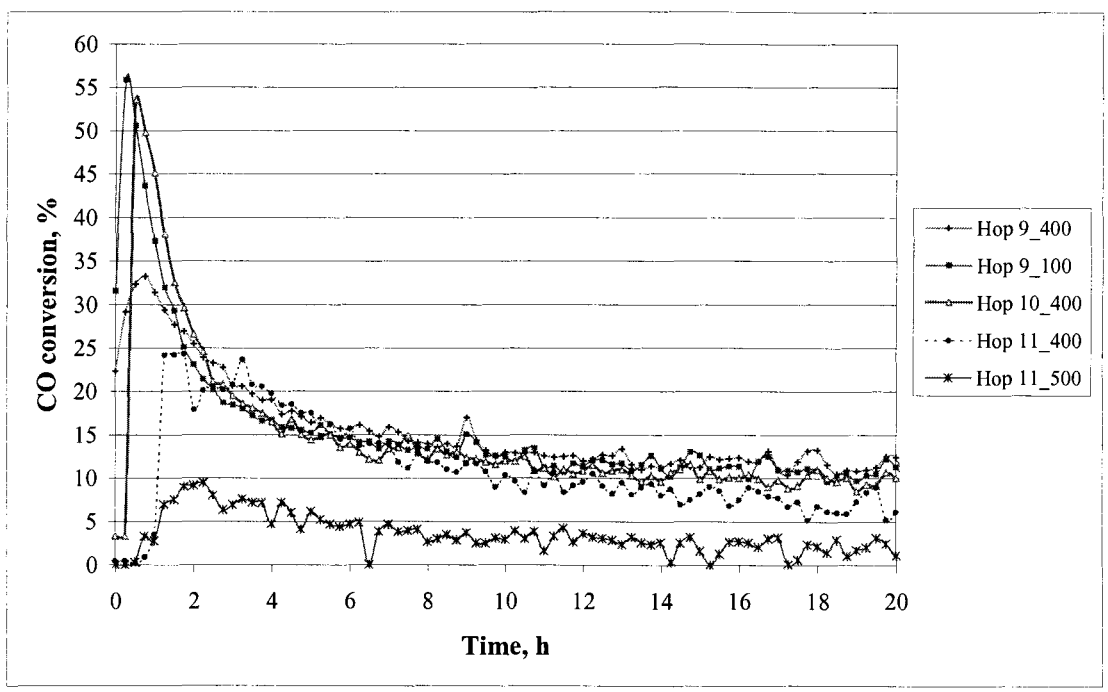


Figure 4. Comparison of activities of catalysts (SG-2157) made with Mg citrate; 0.5 g catalyst, 60 ml/min, room temperature

These catalysts were less active than Hop 0. As was seen with the previous catalysts, the activities decreased over time. There was no significant difference in activity between Hop 9 and 10. Hop 11's performance was worse than the others, but it is possible that this is due to the lower gold loading, and not a reflection of the stage at which the magnesium citrate was added.

A comparison of heat-treatment temperatures in Hop 9 (100°C vs. 400°C) showed no significant difference in activity. This could imply that the citrate was washed out of the catalyst, or that if present, it is not affecting the catalyst's activity adversely. Since Hop 11 showed such low activity, it was decided to heat-treat a sample at 500°C to see if its activity would improve. However, the activity just worsened, probably due to sintering of gold particles and the hopcalite support becoming more crystalline.

C) Zeta potential

Results of CO conversion tests showed that N-140 had a better activity than SG-2157 (see Figure 5).

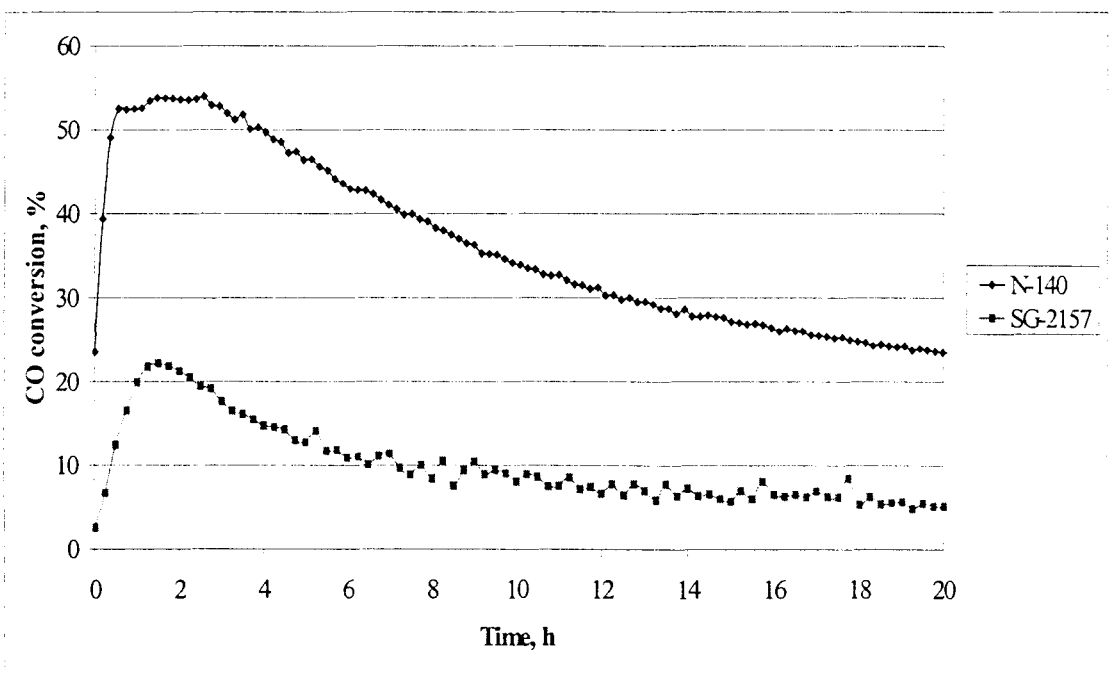


Figure 5. Comparison of activities of N-140 (new hopcalite) and SG-2157 (old hopcalite); 0.5 g catalyst, 60 ml/min, room temperature

This result could be due to N-140 having a larger surface area available for CO conversion. Another factor which needs to be taken into consideration, however, is that of the difference in chemical composition of the two hopcalite batches. The chemical compositions are outlined in Table 6.

Table 6. Chemical compositions (wt %) of SG-2157 and N-140

Hopcalite / Element	SG-2157	N-140
Cu	20.8	15.4
Mn	25.8	36.9
Al	8.24	0.02

The Cu/Mn molar ratios for SG-2157 and N-140 work out to 0.70 and 0.36, respectively. According to Hutchings *et al.*[11], a manganese-rich hopcalite catalyst is more active than a copper-rich hopcalite catalyst. A possible reason for this is that copper forms stable complexes with CO[26]. Thus a high copper surface concentration would result in the blocking of the surface sites. This is consistent with N-140 being the better catalyst. There is also a noticeably larger aluminium concentration on SG-2157, but its contribution to the performance of SG-2157 is not known.

The activities of the two catalysts made at pH 3 are shown in Figure 6.

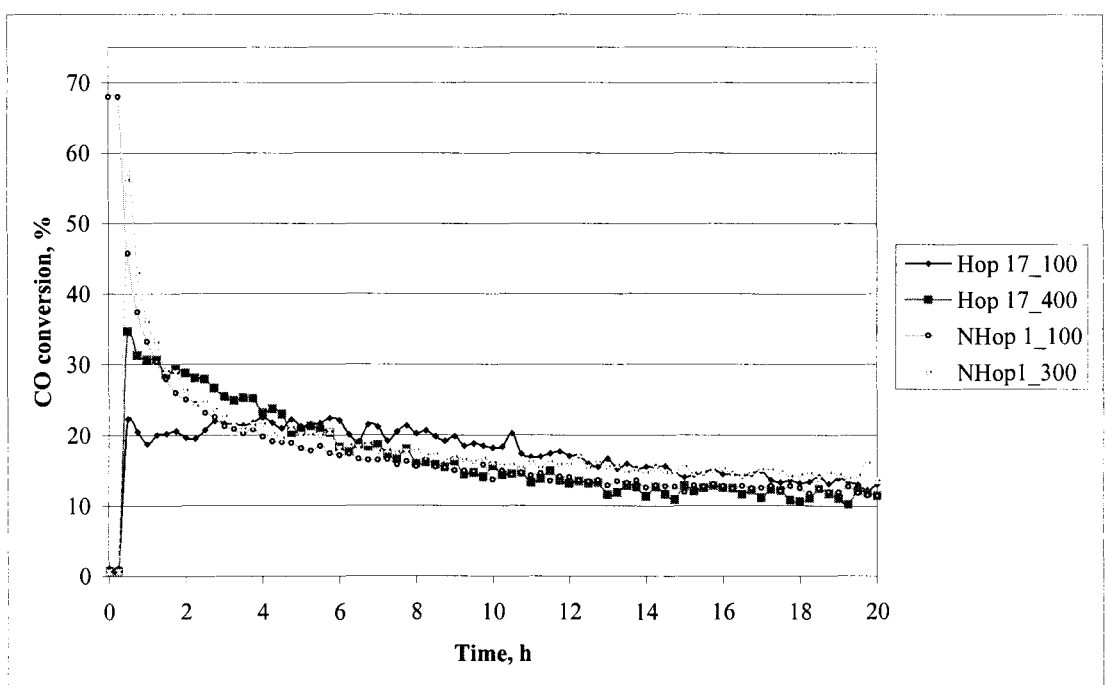


Figure 6. Activities of Hop 17 and NHop 1 catalysts; 0.5 g catalyst, 60 ml/min, room temperature

All the catalysts had similar activities, regardless of the calcination temperatures used, or whether or not Step 4 was omitted from the recipe. It was thought that perhaps the extra hour stirring at temperature was encouraging the formation of large gold clusters. However, omitting Step 4 made no difference to the activity.

4.2. MnO_2

4.2.1. Experimental

Deposition of gold was attempted on two samples of MnO_2. The one batch was high-purity electrolytic MnO_2 (EMD) produced from sodium tum ore, in the Hydrometallurgy Division at Mintek. Catalyst preparation was first attempted on this batch of MnO_2. The second batch was AR grade MnO_2 obtained from Sigma-Aldrich. Both batches were submitted for XRD analysis to determine the MnO_2 crystal structure.

Key to MnO_2 catalyst supports:

Mn = EMD (Mintek) batch

NMn = Sigma-Aldrich batch

The catalysts were prepared using the same method employed for the Au/hopcalite catalysts. All the MnO_2 catalysts were made using *Alternative 2* of Step 3 in the preparation method and were calcined at 200°C. The only deviations to the standard method are reported in Table 7.

Table 7. Changes to standard catalyst preparation method

Catalyst	Deviation from standard method
Mn1	None
Mn2	Omitted Step 4
Mn3	Catalyst made at room temperature
NMn1	Omitted Step 4

The point of zero-charge of the MnO_2 was expected to also be low, as with the hopcalite. These catalysts were therefore also made at pH 3. The gold loadings were increased to be around 3 wt %. 0.25 g catalyst was tested for CO oxidation (flowrate = 60 ml/min; SV = 14 400 ml/g_{cat}/h).

4.2.2. Results and discussion

The measured gold loadings for the **Mn** and **NMn** catalysts are reported in Table 8.

Table 8. Analysed wt % Au loading on MnO_2 catalysts (deposition precipitation)

Catalyst	wt % Au
Mn1	2.8
Mn2	2.8
Mn3	2.7
NMn1	-

The zeta potential of the EMD was measured. Its point of zero charge was found to be low (pH 3.6), as expected.

XRD analysis (copper radiation) showed differences in crystal structure for the MnO_2 supports used. The MnO_2 obtained from Sigma-Aldrich (Figure 7) was in the form of pyrolusite, whereas the MnO_2 produced at Mintek (Figure 8) contained akhtenskite and ramsdellite.

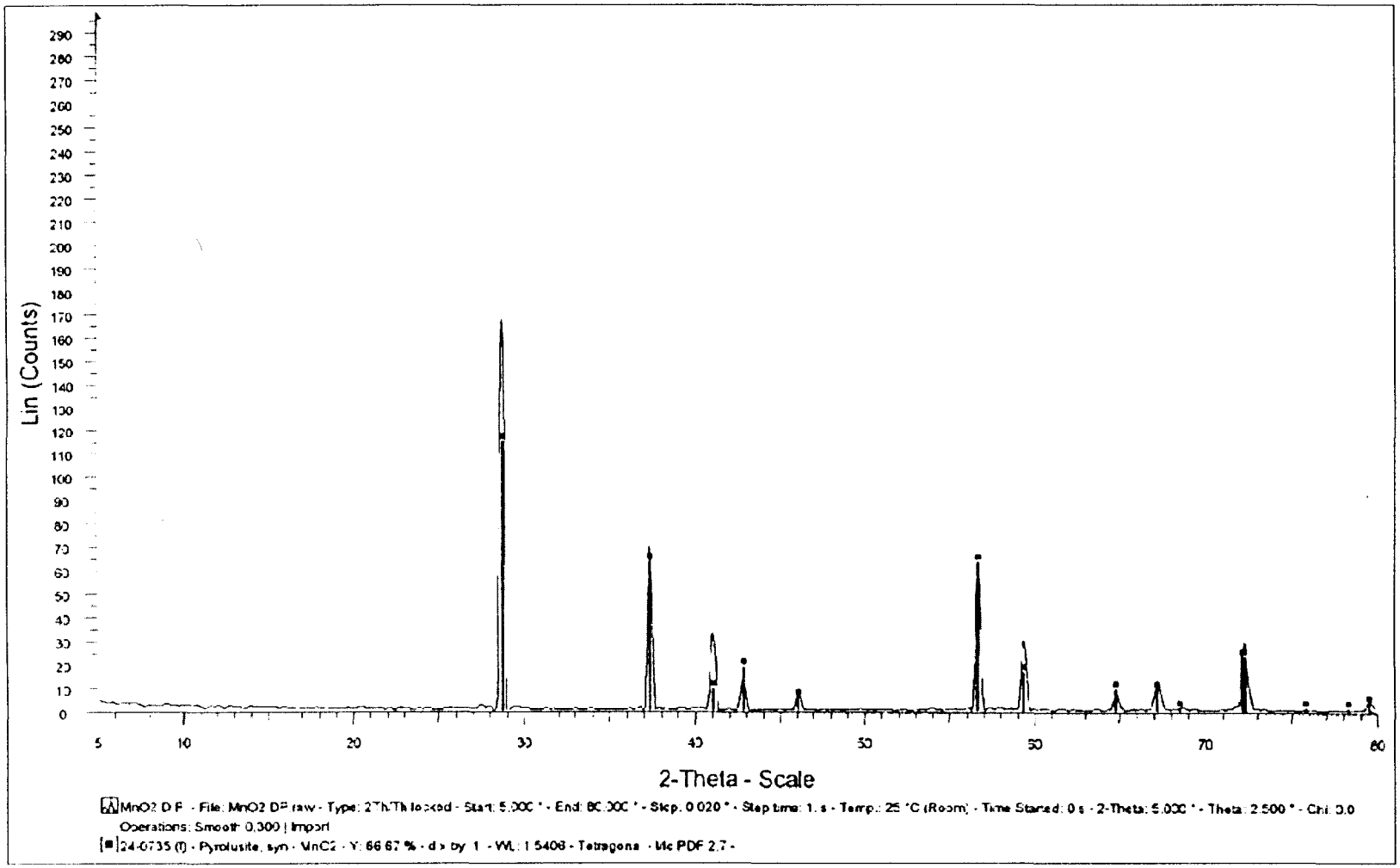


Figure 7. XRD spectrum of MnO_2 received from Sigma-Aldrich

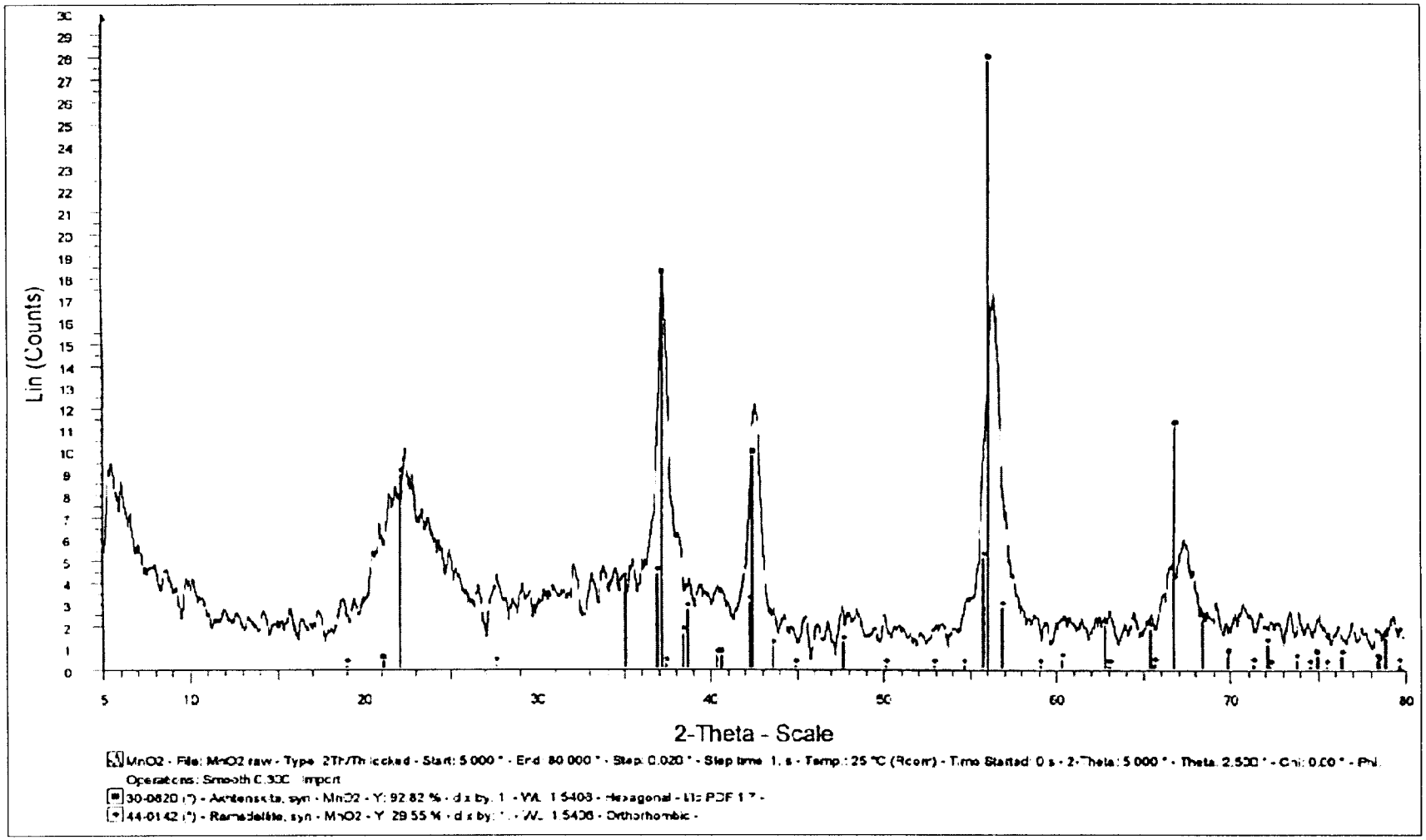


Figure 8. XRD spectrum of electrolytic MnO_2, Hydrometallurgy Division, Mintek

The catalysts made using EMD as a support had similar activities (Figure 9). Thus it was also seen with these catalysts, that changing reaction conditions did not improve the catalyst activities.

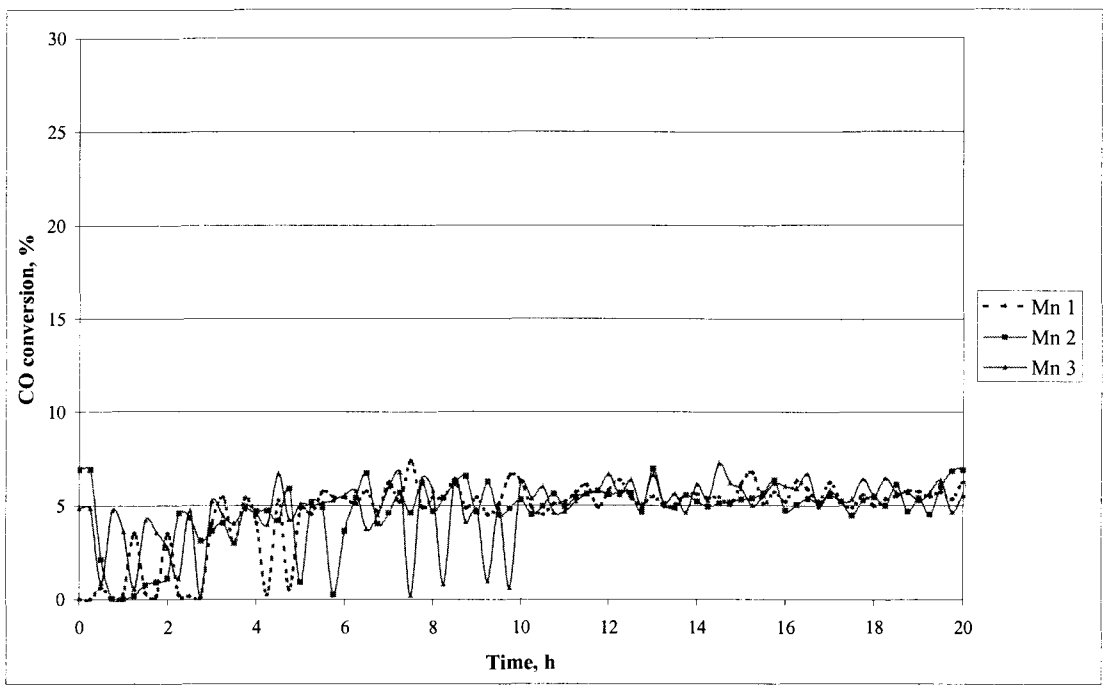


Figure 9. Activities of Mn 1, Mn 2 and Mn 3; 0.25 g catalyst, 60 ml/min; room temperature

SEM images of Mn 1 and Mn 3, showing large gold particles, are depicted in Figures 10 and 11. Numerous gold particles in the size range of 550-1400 nm were visible on both Mn 1 and Mn 3.

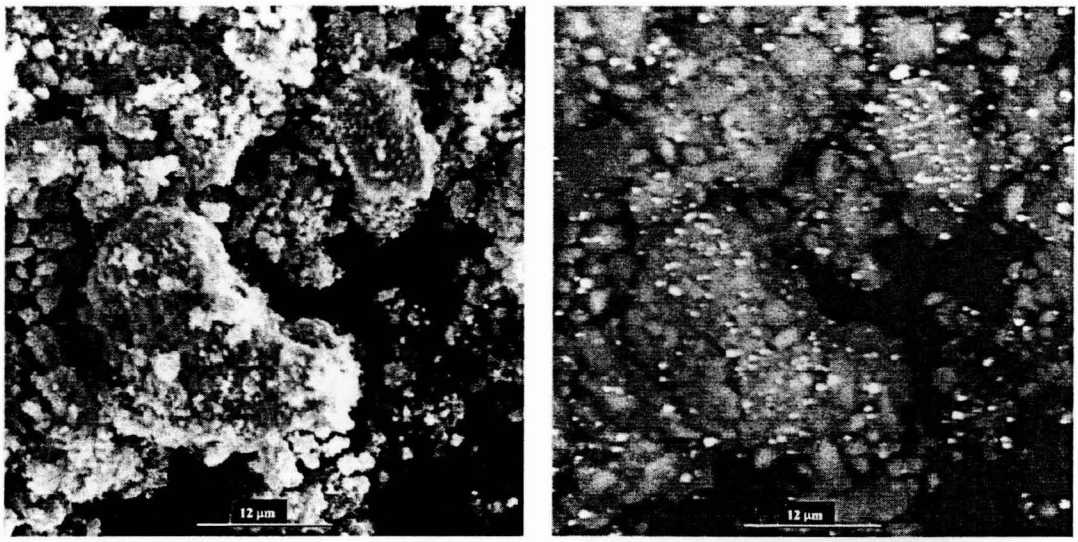


Figure 10. Secondary electron image and backscattered electron image of Mn 1

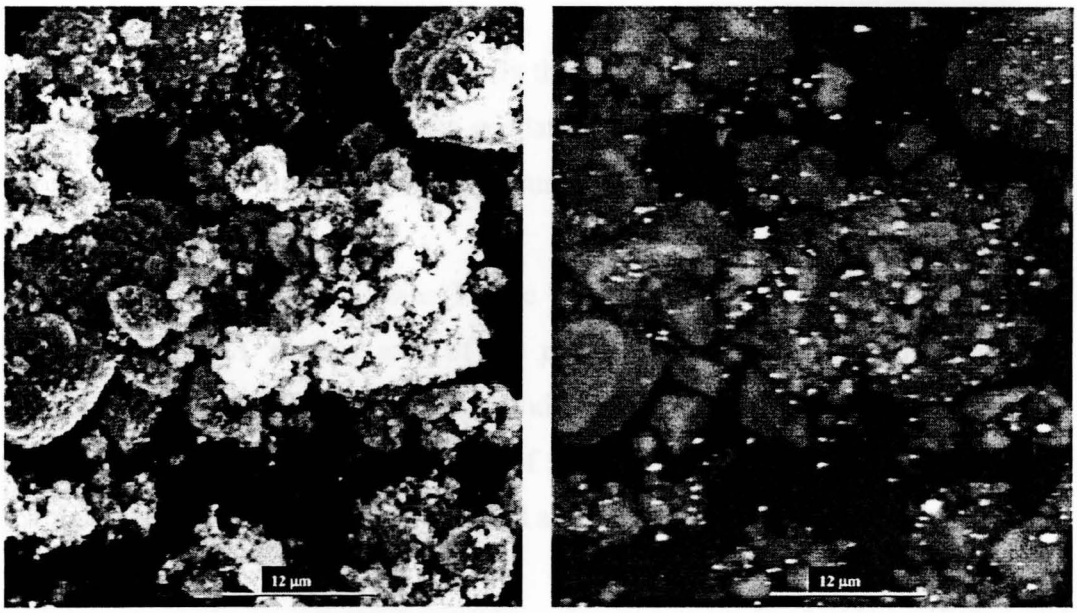


Figure 11. Secondary electron image and backscattered electrom image of Mn 3

Problems were experienced with loading gold onto NMn 1. The gold did not deposit onto the surface of the MnO_2. Rather, what was seen was "sponge-gold", which precipitated out of the solution. Figure 12 (a) shows a SEM image of the precipitated gold and MnO_2 particles. In some instances the gold had precipitated out *over* a MnO_2 particle, as can be seen in Figure 12 (b).

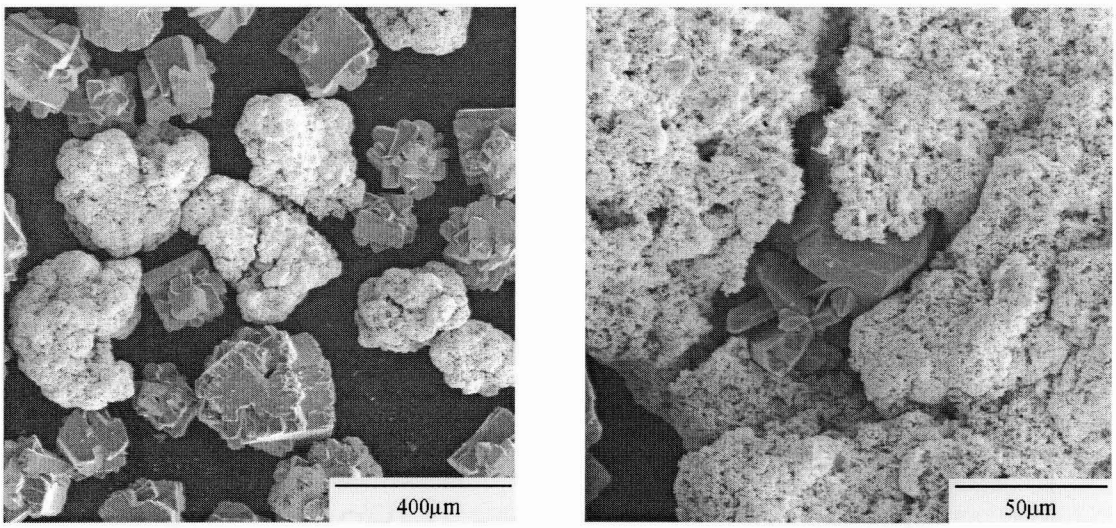


Figure 12. Secondary electron images of NMn 1

EMD is more reactive electrochemically than pyrolusite[34]. The former was also found to be a better oxidant, e.g. in the oxidation of Cr (III)[35]. The lower reactivity of pyrolusite has been attributed to its low surface area and high crystallinity[35].

The XRD spectrum of pyrolusite (Figure 7), does show that it is a highly crystalline material. The BET surface area of the pyrolusite was measured and found to be 0.0009 m^2/g. The EMD on the other hand, was seen to be less crystalline (Figure 8) and was found to have a surface area of 39 m^2/g. The very low surface area of the pyrolusite is probably the reason for gold adsorption not taking place.

None of the deposition-precipitated catalysts were very active. It is felt that this is due to the low zeta potentials of hopcalite and MnO_2. It has been stated that the deposition-precipitation method is ineffective for metal oxides with low points of zero charge, since gold hydroxide cannot be deposited at a low pH[36]. This can be seen in Figure 13, showing the distribution of the various hydrolysed gold species, as a function of chloride concentration and pH[37]. Assuming the equilibria depicted in Figure 13 are attained, then at pH 3 and log $[Cl^-]$ of around -2.7 (calculated from the $HAuCl_4$ concentration present in the starting solution), gold would be in the form of $[AuCl_4]^-$. Hence it would be not be able to deposit as a hydroxide.

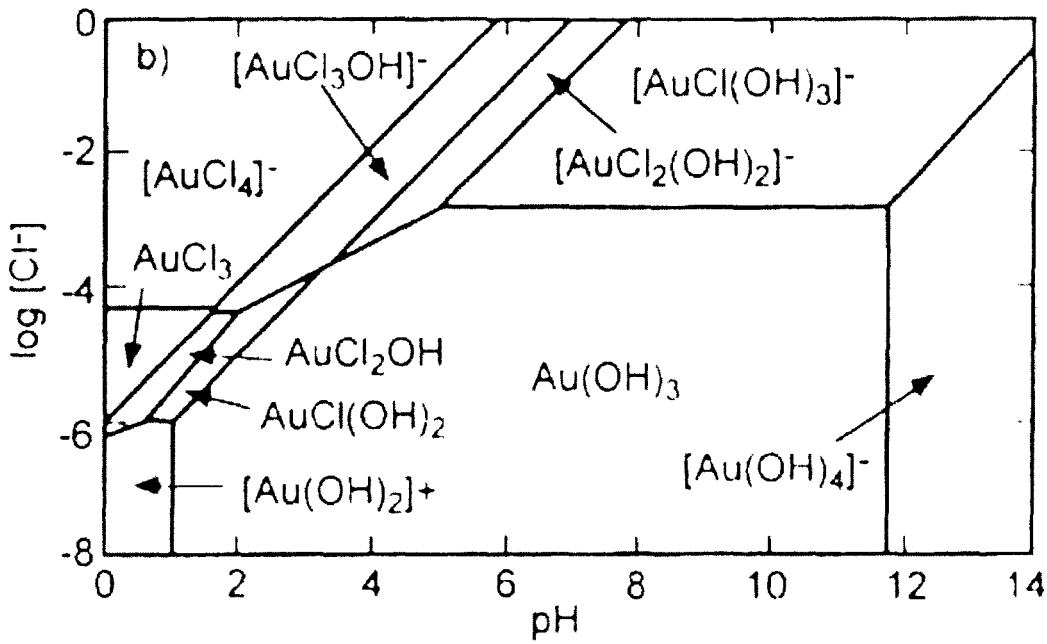


Figure 13. Hydrolysed Au speciation as a function of log [Cl⁻] and pH

Although the catalyst activities are compared by means of their % CO conversion, this is not always an accurate reflection of their activities, since it does not take the amount of gold loaded on the catalyst into account. To do so, the converted μmol CO/g Au/s is calculated. This is a more exact way of comparing the activities. The μmol CO/g Au/s (based on the CO conversion after 20 h) values are shown in Table 9.

Table 9. Calculated μmol CO/g Au/s for Au/hopcalite and Au/MnO_2 catalysts made by the deposition-precipitation method

Catalyst	μmol CO/g Au/s
Hop 0	18
Hop 1	10
Hop 2	9.0
Hop 3	11
Hop 4	18
Hop 5	10
Hop 6	11
Hop 7	13
Hop 8	10
Hop 9	8.7
Hop 10	8.7
Hop 11	6.9
Hop 17	7.0
NHop 1	11
Mn 1	3.5
Mn 2	3.9
Mn 3	3.6

From these results it can be seen that higher activities were obtained on the Au/hopcalite catalysts than on the Au/MnO_2 catalysts.

5. COLLOIDAL GOLD

The preparation of colloidal gold via the THPC route has been reported to yield gold particles between 1-2 nm in diameter[38,39]. It was hoped that making the small gold particles first and *then* depositing them on the support, would yield better catalysts than were obtained using the conventional deposition-precipitation method.

5.1. Hopcalite

5.1.1. Experimental

Since N-140 was more active than SG-2157, it was decided to carry out the colloidal-gold testwork on the former only.

A scaled-up version of the colloidal gold preparation reported by Duff *et al.*[38] was carried out. To 114 ml of deionised water, was added (with stirring) 3.75 ml 0.2 M NaOH and 2.5 ml diluted tetrakis(hydroxymethyl)phosphonium chloride (THPC). The THPC dilution was 1.2 ml 80% THPC diluted to 100 ml. After 2 minutes, $HAuCl_4$ (4.25 ml 50 g/l $HAuCl_4$, made up to 25 ml with water) was added. The solution colour changed to a dark brown a few seconds after $HAuCl_4$ addition, indicating the formation of colloidal gold[38,39].

The colloidal gold solution was then deposited onto the metal oxide support using a modified procedure of Grunwaldt *et al.*[39] Both the metal oxide slurry (5 g metal oxide in 500 ml H_2O) and the colloidal gold solution were taken down to pH 2. The metal oxide slurry was placed in an ultrasonic bath for 15 minutes. Thereafter, the slurry and colloidal gold were mixed together for 2 hours. The time interval between colloid formation and colloid deposition on the support, was 16 h for NHop 2 and Mn 4. For Mn 5, the colloid was deposited on the support immediately after it was prepared.

The catalyst was filtered, washed and dried at 80°C for 2 hours. It was then calcined at 200°C for 4 hours.

The activity of 0.25 g catalyst (flowrate = 60 ml/min, SV = 14 400 ml/g_{cat}/h) was then tested on the rig.

5.1.2. Results and discussion

The activity of NHop 2 (3.3 wt % Au) is shown in Figure 14.

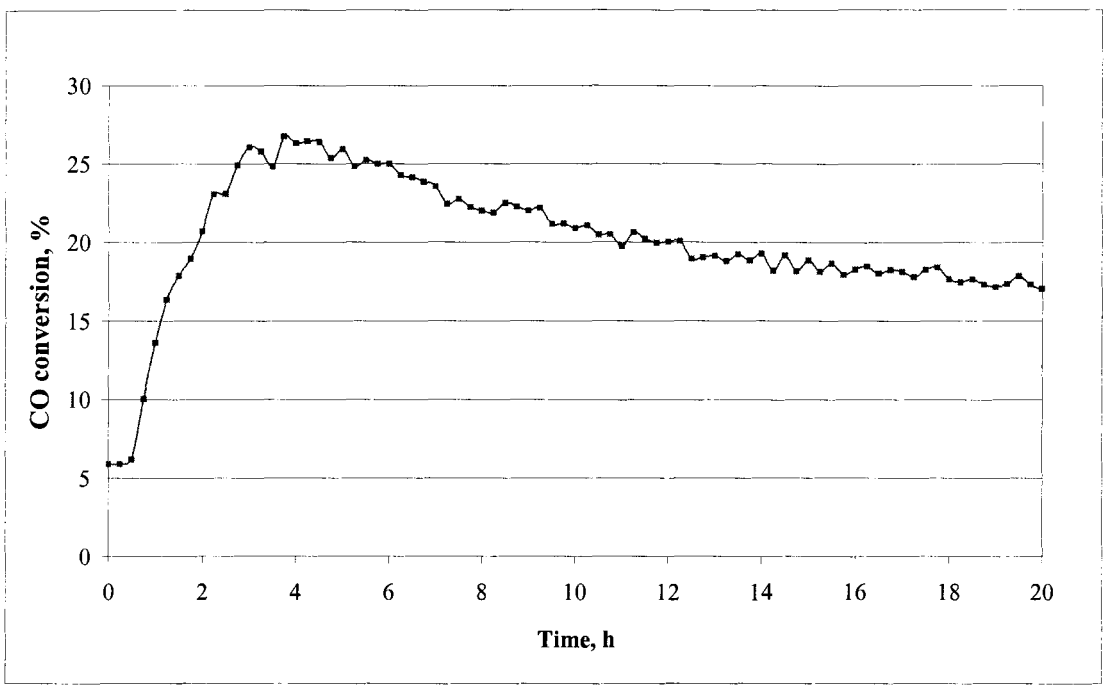


Figure 14. Activity of NHop 2;
0.25 g catalyst,60 ml/min, room temperature

The activity of NHop 2 after 20 h, was 4.6 μmol CO/g Au/s. SEM analysis of the catalyst showed large gold particles on the supports, even very large clusters (Figure 15).

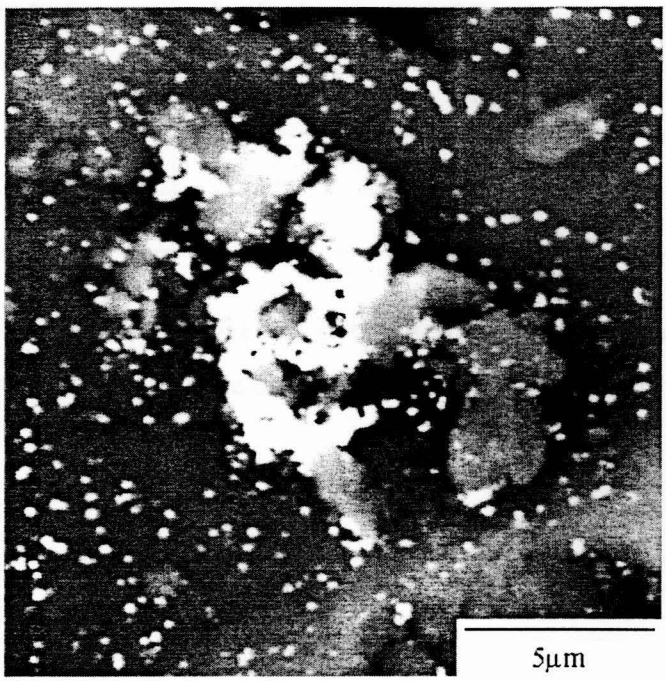


Figure 15. Backscattered- electron image of NHop 2

5.2. MnO_2

5.2.1. Experimental

Only the Mintek-made MnO_2 showed any promise for gold adsorption, so this was used as a support. The method of preparation and deposition of colloidal gold on MnO_2, was identical to that used for hopcalite (see Section 5.1.1).

5.2.2. Results and discussion

The gold loading and catalytic activities (after 20 h) of Mn 4 and Mn 5 are shown in Table 10.

Table 10. Au loading and calculated μmol CO/g Au/s of Mn 4 and Mn 5

Catalyst	wt % Au	μmol CO/g Au/s
Mn 4	3.3	7.7
Mn 5	2.4	3.3

The activity of Mn 4 increased over time, taking a long time to stabilise (Figure 16). SEM analysis showed the presence of large gold particles (Figure17).

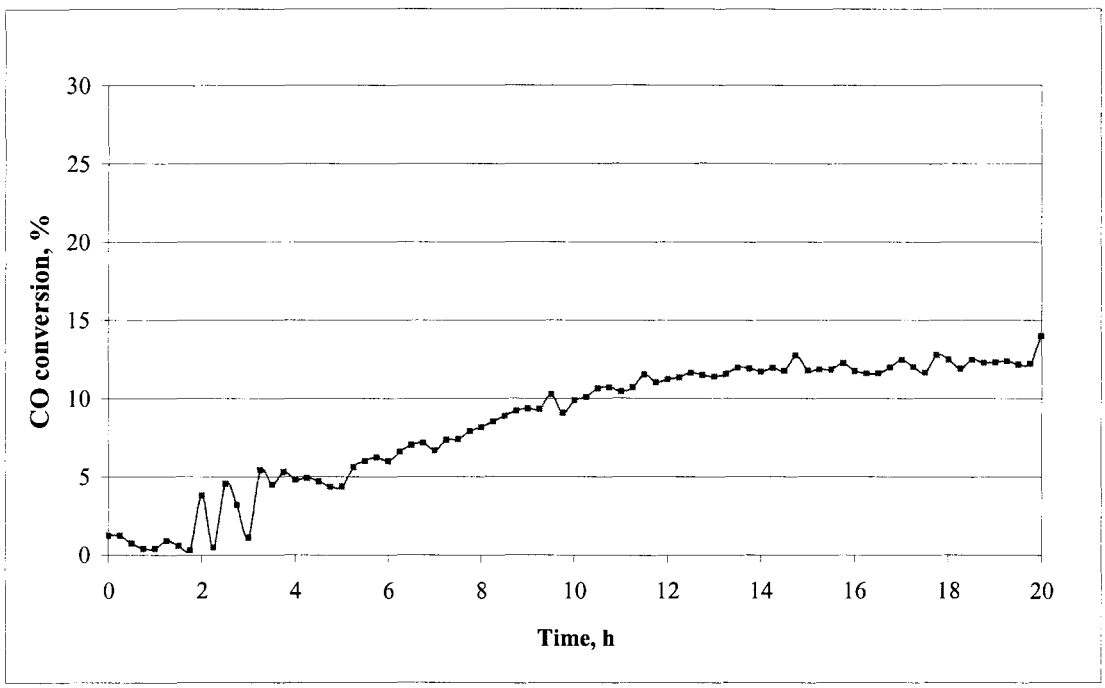


Figure 16. Activity of Mn 4;
0.25 g catalyst,60 ml/min, room temperature

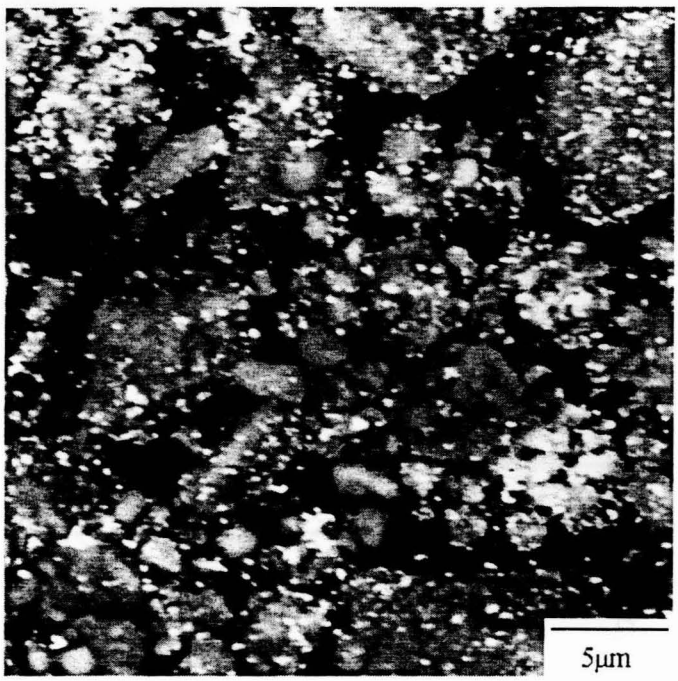


Figure 17. Backscattered electron image of Mn 4

It is apparent from these SEM results and that of NHop 2 (Figure 15), that the colloidal gold agglomerated to form larger colloids. It is possible that this occurred in the 16 hours of standing time before the colloids were deposited onto the supports.

It was noticed that the sol was a deep red colour after 16 hours of standing. This colour has been attributed to gold particles of 17 nm and greater[38]. Although it was claimed by Grunwaldt *et al.*[39] that the colour of the sol only changed to red (i.e. the gold particle size increased) after about 2-3 months, it occurred much faster in this particular instance. It is not understood why this occurred.

In an attempt to prevent the formation of these large gold clusters, it was decided to deposit the colloidal gold onto the support immediately after its preparation. The activity of the catalyst made in this way (Mn 5) is shown in Figure 18.

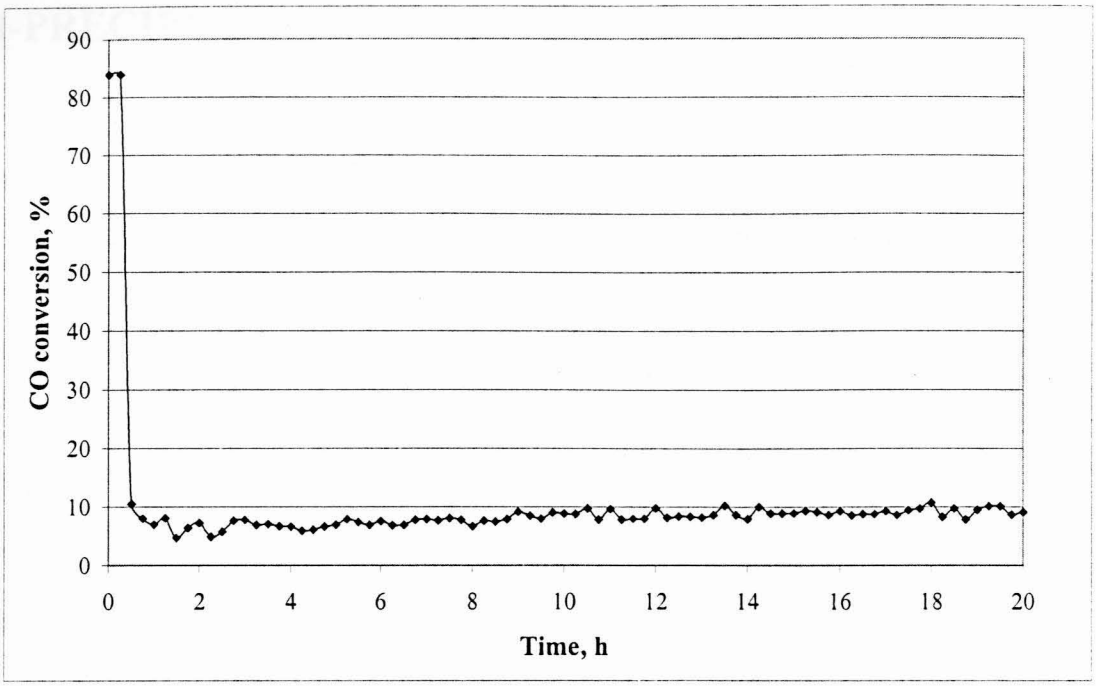


Figure 18. Activity of Mn 5;
0.5 g catalyst,60 ml/min, room temperature

The immediate deposition did not improve the activity of the catalyst. In fact, the activity was worse. Very large gold clusters were also seen on this catalyst (Figure 19).

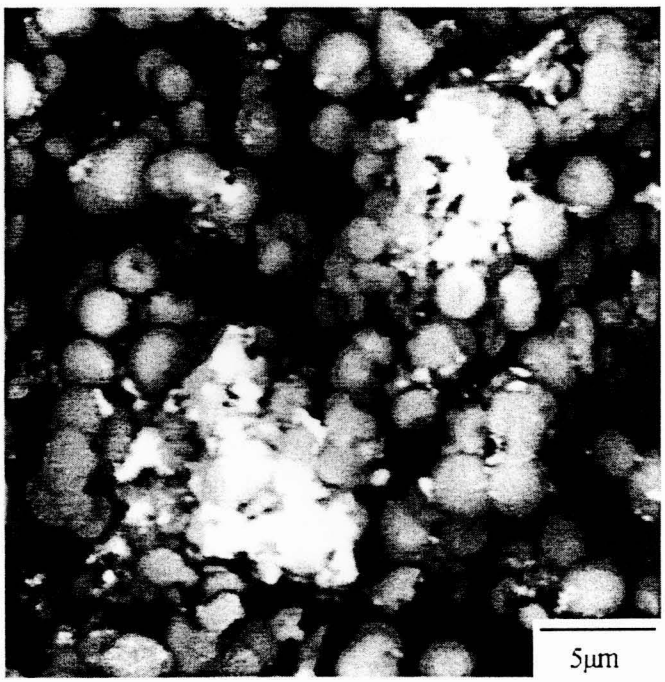


Figure 19. Backscattered electron image of Mn 5

6. CO-PRECIPITATION

The methods of attempting to deposit gold onto metal oxide supports did not yield promising catalysts, so it was decided to investigate the co-precipitation method. The co-precipitation of Au/Mn_xO_y was investigated first, as it was felt that this was a simpler system to study, than the mixed-oxide hopcalite system.

6.1. Mn_xO_y

6.1.1. Experimental

The experimental conditions of CPMn 1 – CPMn 39, are set out in Table 11.

Table 11. Experimental conditions of CPMn 1-39

Catalyst	$HAuCl_4$		Metal salts		Total volume ($HAuCl_4$ + metal salts), *ml*	Temp, ^oC	Ageing time, *min*	Final pH	Base used	Base	
	Conc, *g/l*	Vol, *ml*	Mn nitrate mass, *g*	Ce nitrate mass, *g*						Conc, *M*	Volume (initial), *ml*
CPMn 1	10	45	75		300	25	15	9.0	Na_2CO_3	0.2	180
CPMn 2	10	15	15		200	25	15	10.5	Na_2CO_3	2.0	200
CPMn 3	10	15	15		200	25	15	10.7	Na_2CO_3	1.0	200
CPMn 4	10	15	15		200	25	15	10.2	Na_2CO_3	0.5	200
CPMn 5	10	15	15		200	25	15	9.0	Li_2CO_3	saturated	200
CPMn 5_rpt	10	25	15		200	25	15	9.0	Li_2CO_3	saturated	200
CPMn 6	10	15	15	1.5	200	25	15	9.0	Li_2CO_3	saturated	200
CPMn 7	10	20	15		300	25	15	9.0	Li_2CO_3	saturated	250
CPMn 8	10	20	15		300	25	15	9.0	Li_2CO_3	saturated	250
CPMn 9	10	15	15		300	25	15	9.0	Li_2CO_3	saturated	200
CPMn 10	10	15	15		50	25	15	9.0	Li_2CO_3	saturated	200
CPMn 11	10	15	15		50	25	15	9.0	Li_2CO_3	saturated	200
CPMn 12	10	15	15		65	25	15	9.0	Li_2CO_3	saturated	300
CPMn 13	10	15	15		50	25	15	9.0	Li_2CO_3	saturated	300
CPMn 14	50	3	15		20	25	15	9.0	Li_2CO_3	saturated	200
CPMn 15	10	15	15	1.19	50	25	15	9.0	Li_2CO_3	saturated	200
CPMn 16	10	15	15		50	70	15	9.0	Li_2CO_3	saturated	200
CPMn 17	10	15	15		100	25	15	9.0	Li_2CO_3	saturated	N/A
CPMn 18	10	15	15		100	70	15	9.0	Li_2CO_3	saturated	N/A
CPMn 19	10	15	15		50	25	15	9.6	Li_2CO_3	saturated	300
CPMn 20	10	15	15		50	25	15	9.1	Li_2CO_3	saturated	400

Table 11 continued...

Catalyst	$HAuCl_4$		Metal salts		Total volume ($HAuCl_4$ + metal salts), *ml*	Temp, ^oC	Ageing time, *min*	Final pH	Base used	Base	
	Conc, *g/l*	Vol, *ml*	Mn nitrate mass, *g*	Ce nitrate mass, *g*						Conc, *M*	Volume (initial), *ml*
CPMn 21	10	15	15		50	25	15	10.5	Li_2CO_3/ Na_2CO_3	saturated /1.0	200
CPMn 23	10	15	15		50	25	15	10.2	Na_2CO_3	1.0	200
CPMn 24	50	3	15		50	25	180	10.0	Na_2CO_3	0.5	200
CPMn 25	50	3	15		50	25	10	10.5	Na_2CO_3	1.0	200
CPMn 26	50	3	15		50	25	10	10.1	Na_2CO_3	0.5	200
CPMn 27	50	3	15		50	25	10	10.2	Li_2CO_3	saturated	800
CPMn 28	50	3	15	0.095	50	25	180	10.2	Na_2CO_3	0.5	200
CPMn 29	50	3	15		50	25	10	6.1	Na_2CO_3	0.2	200
CPMn 30	50	3	15		25	25	10	10.7	Na_2CO_3	2.0	200
CPMn 31	50	3	15		23	25	180	10.5	Na_2CO_3	2.0	200
CPMn 33	50	3	15		50	25	180	11.3	Na_2CO_3	0.5	200
CPMn 34	50	3	15		20	25	10	10.7	Na_2CO_3	1.0	200
CPMn 35	50	3	15		50	25	10	8.9	Na_2CO_3	0.4	200
CPMn 36	50	3	15		50	25	10	10.7	Na_2CO_3	2.0	200
CPMn 37	50	3	15		50	25	10	10.5	Na_2CO_3	2.0	100
CPMn 38	50	1	15		50	25	10	10.7	Na_2CO_3	1.0	200
CPMn 39	50	3	15		50	25	180	10.4	Na_2CO_3	1.0	200

Hoflund *et al.*[5] found that if Li_2CO_3 was used as the base instead of Na_2CO_3 in Au/Mn_xO_y catalysts, the lithium acted as a promoter to increase catalyst activity. Therefore both Li_2CO_3 and Na_2CO_3 were tested. In this study, it was not possible to compare concentrations with Li_2CO_3 as was done with Na_2CO_3, due to the poor solubility of Li_2CO_3 in water (13 g/l; 0.18 M maximum). Saturated Li_2CO_3 solutions were used in making the catalysts. Even so, additional Li_2CO_3 had to be pumped in during the metal salt addition so that the pH did not drop below 9. The total volume of Li_2CO_3 usually added in was around 800 ml. Only in the case of CPMn 27, where 800 ml of Li_2CO_3 was added in initially, was no extra Li_2CO_3 pumped in.

For CPMn 2-4 and CPMn 21-39, the final pH was not controlled by pumping in base during the experiment, but rather by using different base concentrations initially.

Cerium-promoted catalysts (CPMn 6, CPMn 15, CPMn 28) were also made to determine if cerium could improve the CO oxidation ability of the Au/Mn_xO_y catalyst.

The catalyst preparation methods are outlined below.

6.1.1.1. Method 1 – co-precipitation (CPMn 1-10, 11,12-16, 19-21, 23)*

The required volume of base was added into the reaction vessel and heated to 25°C. $Mn(NO_3)_2.xH_2O$ and $HAuCl_4$ solution were mixed together and diluted to the required volume. The mixed metal solution was then pumped into the base at a flowrate of 5.9 ml/min. During the metal salt addition, if the pH fell below 9, additional base was pumped in to keep the pH at 9. This pH was chosen because Mn^{2+} precipitates out only at pH 8 and an even higher pH is necessary for effective precipitation[11].

The suspension was stirred for 15 minutes to allow for any further precipitation. Thereafter, it was filtered, washed and subsequently dried at 80°C. A few catalysts were initially calcined at 200°C, but most were calcined at 400°C.

---

* With CPMn 11, a variation was attempted. A solution of $Mn(NO_3)_2$ (35 ml) was first pumped into Li_2CO_3 to precipitate $Mn(OH)_2$. $HAuCl_4$ (15 ml) was then pumped into this slurry. After ageing, the catalyst was filtered, washed and dried at 80°C.

6.1.1.2. Method 2 – inverse co-precipitation (CPMn 17,18)

$Mn(NO_3)_2.xH_2O$ and $HAuCl_4$ solution were mixed together and diluted to 100 ml. The mixed metal salt solution was then poured into the reaction vessel and the desired temperature was set. Saturated Li_2CO_3 was then pumped in to precipitate the metal hydroxides. The final pH was set at 9. When this pH was reached, it was maintained for 15 minutes to ensure complete precipitation. Thereafter, the precipitate was filtered, washed and dried at 80°C. The catalysts were calcined at 400°C.

6.1.1.3. Method 3 – co-precipitation (CPMn 24-39)

The required amount of base was added to the reaction vessel and heated to 25°C. $HAuCl_4$ solution was mixed together with the metal salts, and the solution was made up to the required volume. The mixed metal salt solution was then poured into the base in one aliquot. The suspension was stirred for the required time and then filtered. The solids were washed and subsequently dried at 80°C. The catalysts were calcined at 400°C.

6.1.2. Results and discussion

The gold loadings on the co-precipitated catalysts are shown in Table 12 below.

Table 12. Au loadings on co-precipitated Au/Mn_xO_y catalysts

Catalyst	wt % Au
CPMn 1	1.8
CPMn 2	2.1
CPMn 3	2.4
CPMn 4	2.4
CPMn 5	2.3
CPMn 5_rpt	3.9
CPMn 6	1.9
CPMn 7	3.5

CPMn 8	3.5
CPMn 9	2.6
CPMn 10	2.4
CPMn 11	2.4
CPMn 12	2.4
CPMn 13	2.3
CPMn 14	2.3
CPMn 15	2.1
CPMn 16	2.4
CPMn 17	2.4
CPMn 18	2.1
CPMn 19	2.5
CPMn 20	2.4
CPMn 21	2.5
CPMn 23	2.6
CPMn 24	2.3
CPMn 25	2.5
CPMn 26	2.4
CPMn 27	2.2
CPMn 28	2.3
CPMn 29	4.4
CPMn 30	2.9
CPMn 31	2.9
CPMn 33	2.8
CPMn 34	3.0
CPMn 35	2.9
CPMn 36	2.7
CPMn 37	2.9
CPMn 38	0.99
CPMn 39	2.7

With the exception of CPMn 29 all the catalysts had close to the expected gold loadings. CPMn 29 had a much higher gold loading than was expected, but this is probably due to it having an end pH of 6.1 (Table 11). At this low pH, not all of the manganese would have precipitated out of solution[11].

The catalytic activities of the co-precipitated Au/Mn_xO_y catalysts are tabulated below (Table 13). Since run-times differed for each catalyst (varying between 1.5 to 20 h time on-stream), activities as μmol CO/g Au/s, were calculated using the % CO conversion value at the end of the run.

Table 13. Calculated μmol CO/g Au/s for co-precipitated Au/Mn_xO_y catalysts (CPMn 1-39, calcined at 400°C)

Catalyst	μmol CO/g Au/s
CPMn 1	26
CPMn 2	32
CPMn 3	26
CPMn 4	28
CPMn 5	35
CPMn5_rpt	3.9
CPMn 6	6.0
CPMn 7	3.6
CPMn 8	1.6
CPMn 9	8.9
CPMn 10	29
CPMn 11	13
CPMn 12	27
CPMn 13	34
CPMn 14	28
CPMn 15	7.8
CPMn 16	20
CPMn 17	3.0
CPMn 18	4.7
CPMn 19	15
CPMn 20	23
CPMn 21	29
CPMn 23	32
CPMn 24	383
CPMn 25	382
CPMn 26	274
CPMn 27	238
CPMn 28	119
CPMn 29	166
CPMn 30	23
CPMn 31	24
CPMn 33	2.9
CPMn 34	16
CPMn 35	301
CPMn 36	210
CPMn 37	199
CPMn 38	229
CPMn 39	181

6.1.2.1. Method 1 (CPMn 1-10, 11,12-16, 19-21, 23)*

CPMn 1-CPMn 5 were initially calcined at 200°C. With CPMn 1, as a result of the reagent quantities being tripled, the pH fell rapidly to less than 7. Since the 0.2 M Na_2CO_3 being automatically titrated in was too weak to maintain the pH control (programmed to not fall below pH 9), a saturated Na_2CO_3 solution was simultaneously added in. CPMn 1 did not perform as well in the activity tests as the other CPMn- catalysts (see Figure 20).

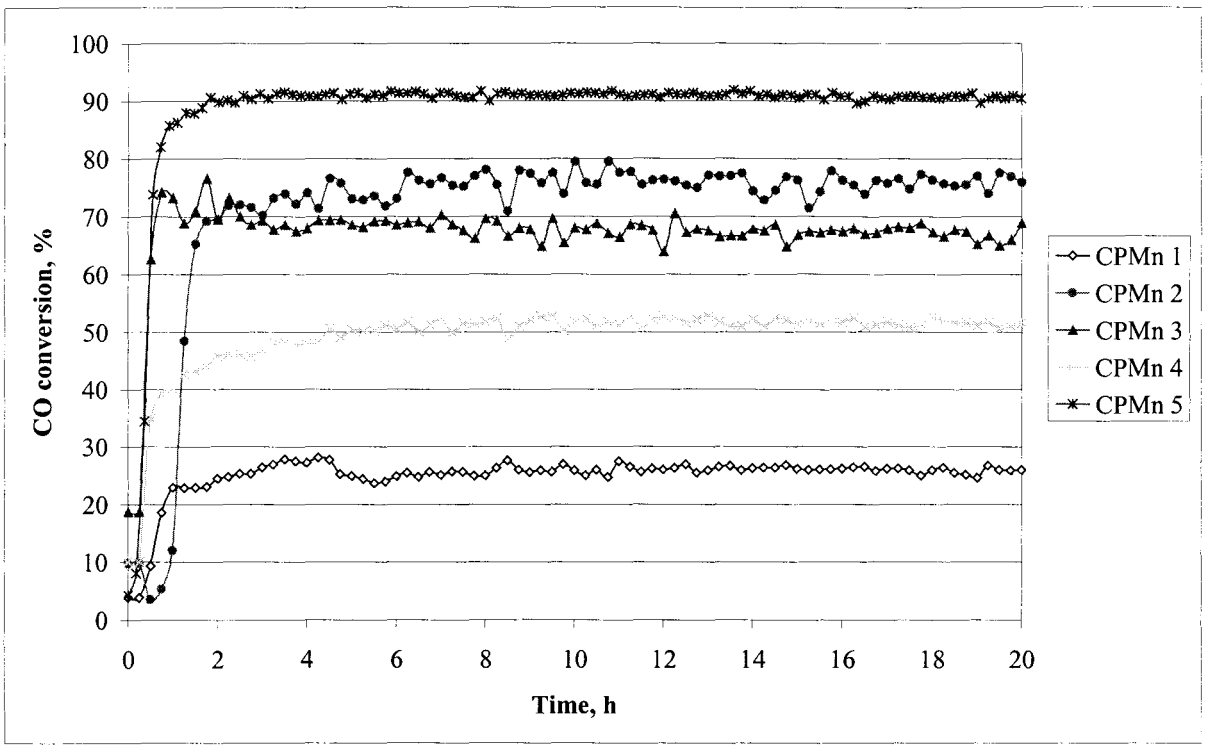


Figure 20. Activities of CPMn 1-5, calcined at 200°C;
0.25 g catalyst (CPMn 1),0.5 g catalyst (CPMn 2-5), 60 ml/min; room temperature

The highest activities so far were obtained on these catalysts – all performed better than the catalysts prepared by deposition-precipitation or colloidal gold methods.

CPMn 5, the catalyst made using Li_2CO_3 as a base, had the best activity. Although it seems as if CPMn 1 had a much lower activity than the others, the test was run on only 0.25 g of the catalyst. There does appear to be some sort of base concentration dependence with the sodium-'promoted' catalysts. Not much difference was observed for CPMn2 and CPMn 3, with 2 M Na_2CO_3 and 1 M Na_2CO_3 respectively. However, CPMn 4 (0.5 M Na_2CO_3)

appeared to have a noticeably lower activity. Taking the gold loading and catalyst masses into account, a clearer picture of the catalyst activities after 20 h, was seen (Table 14).

Table 14. Calculated μmol CO/g Au/s for co-precipitated Au/Mn_xO_y catalysts (CPMn 1-5, calcined at 200°C)

Catalyst	Base	μmol CO/g Au/s
CPMn 1	Na_2CO_3	26
CPMn 2	Na_2CO_3	32
CPMn 3	Na_2CO_3	26
CPMn 4	Na_2CO_3	19
CPMn 5	Li_2CO_3	36

From these results, it can be seen that the activities of CPMn 5 and CPMn 2 are not as different as they appeared to be. So although CPMn 5 has a higher activity, no definite conclusion can be drawn yet about which base yields a more active catalyst.

From the activities measured, a definite base-concentration dependence on activity can be seen for CPMn 2, CPMn 3 and CPMn 4, with catalyst activity decreasing with decreasing base concentration. Although CPMn 1 (0.2 M Na_2CO_3) was more active than CPMn 4, its base concentration cannot be compared here, as saturated Na_2CO_3 was also used in its preparation.

As Hoflund, et al.[5] calcined their catalysts at 400°C, CPMn 2, CPMn 4 and CPMn 5 were also calcined at this temperature. The activities of these catalysts are shown in Figure 21.

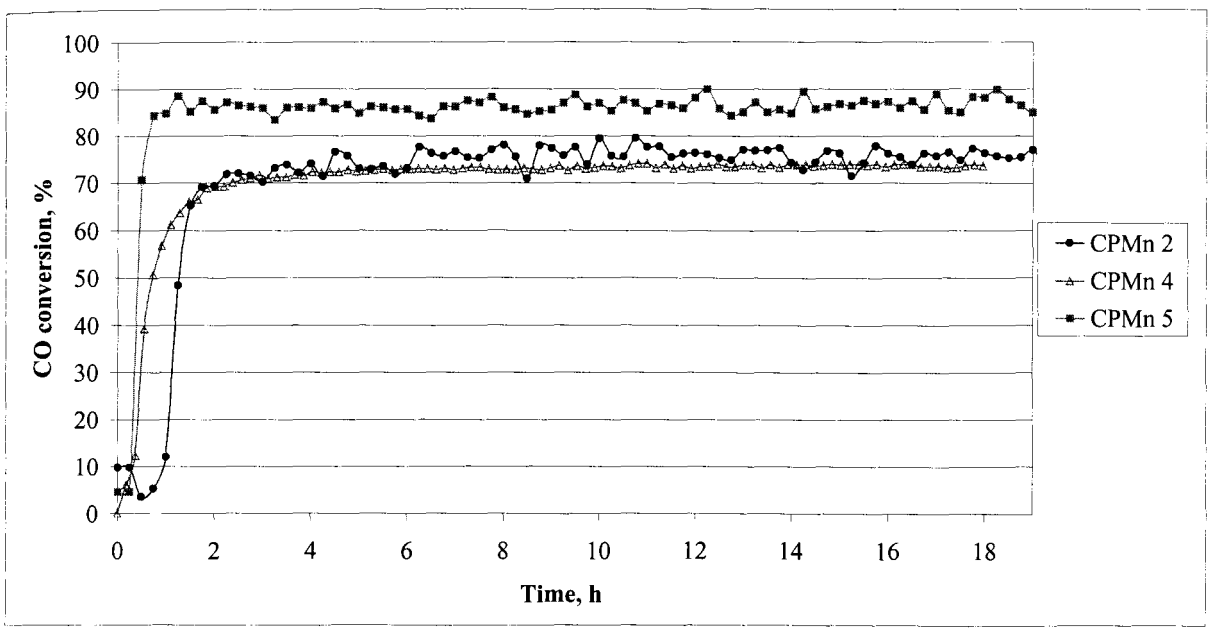


Figure 21. Activities of CPMn 2, 4 and 5, calcined at 400°C; 0.5 g catalyst, 60 ml/min; room temperature

A comparison of the catalytic activities of CPMn 2, 4 and 5 at the calcination temperatures of 200°C (Table 14) and 400°C (Table 13), showed that calcining the catalysts at 400°C had a positive effect for CPMn 4. There was no significant difference in activity with CPMn 2 or CPMn 5. However, it was decided to calcine all future catalysts at 400°C.

The surface area of CPMn 2 was measured, and determined to be $100m^2/g$.

The addition of cerium as a promoter did not effect the hoped-for result. The activity of CPMn 6 is illustrated in Figure 22.

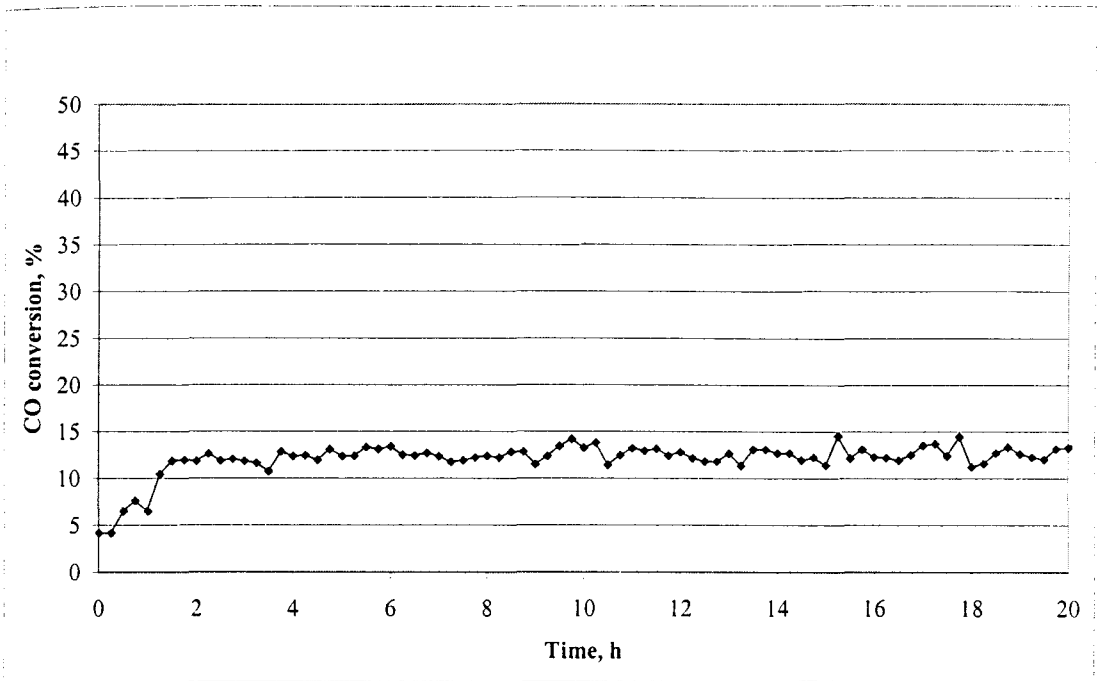


Figure 22. Activity of CPMn6, calcined at 400°C; 0.5 g catalyst, 60 ml/min; room temperature

From this result, it appears as though cerium hinders the performance of the Au/Mn_xO_y catalyst. However, the Ce/Mn molar ratio of 4/6 that was used, is actually the optimum for phenol oxidation. So it is possible that a different Ce/Mn ratio would be required to promote the CO oxidation reaction.

Because CPMn 5 had a higher activity (although slight) than CPMn 2, it was decided to focus efforts on optimising the co-precipitation technique using Li_2CO_3 as the base. Another reason for doing so was that Hoflund *et al.*[5] found the catalysts made with Li_2CO_3 had the highest activities.

The preparation of CPMn 5 was repeated with a higher gold loading (CPMn 5_rpt), but keeping the preparation conditions otherwise identical. However, this catalyst had a much poorer activity than CPMn 5. CPMn 7, 8 and 9 were then made in an attempt to reproduce CPMn 5. The higher gold loadings were still used for CPMn 7 and 8. The base volumes and/or total mixed metal solution volumes were also increased for CPMn 7-9. However, the activity of CPMn 5 could not be duplicated on any of these catalysts (Figure 23).

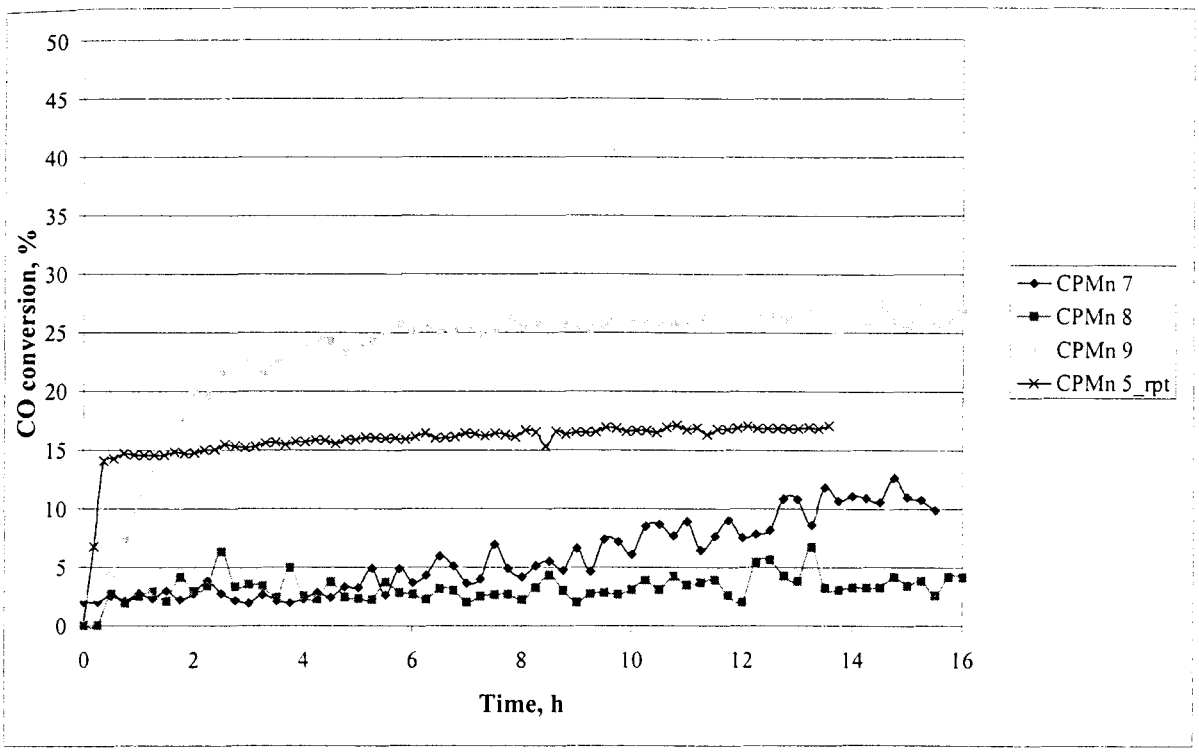


Figure 23. Activities of CPMn 5_rpt, 7-9, calcined at 400°C; 0.5 g catalyst, 60 ml/min; room temperature

Since the conditions being used were not resulting in reproducible catalysts, it was decided to decrease the total volume of the mixed metal salt solution; i.e. the concentration of the solution was increased. The flowrate was maintained and therefore addition of the mixed metal solution was effected more rapidly.

The new preparation method appeared to work, with CPMn 10 performing well with around 75% CO conversion. It was therefore decided to use the more concentrated mixed metal salt solutions for the catalysts made thereafter.

Modifications to the CPMn 10 method were initially made on CPMn 11-16. The CPMn 11 recipe is outlined in the footnote in Section 6.1.1.1. With CPMn 12-14, variations were made to either the total metal volume, base volume, or both. CPMn 15 was made with the addition of cerium nitrate. Since the use of cerium as a promoter was attempted previously, with no success (CPMn 6), another attempt was now made using the recipe of CPMn 10. Also, the 'optimum' Ce/Mn ratio for CO oxidation, was now used in the preparation of CPMn 15. Imamura *et al.*[40] tested the CO oxidation ability of cerium oxide-manganese oxide catalysts

which were co-precipitated in varying ratios, and found the optimum Ce/Mn ratio for CO oxidation to be 5/95 mol %. The same ratio was therefore used in the preparation of CPMn 15.

Since no catalysts had yet been prepared at higher temperatures, CPMn 16 was prepared at 70°C.

A comparison of the activities of CPMn 10-16, 19 and 20, is shown in Figure 24.

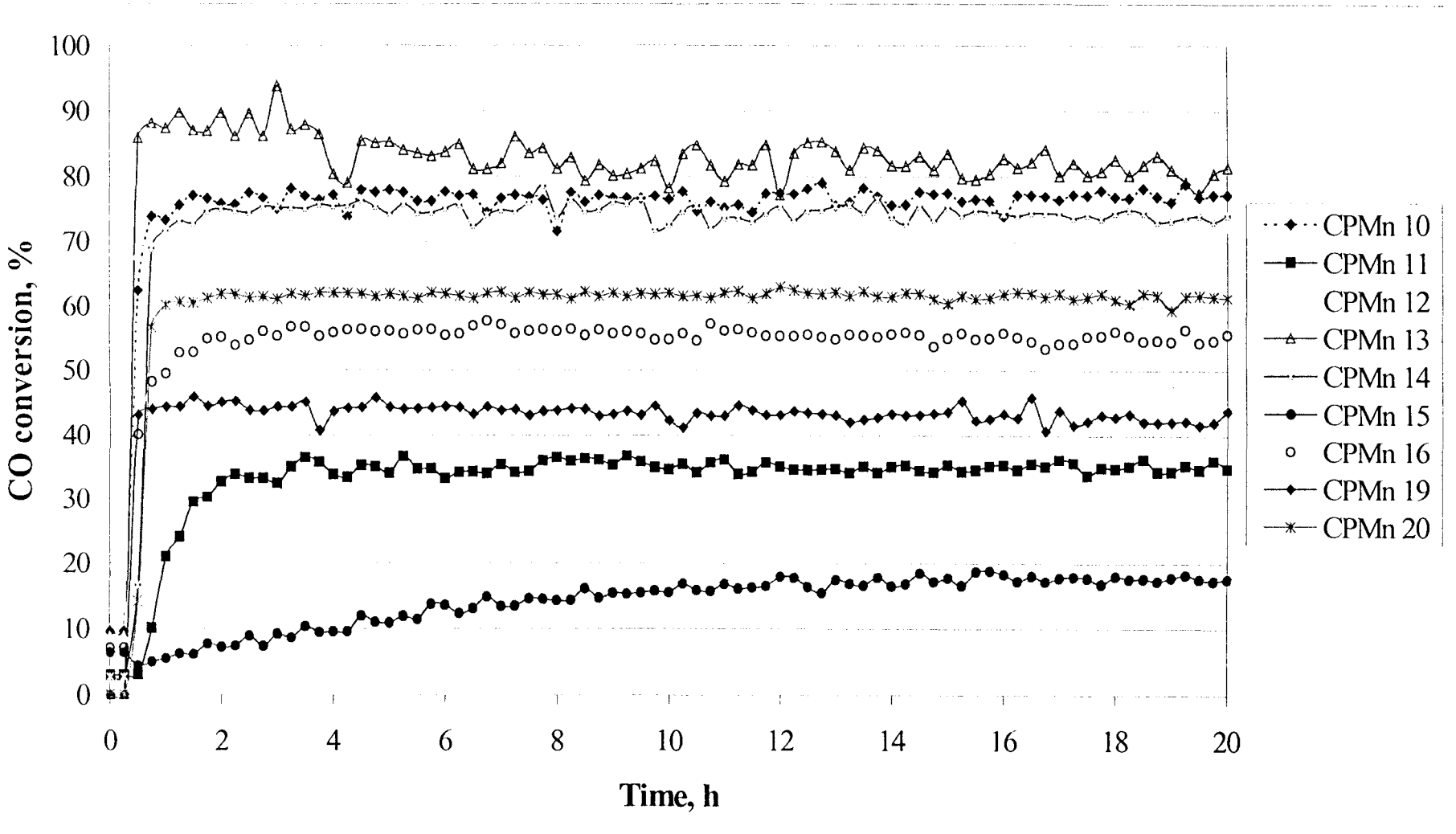


Figure 24. Activities of CPMn 10-16,19, 20; calcined at 400°C; 0.5 g catalyst, 60 ml/min, room temperature

The best-performing catalyst was CPMn 13 (although some deactivation was apparent), followed closely by CPMn 10, CPMn 14 and CPMn 12. Therefore, the variations to mixed metal and/or base volume did not greatly affect the catalysts' activities. However, variations to the mixed metal solution volume were small, which is probably why the activity differences were small. The base volumes, although they varied by large amounts, were just the initial volumes, and extra Li_2CO_3 still had to be added in during the course of the catalyst preparation, to keep the pH at 9. So the variations might not have been significant enough to affect the activities. The similar activities of CPMn 10, 12, 13 and 14 appear to indicate that using a more concentrated mixed metal solution gave more reproducible catalysts.

CPMn 16, the catalyst made at 70°C, did not perform as well as those made at room temperature. It was also seen that depositing gold onto freshly precipitated manganese hydroxide (CPMn 11), and the addition of cerium (CPMn 15), did not yield good results. The CPMn 15 result was disappointing since the optimum Ce/Mn ratio for effective CO oxidation, as reported by Imamura *et al.*[40], was used in the preparation of this catalyst. Imamura *et al.*[40] have stated that at low temperatures, cerium transfers oxygen to Mn_xO_y, and at high temperatures, cerium withdraws oxygen from Mn_xO_y[40]. Therefore, cerium was expected to promote the CO oxidation of the Au/Mn_xO_y catalyst at low temperatures. However, the opposite effect was obtained.

The reaction mechanism for CO oxidation is said to involve the adsorption of CO onto gold particles[19, 36]. Haruta *et al.*[36] discovered in their IR studies, carbonate-like species adsorbed onto the TiO_2 support (this is in agreement with the postulated mechanism of Bond and Thompson[19]). The oxygen atoms responsible for the formation of this species, were provided by the support itself. This would apply to the Mn_xO_y support as well, since the participation of catalyst surface oxygen has been observed previously on Mn_xO_y catalysts[7].

It was therefore expected that the combined effect of the manganese and cerium - with both providing oxygen for CO conversion - would increase the activity. Since it has been found on Au/CeO_x catalysts that the addition of gold increased the oxygen storage capacity of CeO_x to a large extent[17], the oxygen donation to Mn_xO_y was expected to be very high. It was therefore expected that the CO conversion on this catalyst would be high.

A possible reason for the unexpected disappointing activity is that the Au-Ce_xO_y combination resulted in the Mn_xO_y surface becoming too oxygenated. It has been reported that a fully oxygenated Mn_xO_y surface is not active for low temperature CO oxidation[7].

The final two catalysts made with Li_2CO_3 alone were CPMn 19 and CPMn 20. The method for CPMn 19 was identical to that of CPMn 13, except that the end pH of the former was 9.6. It therefore seems that pH 9 is the better pH for lithium-promoted co-precipitated Au/Mn_xO_y catalysts. Since high activities were obtained on catalysts with 300 ml Li_2CO_3 (CPMn 12, 13), it was decided to see the effect of increasing the Li_2CO_3 volume to 400 ml. However, the activity was notably lower in this instance.

The problem experienced throughout the manufacture of lithium-promoted catalysts was that, due to the low solubility of Li_2CO_3, large quantities were required for pH adjustment. A mixture of 0.12 M Li_2CO_3 and 1 M Na_2CO_3 was used in making CPMn 21. The reasons for doing this were:

- The higher concentration Na_2CO_3 would make pH control easier, with smaller volumes of base being used
- There would still be enough Li_2CO_3 to 'promote' the catalyst (i.e. if lithium was indeed a promoter on these catalysts)

Previously, it was seen that the catalyst with Li_2CO_3 (CPMn 5), performed slightly better than the then-best Na_2CO_3 catalyst (CPMn 2). However, these catalysts were prepared with very dilute mixed metal solutions. No catalyst had yet been made with Na_2CO_3, while using a more concentrated mixed metal solution. CPMn 23 was thus made for comparison purposes, using 1 M Na_2CO_3 and the preparation conditions of CPMn 10.

The activities of CPMn 21 and CPMn 23 are shown in Figure 25.

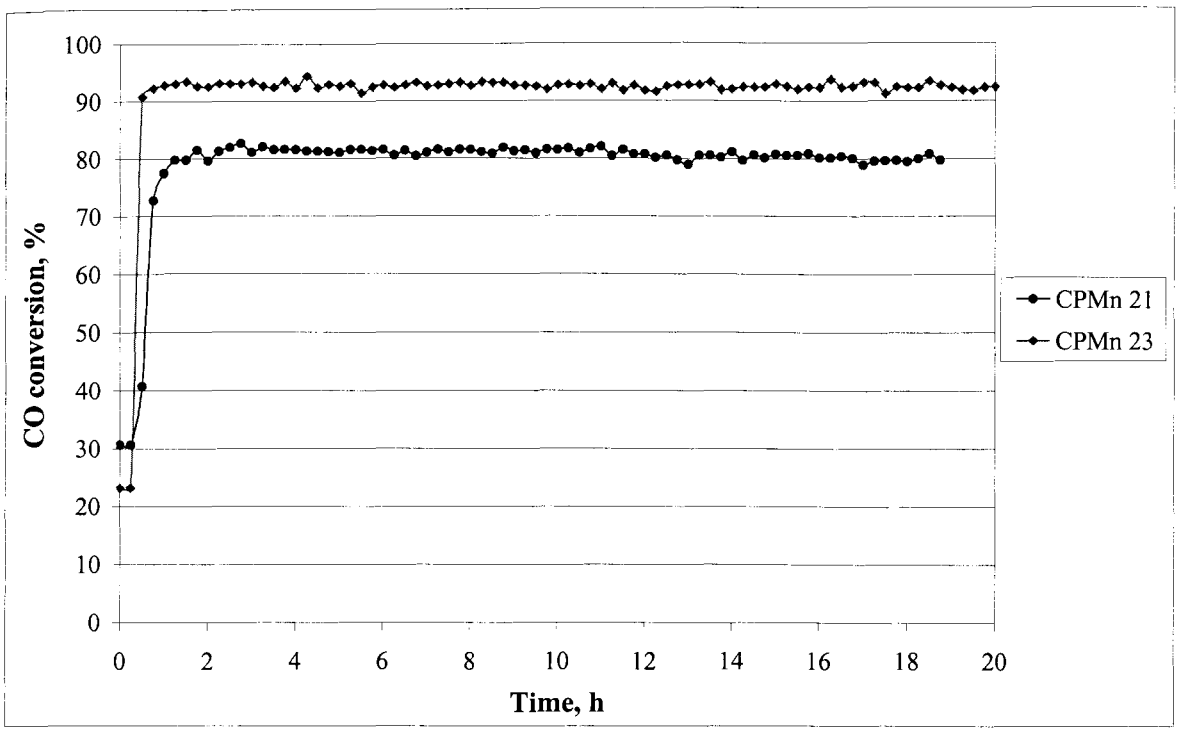


Figure 25. Activities of CPMn 21 and 23, calcined at 400°C; 0.5 g catalyst, 60 ml/min; room temperature

CPMn 21, with its mixture of Na_2CO_3 and Li_2CO_3 , performed well, as did CPMn 23 - the catalyst made with Na_2CO_3. CPMn 23 even appears graphically, to have a slightly higher activity than the lithium-'promoted' CPMn 5. Comparing the activities of these catalysts (Table 13), the activity differences between the best performing sodium- (CPMn 23) and lithium- (CPMn 5) catalysts are actually very close. It is therefore difficult to decide which base is the better one to use.

XRD spectra obtained using Cu radiation (Figure 26) showed no difference in crystal structure between CPMn 10 (made with Li_2CO_3) and CPMn 23 (made with Na_2CO_3). The crystal phases could not easily be identified, however, because of the low degree of crystallinity of these catalysts.

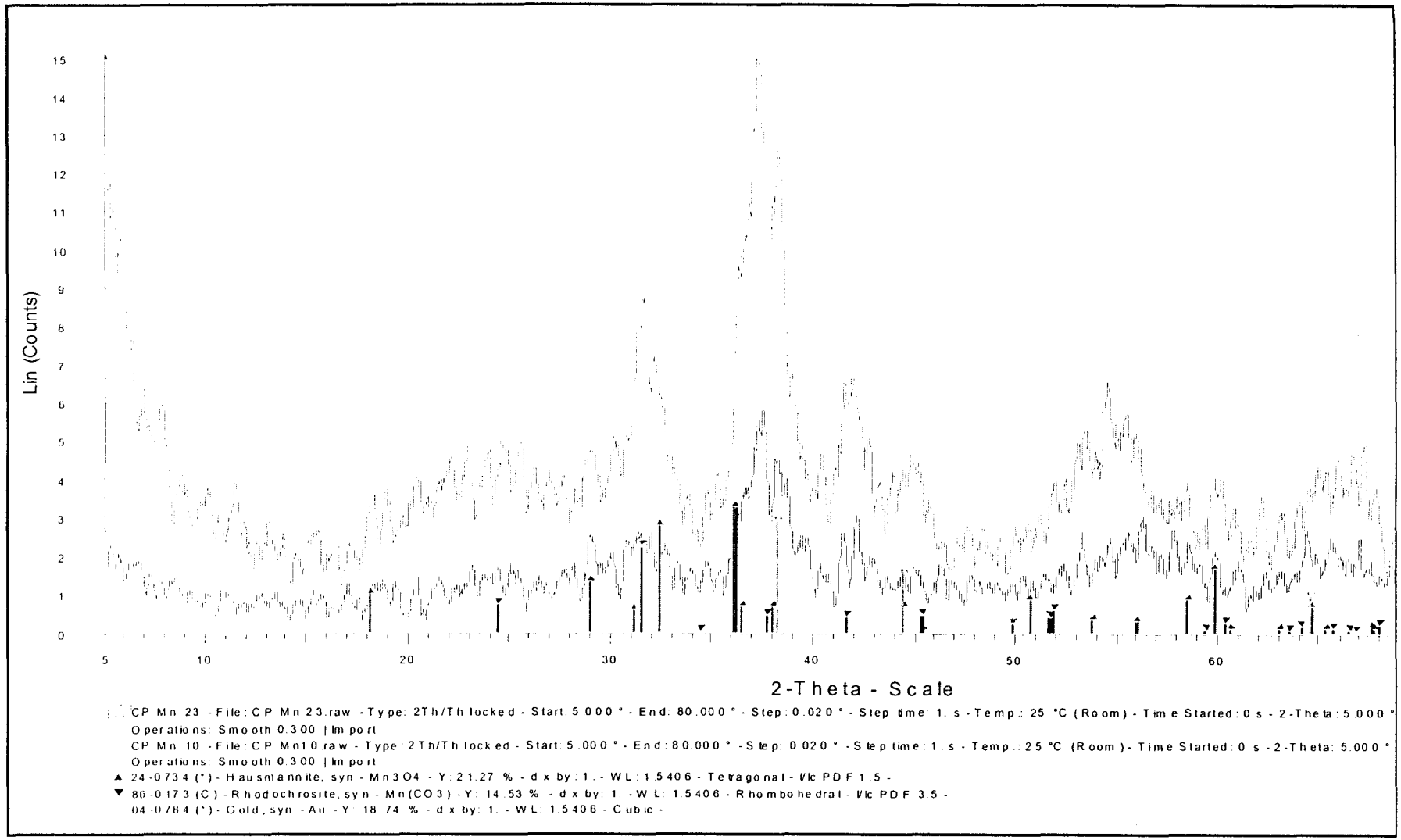


Figure 26. XRD spectra of CPMn 10 (top trace) and CPMn 23 (bottom trace)

The diffractograms appear to show the presence of gold, $MnCO_3$ and Mn_3O_4. XRD studies carried out on co-precipitated Au/Mn_xO_y catalysts by other investigators[16] showed only gold and $MnCO_3$ in the XRD spectra of their fresh catalysts. After catalytic activity tests, it was found that $MnCO_3$ had decomposed into Mn_3O_4, MnO and Mn_2O_3. It was stated that these manganese oxides may be more effective supports for gold and this could explain why catalyst activities increased gradually over time. Increases in activity with increasing time were also seen on CPMn 10 and CPMn 23, which reached maximum activity in 45 minutes and 30 minutes respectively.

6.1.2.2. Method 2 (CPMn 17 and 18)

The activities of the catalysts made by the inverse co-precipitation method, are shown in Figure 27.

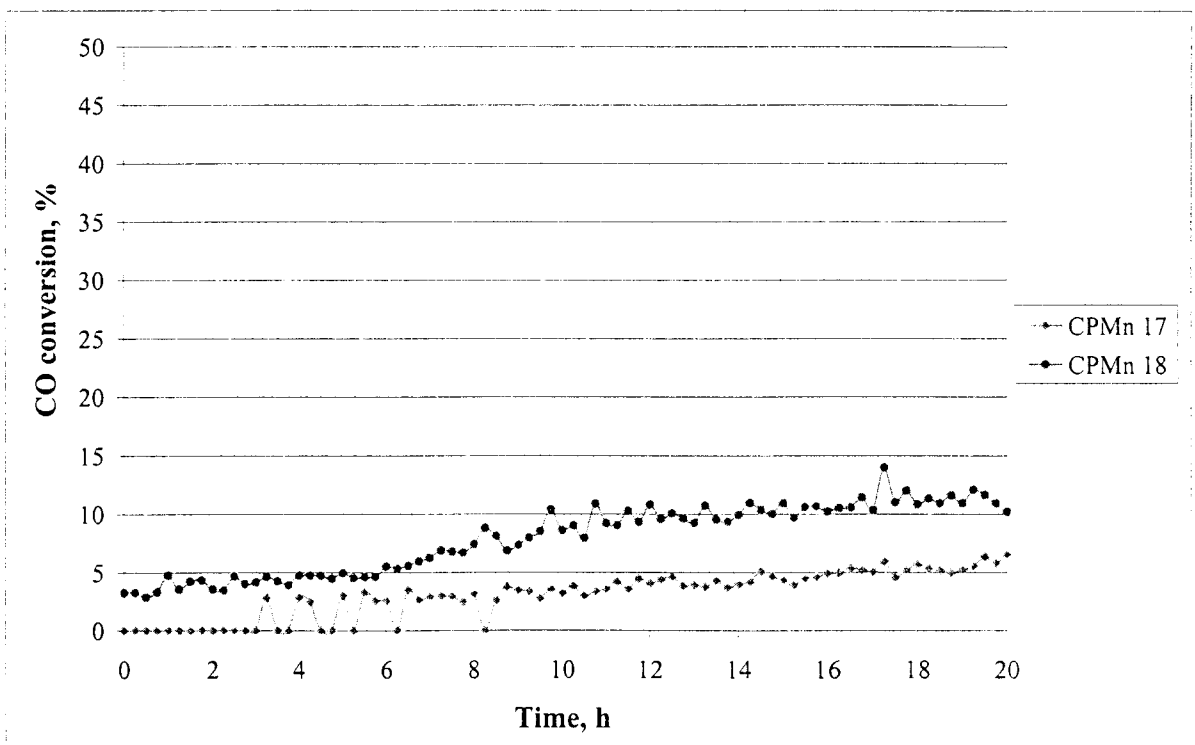


Figure 27. Activities of CPMn 17 and 18, calcined at 400°C; 0.5 g catalyst, 60 ml/min; room temperature

Both CPMn 17 (made at room temperature) and CPMn 18 (made at 70°C) performed poorly. So the inverse co-precipitation method does not appear to work for Au/Mn_xO_y catalysts.

6.1.2.3. Method 3 (CPMn 24 – 38)

In the initial investigations (catalysts made using *Method 1*), the flowrate was set at 5.9 ml/min, to effect the dropwise addition of the mixed metal salts into the base. Due to irreproducibility, the solution volume was decreased and hence the mixed metal salts were pumped in at the same flowrate, but over a shorter period of time (*Method 2*). This led to improved activities. Now in *Method 3*, the effect of adding the metal solution into the base in an instantaneous manner, was studied.

These catalysts proved to be more active than any of the previous catalysts, by an order of magnitude. The results of the activity tests for CPMn 24-28 are shown in Figure 28.

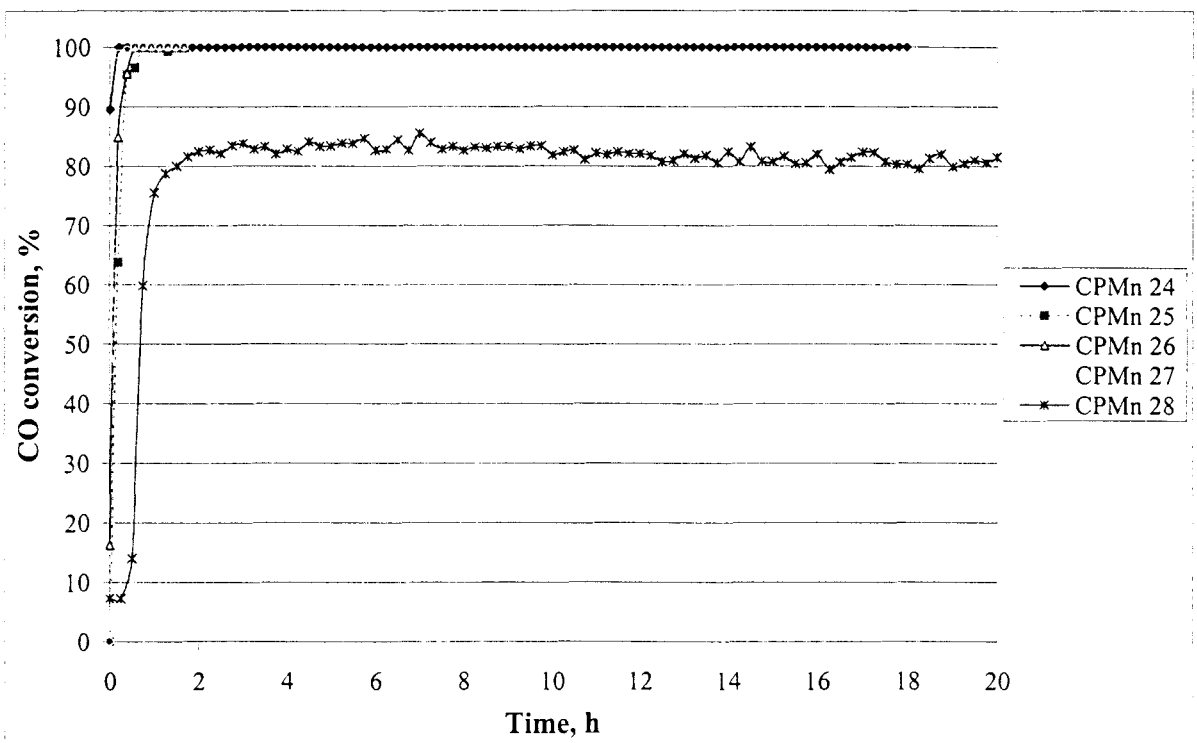


Figure 28. Activities of CPMn 24- 28, calcined at 400°C; 0.5 g catalyst, 60 ml/min; room temperature

All catalysts; except for the cerium-promoted CPMn 28; reached the maximum activity that could be reached under these operating conditions (60 ml/min flowrate, 0.5 g catalyst), within a very short space of time. Much less $Ce(NO_3)_2.6H_2O$ (8 % of the mass used for CPMn 15) was added in this time than previously, due to poor activities being obtained on those

catalysts. So it was hoped that the addition of less cerium (expected Ce/Mn ratio = 0.4/99.6) would oxygenate the manganese support just enough to promote the reaction. However, even the addition of a minute amount of cerium affected the activity of the catalyst adversely. So cerium does not appear to have any potential as a promoter for CO oxidation, on Au/Mn_xO_y catalysts.

Just to ensure that the added amount of cerium was precipitating out at the correct proportions to manganese in the catalysts, CPMn 15 and CPMn 28 were analysed for cerium and manganese. The expected and actual mol % of cerium and manganese are tabulated below (Table 15). From these values it can actually be seen that cerium and manganese precipitated out in proportions very similar to those used in the starting solutions.

Table 15. Comparison of expected and actual Ce and Mn molar proportions

Catalyst	Expected metal ratio on catalyst, %		Actual metal ratio on catalyst, %	
	Ce	Mn	Ce	Mn
CPMn 15	5	95	6	94
CPMn 28	0.4	99.6	0.6	99.4

The fact that the remainder of the catalysts reached maximum activity *despite* differences in base type, base concentration and ageing times (Table 11), leads to the conclusion that the rate of addition of the mixed metal salts is a very important factor in the preparation of these catalysts. From the above results, it can be seen that instantaneous precipitation is the best method evaluated so far, for co-precipitated Au/Mn_xO_y catalysts.

The same conclusion was reached by Haruta *et al.*[41], who initially specified dropwise addition in a patent. However, in a more recent paper, Haruta and Daté[42] report that during the catalyst preparation, the metal hydroxide precursors should be precipitated instantaneously to obtain a homogeneous size distribution.

Since the activities of the catalysts made by means of instantaneous precipitation were very high, the testing conditions had to be changed. So the catalyst mass was reduced to 0.25 g and the gas flowrate was increased to 400 ml/min (SV = 96 000 $ml/g_{cat}/h$).

The effect of base (Na_2CO_3) concentration on activity was tested again, with the new preparation method. A catalyst was also made using saturated Li_2CO_3 solution. To avoid having to pump in Li_2CO_3, to prevent the pH dropping to below 9 once the mixed metal salt solution was added in, a large volume of Li_2CO_3 (800 ml) was added into the reaction vessel at the start.

The activities of the catalysts are shown in Figure 29.

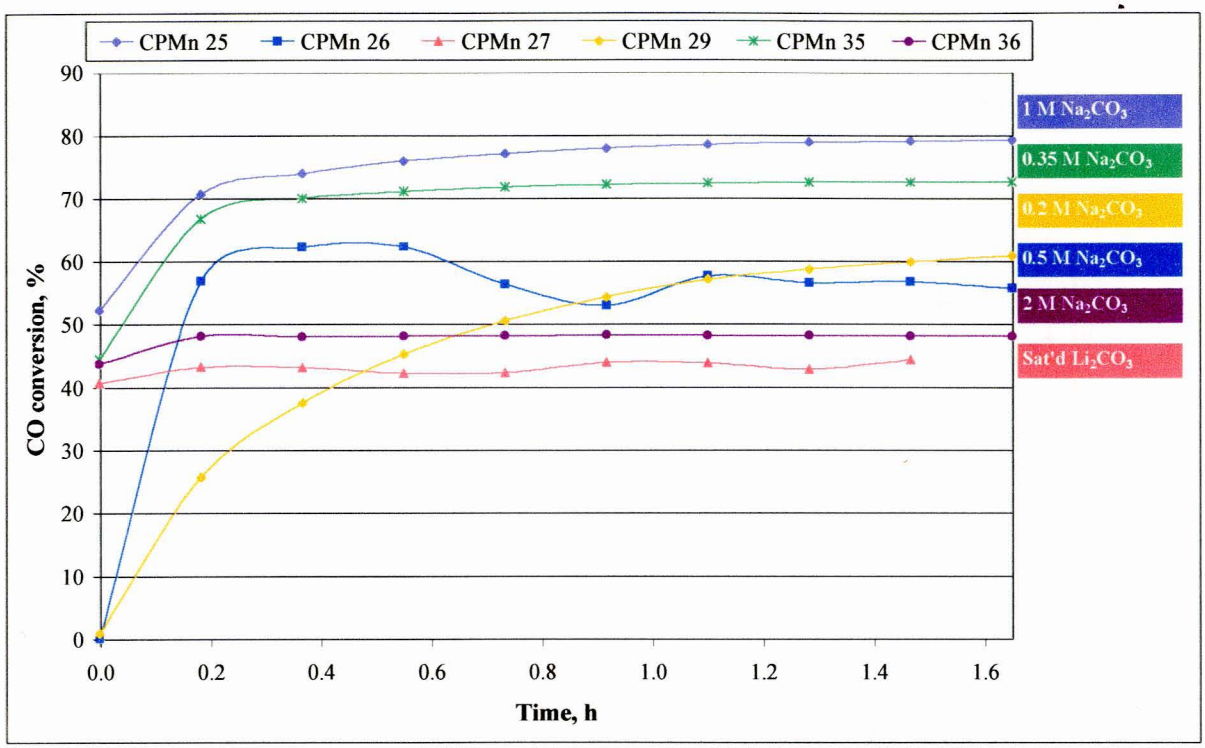


Figure 29. Comparison of co-precipitated catalysts made using different base concentrations; 10 minutes ageing, calcined at 400°C; 0.25 g catalyst, 400 ml/min; room temperature

The catalyst made with Li_2CO_3 - CPMn 27 - appeared to have the lowest activity of all. CPMn 27 had a final pH of 10.2. The sodium-'promoted' catalyst with the closest final pH to CPMn 27 was CPMn 26 (0.5 M Na_2CO_3; end pH 10.1), which performed better than CPMn 27. Taking the gold loading into account (Table 13), CPMn 26 was still seen to have a higher activity than CPMn 27, but the latter was also seen to not have the lowest activity after all. CPMn 27 had a higher activity than CPMn 29 (0.2 M Na_2CO_3) and CPMn 36 (2 M Na_2CO_3).

Although lithium-'promoted' Au/Mn_xO_y catalysts were reported to be more active than sodium-'promoted' catalysts by Hoflund *et al*[5], the same result has not been found in this study. The previously-made catalysts, such as CPMn 5, were not convincingly higher in activity than the catalysts made with Na_2CO_3. However, using the new preparation method, the catalyst made with Li_2CO_3 has a much lower activity than catalysts such as CPMn 25 and CPMn 35.

The two worst performing catalysts, CPMn 29 and CPMn 36, were made using the lowest- and highest- concentrations of Na_2CO_3, respectively. A histogram profile of the catalytic activity for the different Na_2CO_3 concentrations used (bar graph), is shown in Figure 30. The final pH's of these catalysts are also shown (line graph).

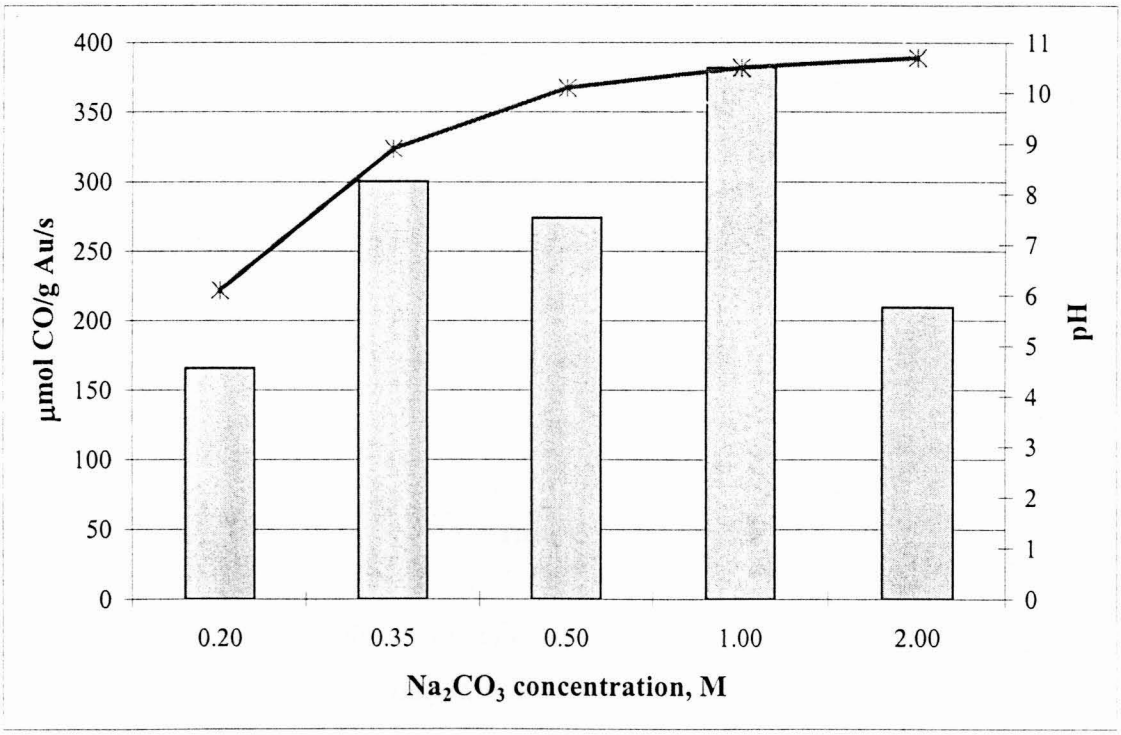


Figure 30. Dependence of activity on Na_2CO_3 concentration

In this graph, the relationship between Na_2CO_3 concentration and activity can be seen more clearly. 1 M Na_2CO_3 appears to be the best concentration to use. CPMn 35, the catalyst made using 0.35 M Na_2CO_3 (end pH 8.9) also performed well, although its activity was still significantly lower than CPMn 25 (1 M Na_2CO_3).

The surface area of CPMn 25 was determined to be 121 m^2/g. This is higher than that of CPMn 10 (100 m^2/g), made using Method 1. So the much higher activity is possibly due partly to the higher surface area of the catalyst.

CPMn 24 was made using exactly the same conditions as CPMn 26, with 0.5 M Na_2CO_3 as the base, except that CPMn 24 was aged for 3 h.

CPMn 24 was more active than CPMn 26 (Figure 31).

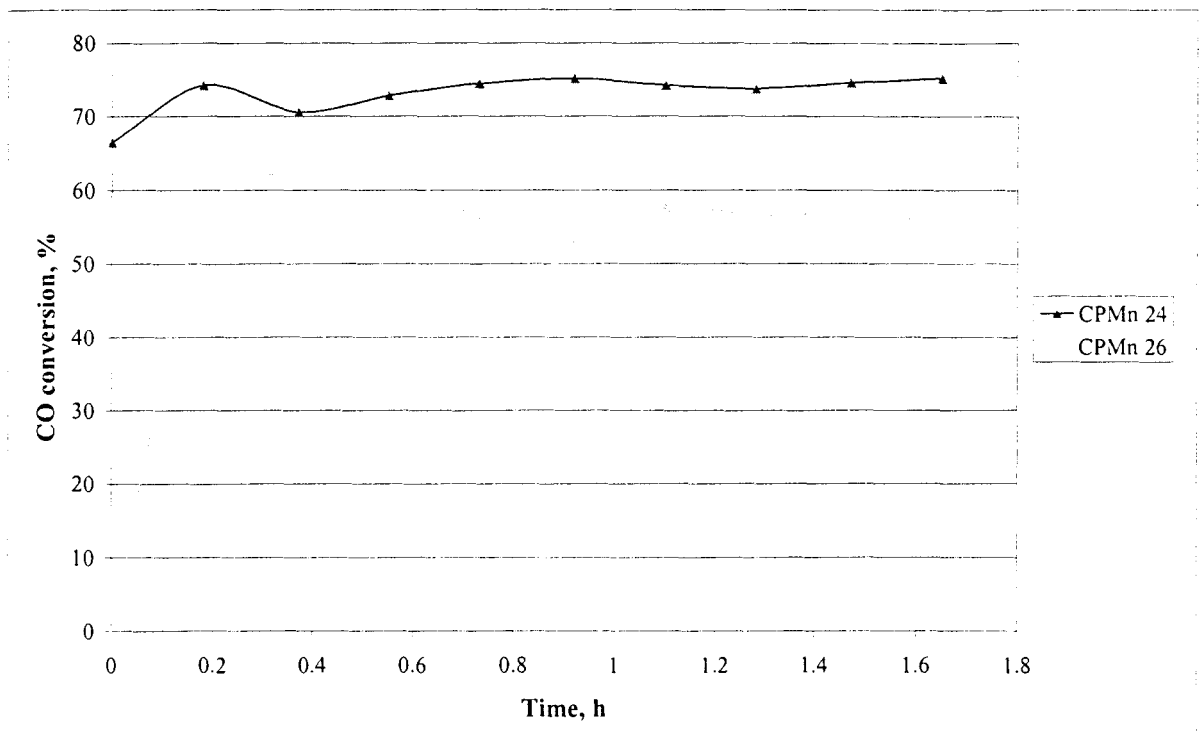


Figure 31. Comparison of activities of CPMn 24 and CPMn 26; 0.25 g catalyst, 400 ml/min; room temperature

CPMn 24 actually had an activity close to that of CPMn 25 (see Table 13). In order to determine whether 3 h ageing is definitely better than 10 minutes ageing, the recipe for CPMn 25 was repeated, but with 3 h ageing. The activity of this catalyst, CPMn 39, as compared to CPMn 25, is shown in Figure 32. As can be seen, the longer ageing time proved to be detrimental to the catalyst in this case. It is possible that the optimum ageing time differs, depending on the base concentration. However, not enough work has been done on ageing, so no conclusive results can be drawn from this.

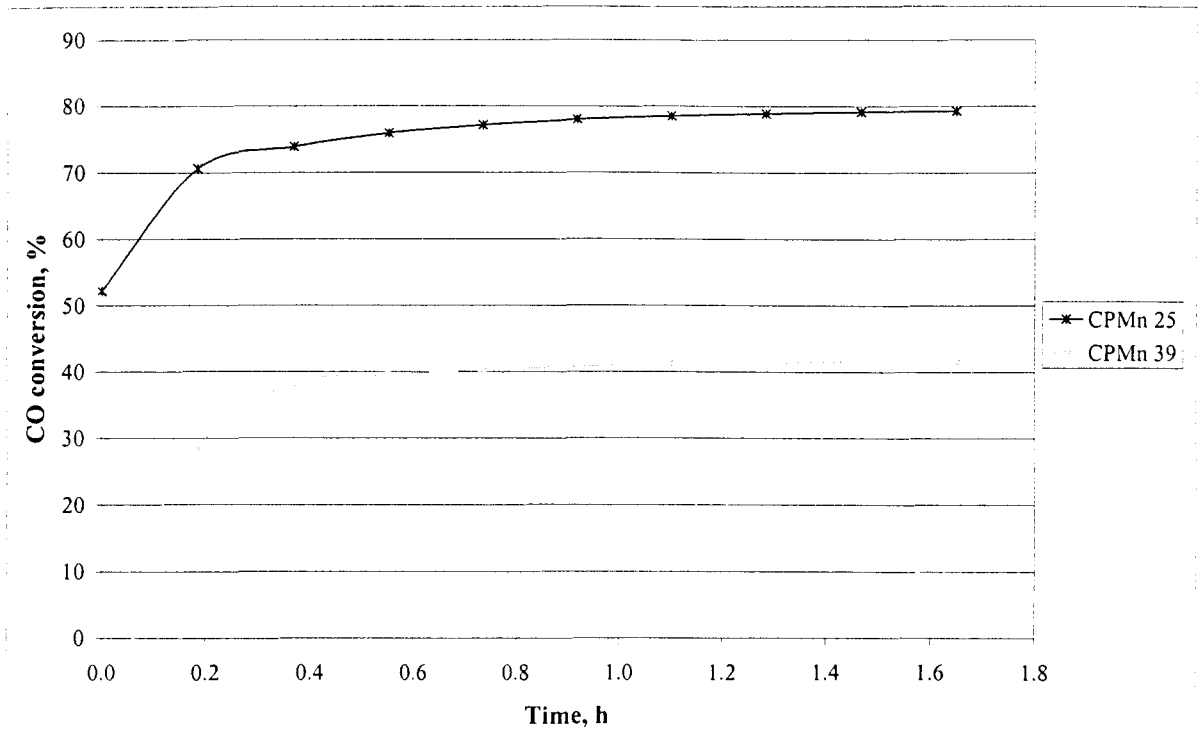


Figure 32. Comparison of activities of CPMn 25 and CPMn 39; 0.25 g catalyst, 400 ml/min; room temperature

For catalysts CPMn 30, 31 and 33, magnesium citrate was used. In a patent by Haruta *et al* [41], after co-precipitation with Na_2CO_3, a 6 g/l magnesium citrate solution was added to the slurry and stirred for an hour. They found that the catalysts made with magnesium citrate had lower CO conversion temperatures than those without.

It has been stated that in co-precipitation, there are 3 steps[22]:

a) supersaturation
b) nucleation (formation of small particles)
c) growth (agglomeration of the small particles)

To obtain small particles, a condition of high supersaturation is required. In this condition, the rate of nucleation is much higher than the rate of growth.

In order to obtain highly saturated metal solutions, both $Mn(NO_3)_2$ and/or $HAuCl_4$ solutions were dissolved in 50 ml and then boiled down to 20 ml (CPMn 30); or *only* $Mn(NO_3)_2$ was boiled down to 20 ml, and $HAuCl_4$ was added in thereafter (CPMn 31). In keeping with

supersaturation, 2 M Na_2CO_3 was used for precipitation. After precipitation, 200 ml of a 6 g/l magnesium citrate solution[41] was added in. The activities of CPMn 30 and CPMn 31 are shown in Figure 33.

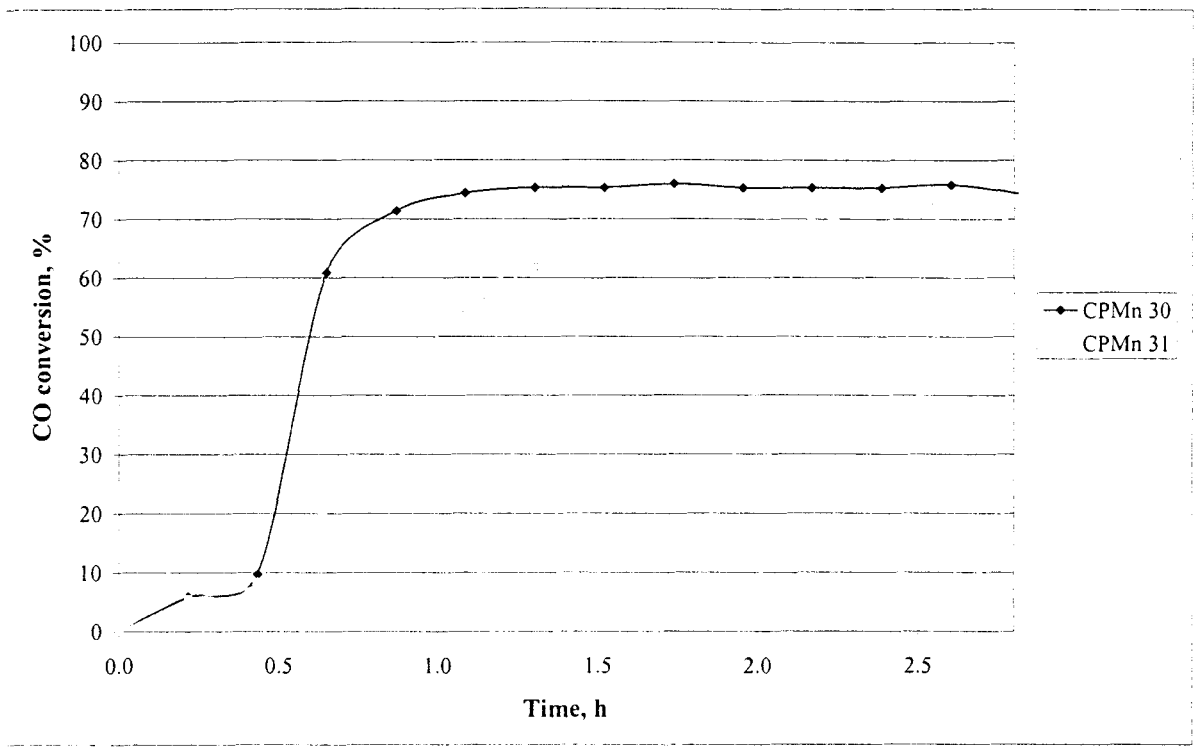


Figure 33. Comparison of activities of CPMn 30 and CPMn 31; 0.5 g catalyst, 60 ml/min; room temperature

Activities of CPMn 30 and CPMn 31 were not promising. Whether this was because of the addition of citrate or because of the metal solution/s being concentrated by boiling, was not certain. In an attempt to evaluate these factors, CPMn 33 and CPMn 34 were prepared.

To determine whether the addition of citrate had a negative effect on the activity, CPMn 33 was made. Exactly the same method as CPMn 24 was used, but 200 ml of a 6 g/l magnesium citrate solution was added in at the start of ageing. The activity of this catalyst is shown in Figure 34.

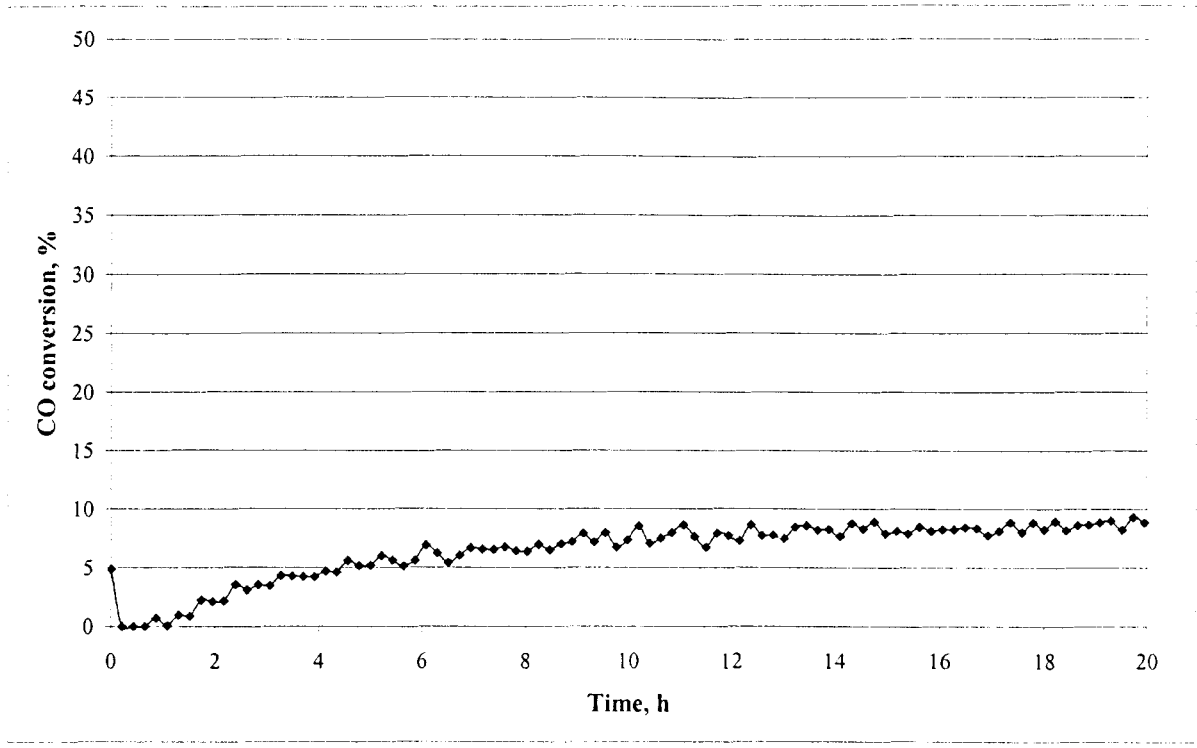


Figure 34. Activity of CPMn 33;
0.5 g catalyst, 60 ml/min; room temperature

As can be seen from the above graph, the addition of magnesium citrate definitely affects the performance of the catalyst. During the 3 h ageing, it was noticed that the pH went up from 7.3 (the pH went down from 10 to 7.3 immediately upon addition of magnesium citrate) to 11.3. It is possible that, had the ageing time been shorter, the activity would have been higher. However, it is doubtful that the catalyst would have had as high an activity as that of CPMn 24.

To determine the effect of using a more concentrated mixed metal salt solution on the performance of the Au/Mn_xO_y catalysts, CPMn 34 was prepared. However, instead of boiling the metal salt solution to a volume of 20 ml, the $Mn(NO_3)_2$ was dissolved in a very small volume of water, and along with the $HAuCl_4$, was made up to only 20 ml. The method of preparation used was the same as that of the most active catalyst, CPMn 25. The activity of CPMn 34 is shown in Figure 35.

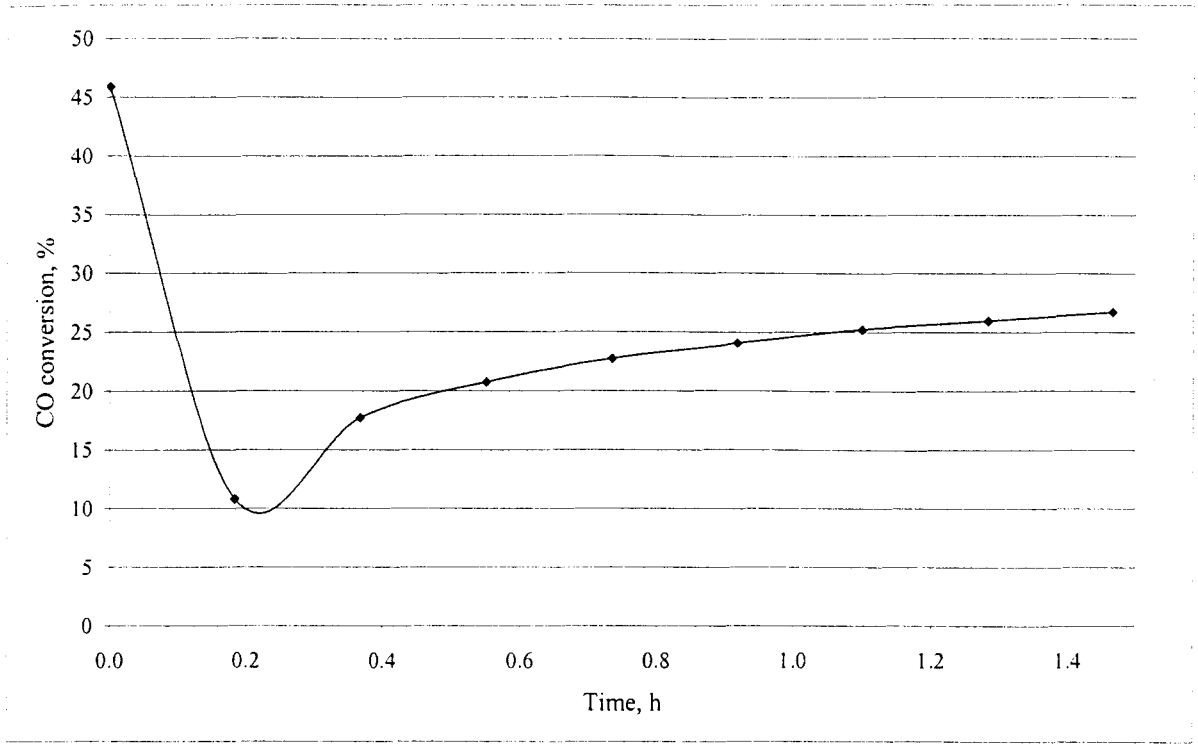


Figure 35. Activity of CPMn 34;
0.25 g catalyst, 60 ml/min; room temperature

So from these results (Figures 34 and 35) it can be seen that although a concentrated mixed metal salt solution is required, it also should not be too concentrated; and the use of magnesium citrate during the preparation of the catalyst, is also not beneficial to the catalyst activity.

It has been reported that Cl^- (originating from the $HAuCl_4$ precursor) poisons the active site of gold catalysts, therefore the catalysts should be washed thoroughly to remove residual Cl^- [7, 23]. Recently it has been reported that Cl^- also causes gold sintering in the catalysts[43, 44, 45]. The proposed structure [43], showing the cause of gold sintering during calcination of the catalyst, is illustrated in Figure 36 (a). Cl^- ions complex the gold species, forming Au-Cl-Au bridges. The Cl^- ions are then removed during calcination, resulting in gold sintering. The formation of large gold particles then leads to a decrease in catalytic activity. It has been claimed that washing of the catalyst with a solution of aqueous ammonia[43, 45] or magnesium citrate[44], to remove the Cl^- (Figure 36 (b)), resulted in catalysts with small gold particles.

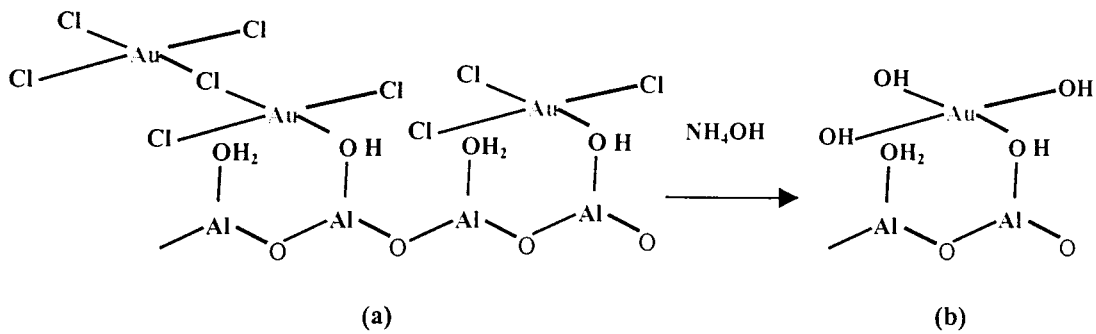


Figure 36. (a) Proposed structure, leading to sintering on a Au/Al_2O_3 catalyst; (b) Displacement of Cl^- by OH^-, so that the complexation shown in (a) does not occur [43]

It was found that treating catalysts with magnesium citrate after drying but *before* calcination, resulted in catalysts with smaller gold particles and higher activities[44]. A sample of dried, uncalcined CPMn 35, was suspended in 200 ml of a 1.25 g/l magnesium citrate solution and stirred for an hour. Thereafter, the catalyst was filtered, washed, dried and calcined at 400°C for 4 h.

The first co-precipitated Au/Mn_xO_y catalysts that were made (CPMn 1-5), were initially calcined at 200°C and later at 400°C. The latter was found to be the better calcination temperature. However, an intermediate temperature of 300°C was not tested. An uncalcined sample of CPMn 35 was therefore calcined at 300°C.

A comparison of the activity of CPMn 35, calcined at 300°C and 400°C, and after treatment with magnesium citrate, is shown in Figure 37.

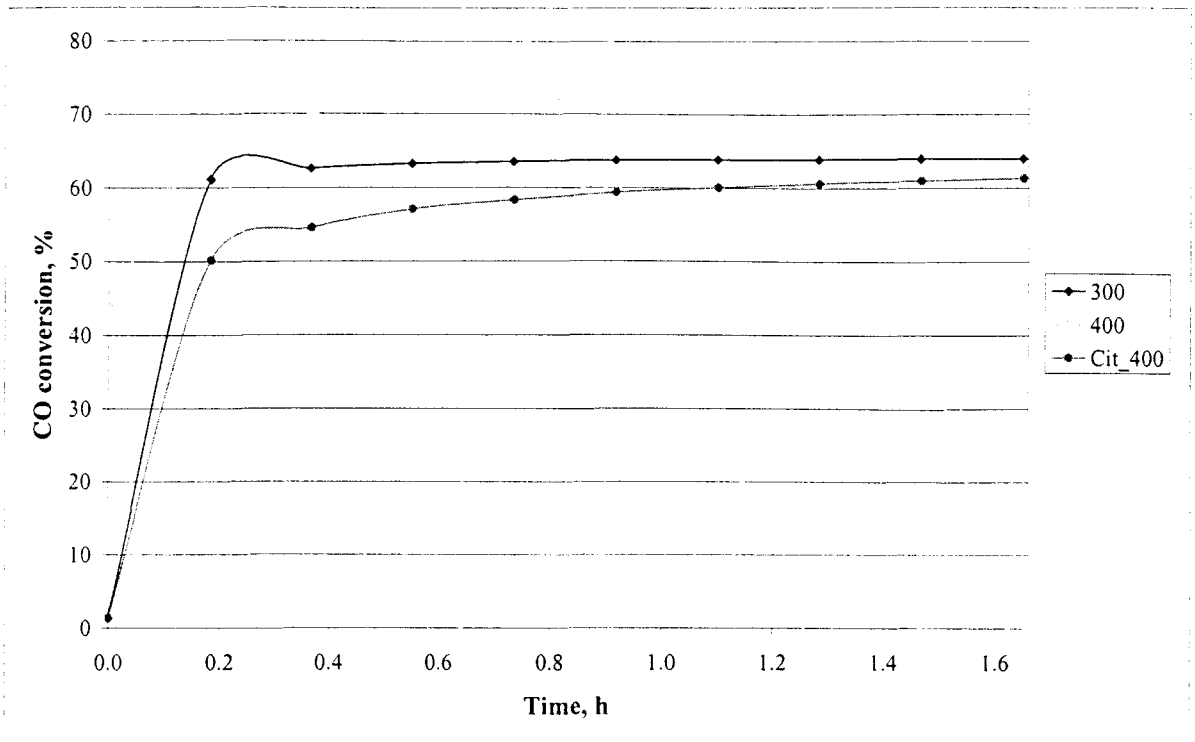


Figure 37. Effect of calcination temperature and citrate washing on the activity of CPMn 35; 0.25 g catalyst, 400 ml/min; room temperature

From these results, it is clear that treating the dried catalyst with magnesium citrate solution does not improve the activity but rather causes deterioration of the catalyst's activity. It was also found that calcining the catalyst at 300°C results in a lower activity than calcination at 400°C.

The effect of base concentration on activity has already been seen, with 200 ml of base of a certain concentration being used to precipitate the metal hydroxides. However, whether the activity was dependent on the Na_2CO_3 concentration or the actual Na_2CO_3 mass, had not been explored.

Thus CPMn 37 was made, using 100 ml of 2 M Na_2CO_3. This is equivalent in mass Na_2CO_3 to 200 ml of a 1 M Na_2CO_3 solution – which is the condition under which CPMn 25 is made. A comparison of the activities of CPMn 25, CPMn 36 (200 ml of 2 M Na_2CO_3) and CPMn 37, is depicted in Figure 38.

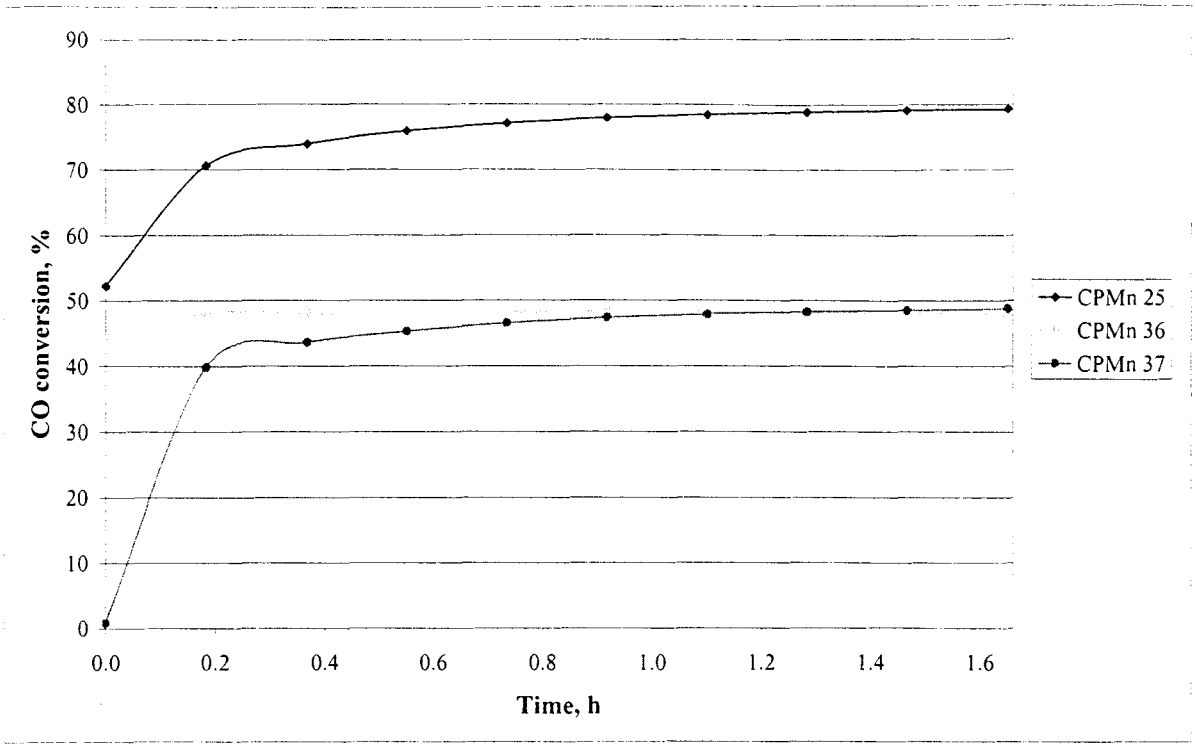


Figure 38. Comparison of activities of CPMn 25, CPMn 36 and CPMn 37; 0.25 g catalyst, 400 ml/min; room temperature

These results show that it is the Na_2CO_3 concentration, rather than the amount of Na_2CO_3 present, which affects the activity. CPMn 36 and CPMn 37, both made with 2 M Na_2CO_3, had very similar activities; whereas CPMn 25, made with 1 M Na_2CO_3, had a much higher activity.

Attempts to carry out XRD analysis with copper radiation, on the catalysts made using Method 3, were very unsuccessful. The catalysts were very amorphous so no clear deductions could be made from the results obtained. It has been reported that the precipitation of supersaturated solutions lead to numerous small particles, resulting in the possibility of amorphous precipitates being achieved[22]. Catalysts made using Method 3 were found to have very small metal oxide particles - in fact - much smaller than those catalysts made using Methods 1 and 2.

The secondary electron images of CPMn 5, CPMn5_rpt (Method 1), CPMn 10 (Method 2) and CPMn 24 (Method 3), are shown in Figures 39-42.

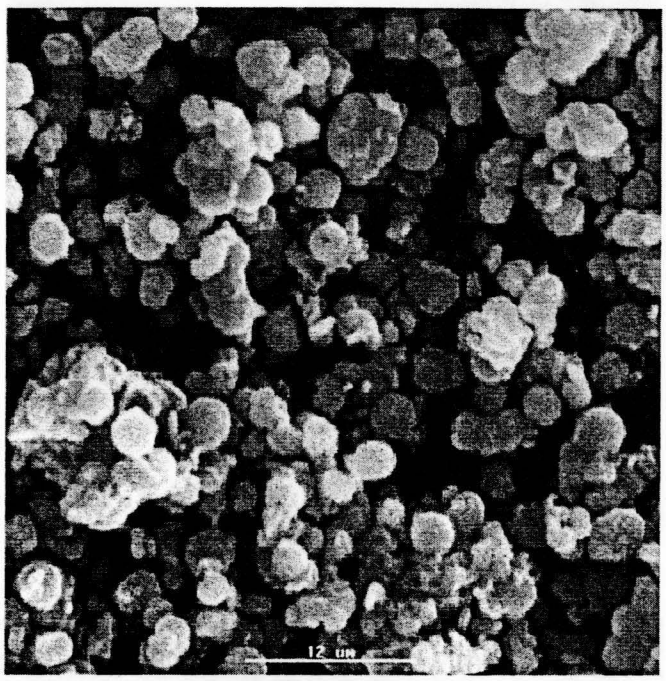


Figure 39. Secondary electron image of CPMn 5, 2000 X magnification

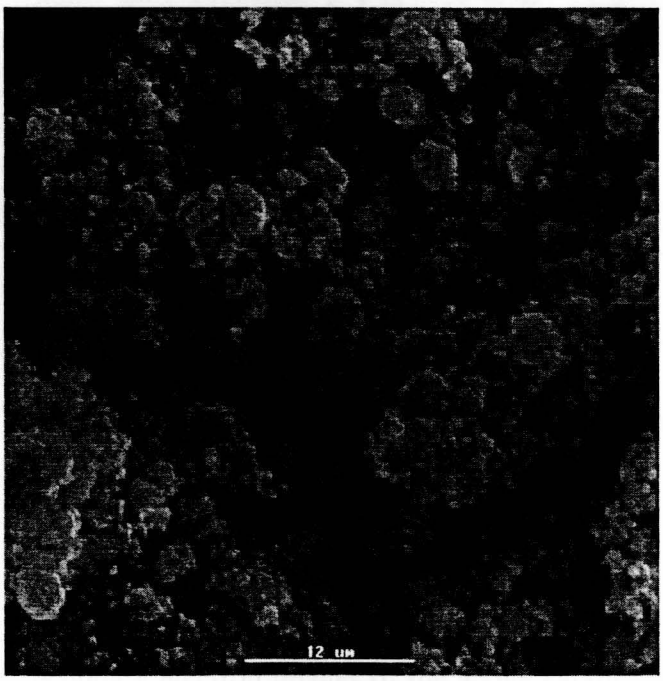


Figure 40. Secondary electron image of CPMn 5 (repeat), 2000 X magnification

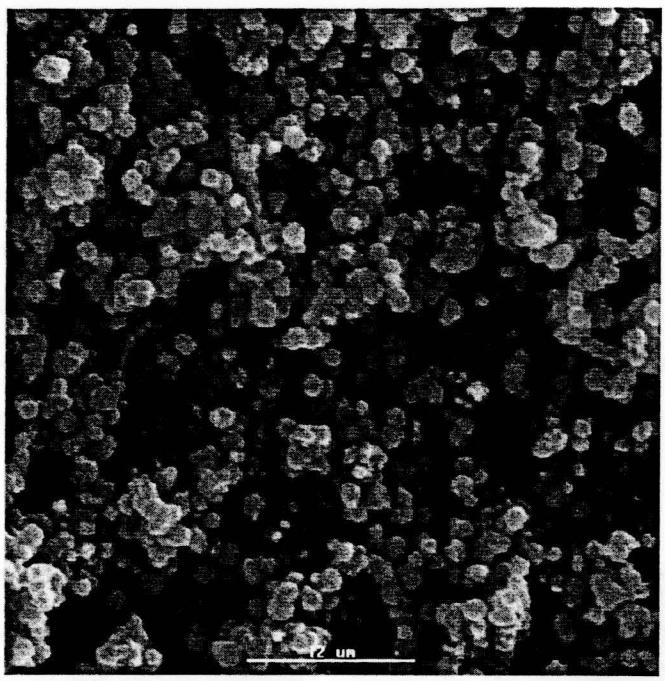


Figure 41. Secondary electron image of CPMn 10, 2000 X magnification

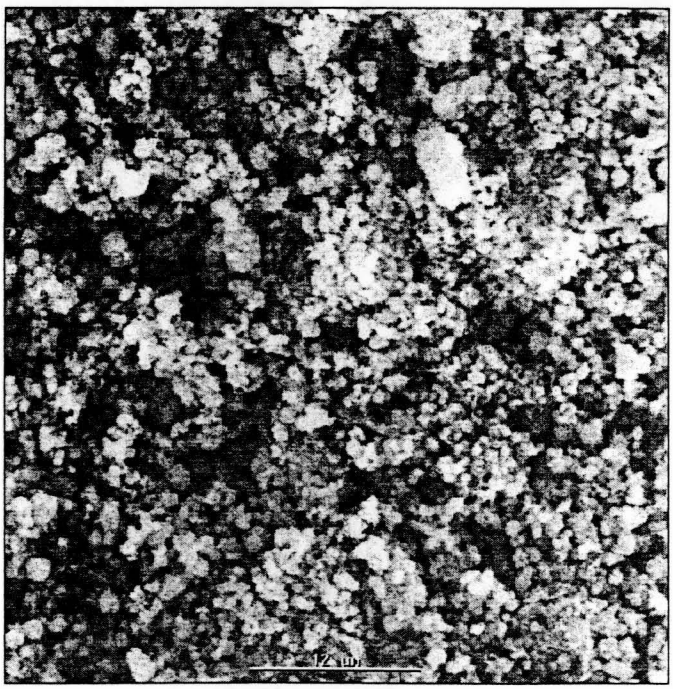
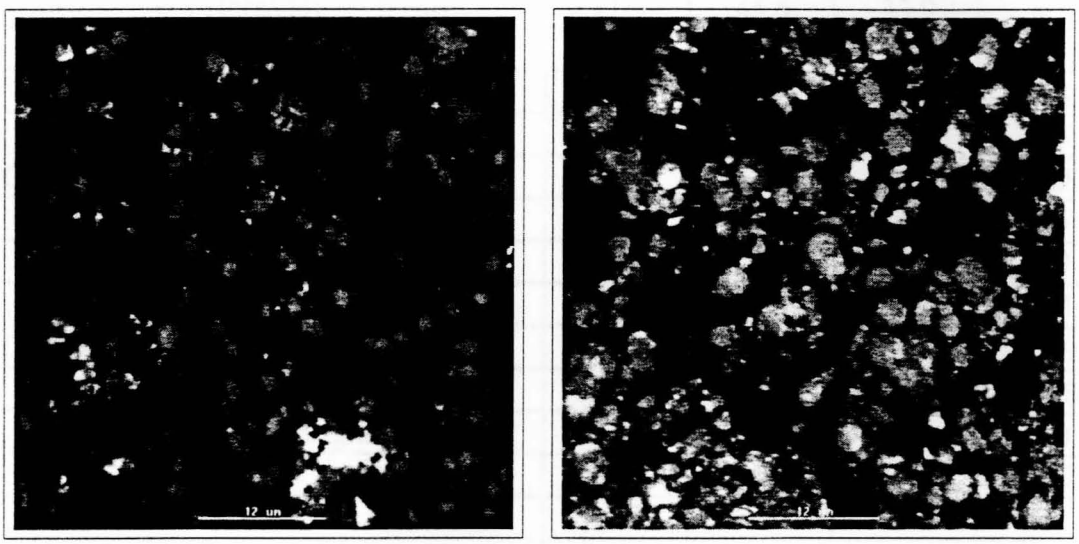


Figure 42. Secondary electron image of CPMn 24, 2000 X magnification

The influence of the concentration and addition rate of the mixed metal salt solution could clearly be seen on the secondary electron images of the above catalysts. CPMn 5 and CPMn 5_rpt, made by means of a dilute mixed metal salt solution (200 ml) added into the base over

a time period of 34 minutes, had large metal oxide particles. The activity difference between the two can be explained by CPMn 5 having a more ordered arrangement of particles, whereas CPMn 5_rpt consists of large disordered clusters, with variations in particle size. The backscattered scanning electron images of CPMn 5 and CPMn 5_rpt (Figure 43), showed the presence of gold clusters on both, but many more on CPMn 5_rpt. CPMn 10, made by the addition of a more concentrated mixed metal salt solution into the base over a period of just under 9 minutes, had a more ordered arrangement- and also consisted of smaller support particles- than CPMn 5 and CPMn 5_rpt.



a **b**

Figure 43. Backscattered electron images of (a) CPMn 5 and (b) CPMn 5_rpt

From a comparison of Figures 39-42, it is apparent that the instantaneous addition of a small volume of mixed metal salt solution into the base yields smaller precipitates. These conditions obviously favour nucleation over crystal growth.

Due to the problems experienced with X-ray diffraction analysis using copper radiation, it was attempted to determine the manganese valency and Mn_xO_y species by means of HRSEM with attached EDS. A few catalysts were selected and various sites on each catalyst were analysed by EDS. The compositions and descriptions of the chosen sites for these catalysts are shown in Table 16. These HRSEM images, with the marked sites, are shown in Appendix C.

Table 16. Compositions of selected Au/Mn_xO_y catalysts as determined by HRSEM- EDS

Catalyst		wt % C	wt % O	wt % Mn	wt % Au
CPMn 10	1 (large bright cluster)	3.2	28.1	39.9	28.8
	2 (large bright cluster)	4.5	31.2	40.9	23.4
	3 (oxide)	9.8	46.5	39.1	4.6
CPMn 24	A 1 (v. small bright spot)	9.7	20.6	12.3	4.9
	2 (small bright spot)	12.2	22.4	10.0	16.6
	3 (oxide)	14.1	38.4	21.4	0.0
	B 1 (large bright spot)	10.6	40.1	34.2	15.2
	2 (large bright spot)	10.4	40.6	36.1	12.9
	3 (small bright spot)	9.6	38.6	21.7	30.1
	4 (small bright spot)	10.7	40.7	22.5	26.1
	C 1 (threads)	11.3	45.5	33.9	9.3
	2 (small bright spot)	9.9	41.6	28.1	20.4
	3 (threads)	8.1	39.6	47.0	5.4
	4 (threads)	12.2	43.4	35.4	9.0
CPMn 27	1 (large bright spot)	7.9	33.7	27.8	21.8
	2 (large bright spot)	7.3	37.6	35.3	7.5
	3 (oxide)	11.0	40.9	30.1	0.0
	4 (oxide)	7.6	37.4	38.7	1.7
CPMn 27u	1 (large bright cluster)	12.5	46.1	28.5	12.9
	2 (small bright spot)	10.3	40.7	38.2	10.8
	3 (small bright spot)	13.1	46.4	32.5	8.0
	4 (part of 1's cluster)	12.7	44.1	32.0	11.2
	5 (oxide)	17.4	54.6	28.0	0.0
CPMn 28	1 (large bright spot)	11.2	46.1	28.5	20.0
	2 (small bright spot)	10.1	40.7	38.2	22.2
	3 (oxide)	13.1	46.4	32.5	0.0
	4 (small bright spot)	0.0	44.1	32.0	35.9

Carbon was seen to be present in practically all the sites – pointing to the possibility of $MnCO_3$ being present. All the bright spots/clusters were seen to have large concentrations of gold. The 'oxide' sites (darker areas of the images) either did not have any gold present, or had much smaller concentrations than were found on the brighter areas. These results were not unexpected. A surprising observation was made on CPMn 24, however, of very fine, bright 'threads' running along the surface of the catalyst. When these threads were analysed by EDS, gold of < 10 wt % concentration, was found. A HRSEM image (at 10 000 X magnification) of CPMn 24 with bright 'threads' is shown in Figure 44.



Figure 44. HRSEM image of CPMn 24 (secondary/backscattered combination)

From the manganese and oxygen compositions listed in Table 16, the Mn/O ratios were calculated for each site in an attempt to determine the manganese species and hence the manganese valency for each site. The Mn/O ratios for the possible manganese compounds are listed in Table 17, and the calculated Mn/O ratios for each site are listed in Table 18.

Table 17. Calculated Mn/O ratios for possible manganese compounds

Compound	mols Mn	mols O	Mn/O
MnO	1	1	1.00
MnO_2	1	2	0.50
Mn_2O_3	2	3	0.67
Mn_3O_4	3	4	0.75
$MnCO_3$	1	3	0.33

Table 18. Mn/O ratios on analysed sites of CPMn 10, 24, 27 and 28

Catalyst		wt % Mn	wt % O	mols Mn	mols O	Mn/O
CPMn 10	1 (large bright cluster)	39.9	28.1	0.73	1.76	0.41
	2 (large bright cluster)	40.9	31.2	0.75	1.95	0.38
	3 (oxide)	39.1	46.5	0.71	2.90	0.25
CPMn 24	A 1 (v. small bright spot)	12.3	20.6	0.22	1.29	0.17
	2 (small bright spot)	10.0	22.4	0.18	1.40	0.13
	3 (oxide)	21.4	38.4	0.39	2.40	0.16
	B 1 (large bright spot)	34.2	40.1	0.62	2.51	0.25
	2 (large bright spot)	36.1	40.6	0.66	2.54	0.26
	3 (small bright spot)	21.7	38.6	0.39	2.41	0.16
	4 (small bright spot)	22.5	40.7	0.41	2.54	0.16
	C 1 (threads)	33.9	45.5	0.62	2.84	0.22
	2 (small bright spot)	28.1	41.6	0.51	2.60	0.20
	3 (threads)	47.0	39.6	0.86	2.47	0.35
	4 (threads)	35.4	43.4	0.64	2.71	0.24
CPMn 27	1 (large bright spot)	27.8	33.7	0.51	2.11	0.24
	2 (large bright spot)	35.3	37.6	0.64	2.35	0.27
	3 (oxide)	30.1	40.9	0.55	2.56	0.21
	4 (oxide)	38.7	37.4	0.70	2.34	0.30
CPMn 27u	1 (large bright cluster)	28.5	46.1	0.52	2.88	0.18
	2 (small bright spot)	38.2	40.7	0.70	2.55	0.27
	3 (small bright spot)	32.5	46.4	0.59	2.90	0.20
	4 (part of 1's cluster)	32.0	44.1	0.58	2.76	0.21
	5 (oxide)	28.0	54.6	0.51	3.42	0.15
CPMn 28	1 (large bright spot)	28.5	46.1	0.52	2.88	0.18
	2 (small bright spot)	38.2	40.7	0.70	2.55	0.27
	3 (oxide)	32.5	46.4	0.59	2.90	0.20
	4 (small bright spot)	32.0	44.1	0.58	2.76	0.21

The Mn/O ratios in most instances, were much lower than the ratios for any of the expected compounds. Except for a few values which indicated $MnCO_3$, and one value of 0.41 which indicated possibly MnO_2 and/or $MnCO_3$, none of the other values could be attributed to any of the possibilities. Since $MnCO_3$ was reported to have undergone conversion to Mn_3O_4, MnO and Mn_2O_3 after CO oxidation tests[16], a used sample of CPMn 27 was also included in the HRSEM analysis. However, the Mn/O ratios of this sample, CPMn 27u, were also very low, so there was no indication from these ratios that these oxides existed.

It was then attempted to analyse the catalysts by XRD again, but this time, using molybdenum radiation. The X-ray diffraction pattern obtained had better resolution than that using copper radiation.

The XRD patterns of CPMn 24 before and after activity tests, were compared to see if there was any difference in composition (Figure 45). However, there was no difference in XRD patterns for the fresh and used catalyst. $MnCO_3$ was present in both, along with MnO_2, Mn_2O_3, Mn_3O_4 and MnO. Multiple Mn_xO_y species were also seen on co-precipitated Au/Mn_xO_y catalysts, characterised by AES (Auger electron spectroscopy), XPS (X-ray photoelectron spectroscopy) and ISS (ion scattering spectroscopy)[6].

XRD studies on $Ag\text{-}Mn_2O_3$ co-precipitated catalysts showed that as the silver content was increased, there was more intimate mixing of silver and Mn_2O_3, resulting in the XRD peaks became broader and more unresolved[1]. Assuming that the same applies to Au/Mn_xO_y catalysts, it was decided to make a Au/Mn_xO_y catalyst with a 1 % gold loading, to see if a sharper diffraction pattern could be obtained. A comparison of this catalyst (CPMn 38) with CPMn 24, is shown in Figure 46. No difference in morphology was seen on these catalysts, and CPMn 38 was only slightly more crystalline than CPMn 24.

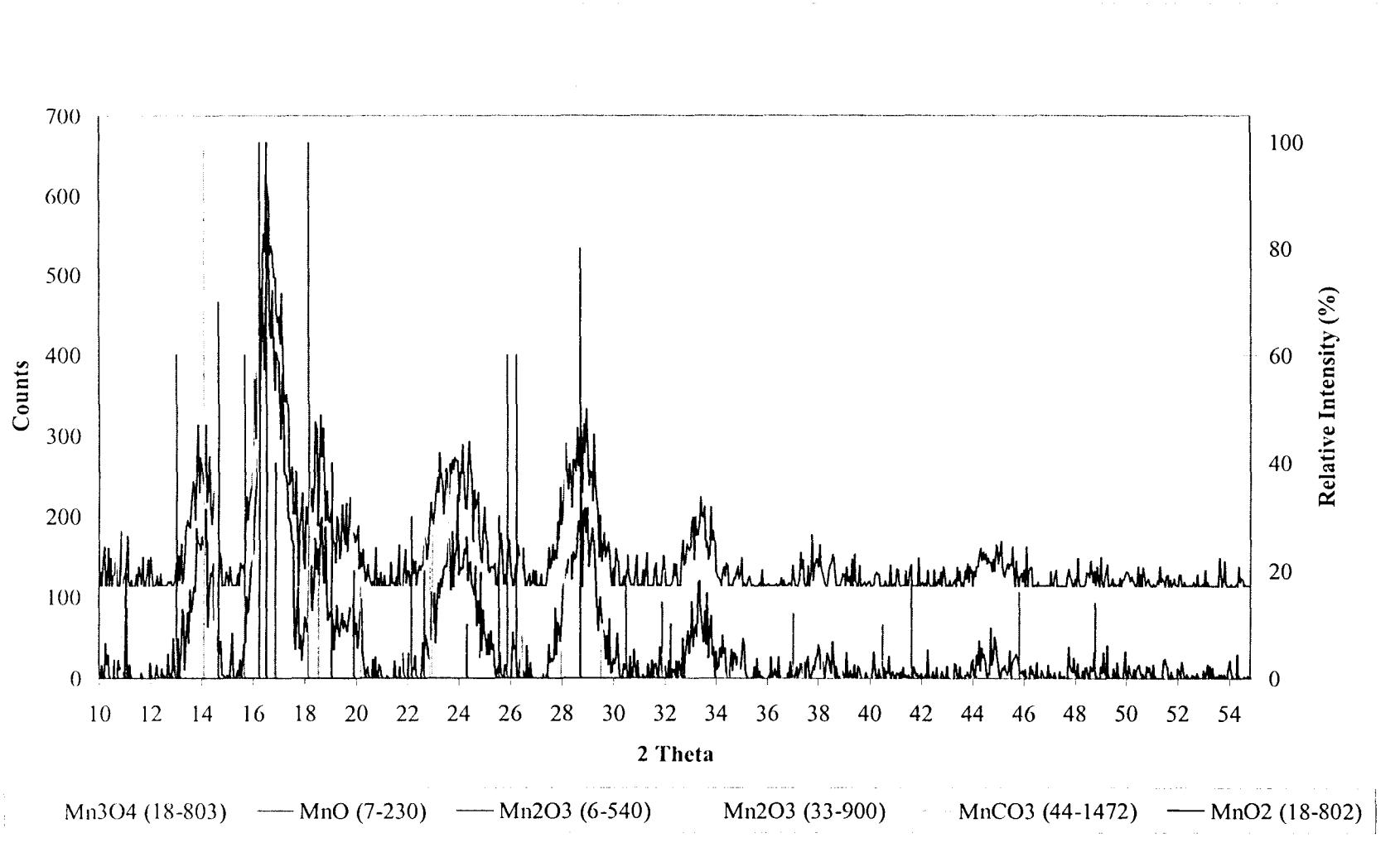


Figure 45. XRD spectra of CPMn 24 (bottom trace) and CPMn 24_ used (top trace)

(Background correction, Kα2 lines stripped, CPMn 24_used spectrum offset)

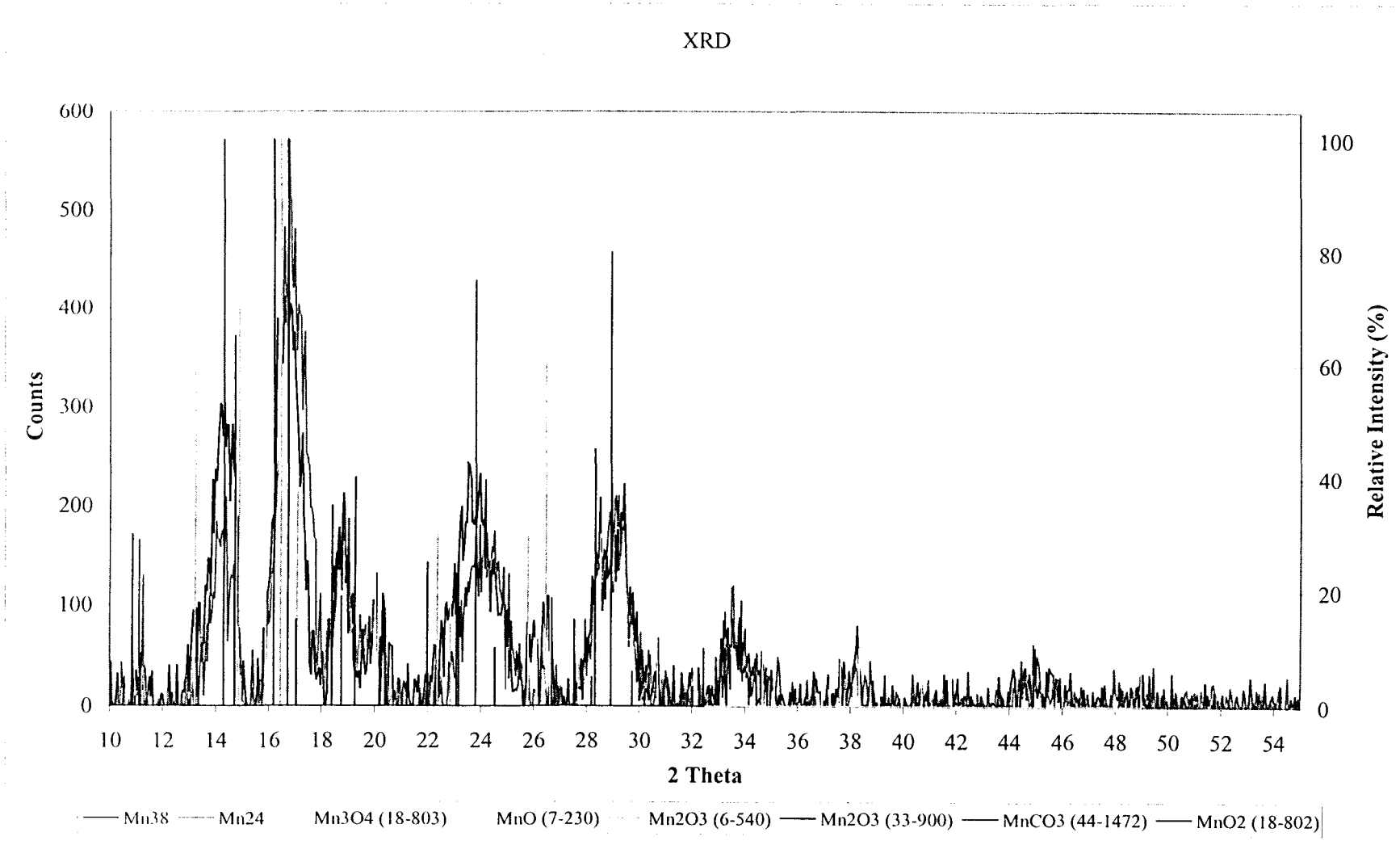


Figure 46. XRD spectra of CPMn 24 and CPMn 38

(Background correction, Kα lines stripped)

The CPMn- catalysts were studied under high resolution SEM in order to determine the gold particle sizes of the catalysts, as well as to take a closer look at the morphology of the catalysts. Some interesting images were seen during the course of the HRSEM investigation.

CPMn 10, made using Method 1, had many gold clusters in the range of 20-50 nm. It has been reported in literature that the Au/Mn_xO_y co-precipitated catalyst consisted of densely packed and loosely coagulated manganese compounds, and gold particles were more prominent on the latter[16]. As can be seen in Figure 47, the same phenomenon was observed on CPMn 10, where gold seemed to be more localised on the smaller, more 'feathery' fractions of the support. The larger support particles, which the gold tended not to sit on so much, appeared to have a more uniform shape than the smaller particles.

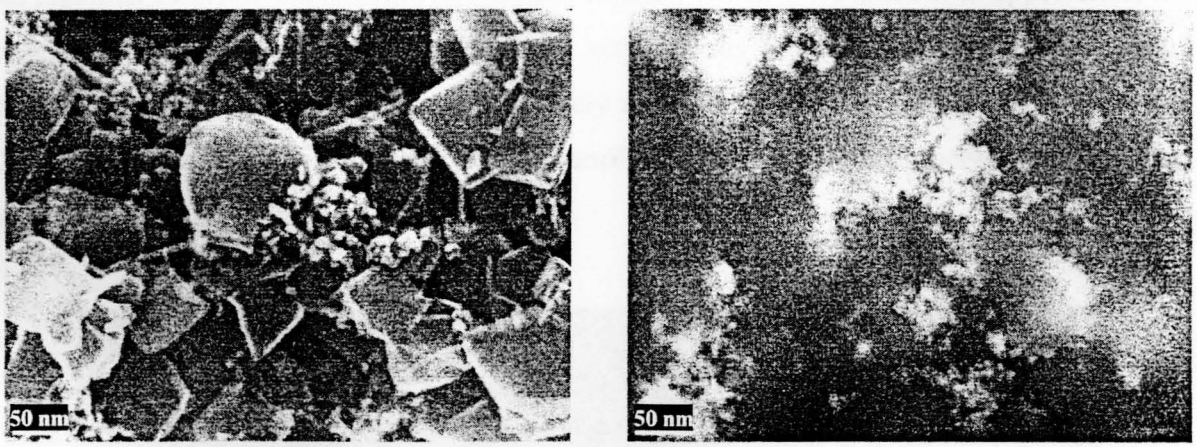
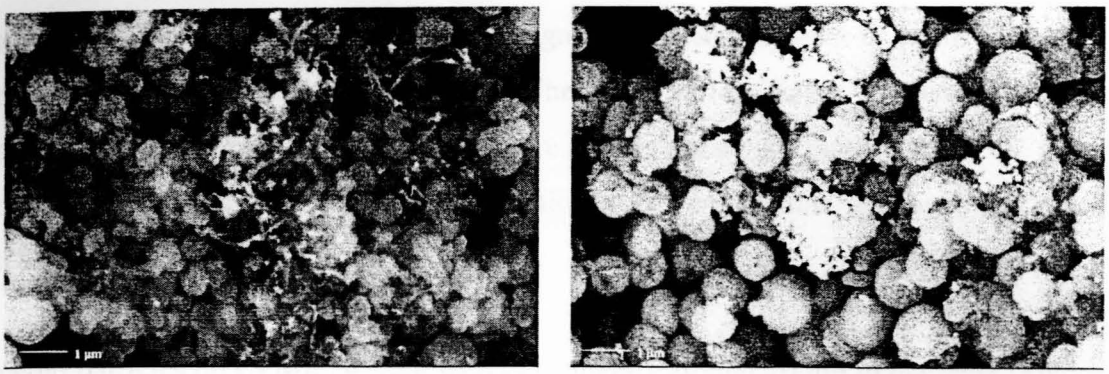


Figure 47. Secondary electron image and backscattered electron image of CPMn 10

The same observation of the gold sitting on the small, feathery particles, was made on CPMn 27 (made using Li_2CO_3 and Method 3). This is very different to the morphology of CPMn 24, made with Na_2CO_3, where the gold tends to run more in 'threads' along the support, and there is just the occasional gold cluster (shown in Figure 44). The support particle sizes of CPMn 27 and CPMn 24 - although made using the same preparation method – differed significantly, with the particles of CPMn 24 being smaller than CPMn 27. There were definitely also larger clusters of gold on CPMn 27. A comparison of the HRSEM images of CPMn 24 and CPMn 27 at 10 000 X magnification, is shown in Figure 48.



a b

Figure 48. HRSEM images of (a) CPMn 24 and (b) CPMn 27 (secondary/backscattered combination)

A startling observation was made upon increasing the magnification on CPMn 27. Unlike all the previous catalysts made with Na_2CO_3 and Li_2CO_3, which were smooth in appearance, the larger support particles on CPMn 27, were very fibrous in appearance (Figure 49). This unusual appearance, which was most definitely not seen on catalysts such as CPMn 5 and CPMn 10 (Method 1; Li_2CO_3), can only be attributed to the difference between preparation methods.

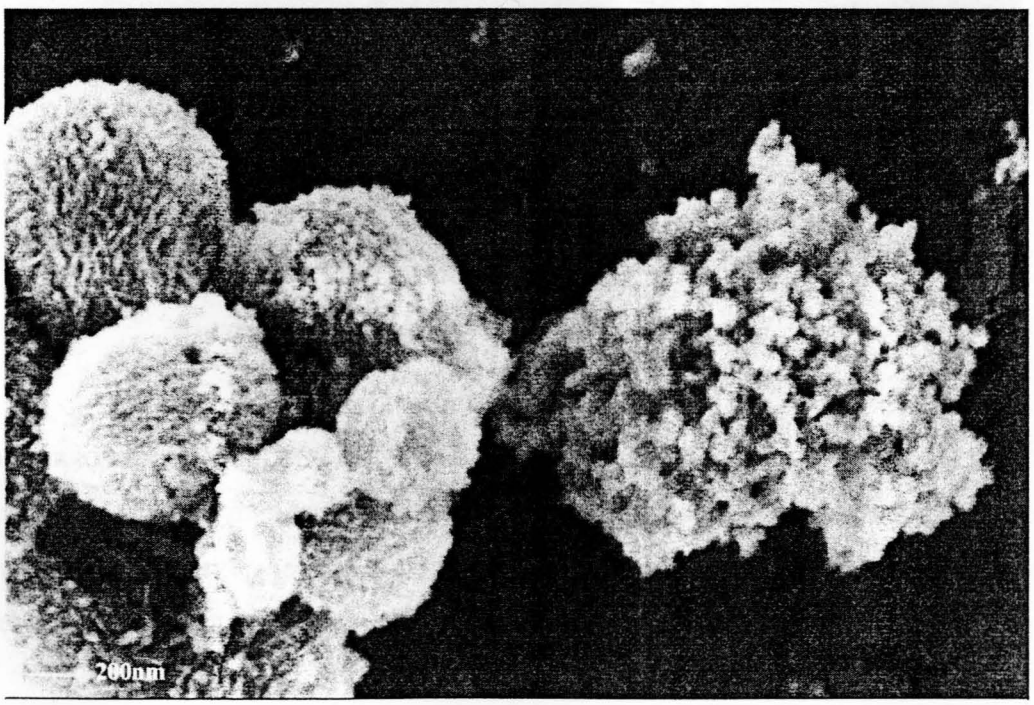


Figure 49. Secondary electron image of CPMn 27

The more 'feathery' particles upon higher magnification, did not look as feathery anymore. In fact, they appeared to be quite structured. The Mn/O ratios (Table 18) were compared for these 2 different types of support structure to determine if there was a difference in composition between them. However, the ratios were very similar, and were too low to be matched to the possibilities.

The gold particles on CPMn 24 were seen to be mainly around 20 nm in diameter (Figure 50). There were also particles as small as 7 nm and as large as 40 nm. The particles tend to cluster in rows, and these are probably the 'threads' that were seen at lower magnification.

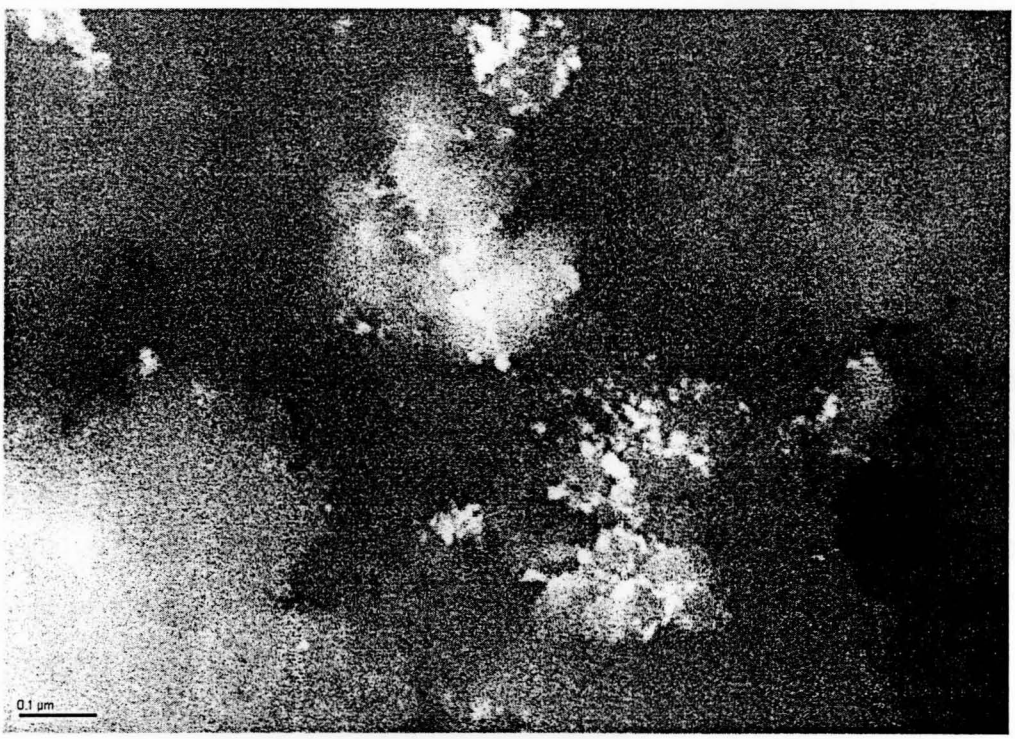


Figure 50. Backscattered electron image of CPMn 24

Although many large gold particles were found on CPMn 24, the high activity of this catalyst is probably due to the manganese oxide support being an active support. It will therefore compensate for the larger gold particles in activity[20]. There may also be even smaller gold particles present, which cannot be seen or measured at this magnification.

6.1.3. Comparison of CPMn- catalysts with those of Hoflund *et al.*[5]

Hoflund *et al.*[5] stated that co-precipitated Au/Mn_xO_y catalysts made with Li_2CO_3 performed better than those made with Na_2CO_3. However, for Method 3 (the best preparation method), the best-performing catalysts made with Na_2CO_3 had significantly higher activities than the catalyst made with Li_2CO_3 and Method 3. Although their preparation method was not outlined in that paper[5], it has been stated in a paper in which Hoflund was a co-author[6], that the mixed metal solutions were added dropwise into the base. Assuming that this was the preparation method used when the different bases were compared, it then corroborates the results found using Method 1 (dropwise addition) - where CPMn 5 (made with Li_2CO_3) performed better than CPMn 2 (made with Na_2CO_3) - although CPMn 5 was not reproducible.

Activities of the Au/Mn_xO_y catalysts made in this study could not be compared with those of Hoflund *et al.*[5], by the usual means of calculating the μmol CO/g Au/s, since they did not provide the actual gold loadings on their catalysts. Rather, their reported percent gold loadings were based on the molar ratio of gold to manganese in the precursor solution. Using this basis (i.e. molar ratio of gold to manganese in precursor solution), the activities of catalysts prepared in this study, were compared to those of Hoflund *et al.* (Table 19). The comparison of these catalysts is not very accurate, since there are differences in the testing conditions which would impact on the activity. The Hoflund catalysts were tested at 55°, while the CPMn- catalysts were tested at room temperature (19-22°C). Also, while the CPMn- catalysts were tested in 1% CO in air, the Hoflund catalysts were tested in a 1% CO /0.5 % O_2 in helium mixture.

Table 19. Comparison of CPMn- catalysts with co-precipitated catalysts of Hoflund et al.[5]

Catalyst	% Au (Au/Mn in precursor soln)	Activity test					Calculated
		% CO in gas mix.	Catalyst mass, *g*	Gas flowrate, *ml/min*	Space velocity, $ml/g_{cat}/h$	CO conversion, %	μmol CO/g Au/s
CPMn 5	1.46	1	0.50	60	7200	87	53.2
CPMn 24	1.46	1	0.25	400	96000	75	611
CPMn 25	1.46	1	0.25	400	96000	79	644
Hoflund_2%	2	1	0.05	10	12000	72	53.6
Hoflund_5%	5	1	0.05	10	12000	80	23.8
Hoflund_10%	10	1	0.05	10	12000	88	13.1
Hoflund_15%	15	1	0.05	10	12000	60	5.95

Hoflund *et al.* claimed that that the 10 % catalyst performed the best, since it had the highest CO conversion. However, taking the gold loading into account, it can be seen (Table 19) that the 2 % catalyst actually performed the best, and any further increase in the amount of gold in the precursor solution, resulted in lower activities.

The CPMn- catalysts contained 1.46 % Au in the precursor solution. CPMn 24 and CPMn 25 were far more active than the catalysts made by Hoflund *et al.* This can be attributed to Method 3 (instantaneous precipitation). The activity of CPMn 5, made by means of dropwise addition, ties in well with that of the 2 % Hoflund catalyst. Because of the differences in testing conditions, a more accurate assessment could not be made. Having more oxygen in the test-gas would have favoured greater CO conversion for the CPMn- catalysts. However, the CPMn-catalysts were also tested at much lower temperatures than the Hoflund catalysts, and still proved to be more active. The surface area of the best-performing catalyst (CPMn 25) was double that of the catalysts made by Hoflund *et al.* (reported to be around 60 m^2/g).

6.2. Hopcalite

6.2.1. Experimental

As with the CPMn- catalysts, 3 different preparation methods were attempted.

6.2.1.1. Method 1 – co-precipitation (CPHop 1-2)

The required volume of base was added into the reaction vessel and heated to 25°C. $Mn(NO_3)_2.xH_2O$, $Cu(NO_3)_2.3H_2O$ and $HAuCl_4$ were mixed together and made up to 50 ml. This mixed metal solution was then pumped into the base at a flowrate of 5.9 ml/min. For CPHop 1, because of the low solubility of Li_2CO_3, additional base was pumped in to keep the pH at 9.

The suspension was stirred for 15 minutes to allow for any further precipitation. Thereafter, it was filtered, washed, dried at 80°C and subsequently calcined at 400°C.

6.2.1.2. Method 2 – inverse co-precipitation (CPHop 4)

$Mn(NO_3)_2.xH_2O$, $Cu(NO_3)_2.3H_2O$ and $HAuCl_4$ were mixed together and diluted to 100 ml. The mixed metal salt solution was then poured into the reaction vessel and the temperature was taken up to 70°C. 0.5 M Na_2CO_3 was then pumped in to precipitate the metal hydroxides. The end pH was set at 8.9. After the target pH was reached, the catalyst was aged overnight. Thereafter, the precipitate was filtered, washed and dried at 80°C. The catalyst was calcined at 400°C.

6.2.1.3. Method 3 – co-precipitation (CPHop 3)

200 ml of base was added to the reaction vessel and heated to 25°C. $HAuCl_4$, $Mn(NO_3)_2.xH_2O$ and $Cu(NO_3)_2.3H_2O$ were mixed together, and the solution was made up to 50 ml. The mixed metal salt solution was then poured into the base in one aliquot. The suspension was stirred for 3 hr, then filtered, washed and subsequently dried at 80°C. The catalyst was calcined at 400°C.

The experimental conditions of CPHop 1 – CPHop 4 are set out in Table 20.

Table 20. Experimental conditions of CPHop 1-4

Catalyst	$HAuCl_4$		Metal salts		Total volume	Temp,	Ageing	End pH	Base	Base	
	Conc, *g/l*	Vol, *ml*	Mn nitrate mass, *g*	Cu nitrate mass, g	($HAuCl_4$ + metal salts), *ml*	^{o}C	time, *min*		used	Conc, *M*	Volume (initial), *ml*
CPHop 1	10	15	10.5	4.42	50	25	15	9.0	Li_2CO_3	saturated	400
CPHop 2	10	15	10.5	4.42	50	25	15	9.3	Na_2CO_3	1.0	200
CPHop 3	10	15	10.5	4.42	50	25	180	10.0	Na_2CO_3	1.0	200
CPHop 4	50	3	10.5	4.42	100	70	780	9.0	Na_2CO_3	0.5	N/A

6.2.2. Results and discussion

The analysed gold loadings on the Au/hopcalite catalysts, are tabulated in Table 21.

Table 21. Gold loadings on co-precipitated Au/hopcalite catalysts

Catalyst	wt % Au
CPHop 1	2.2
CPHop 2	2.3
CPHop 3	2.3
CPHop 4	2.2

The optimum Cu/Mn molar ratio for hopcalite catalysts was found to be 0.5[11]. So the copper and manganese nitrates were mixed together in the starting solution in the same ratio. In order to ascertain whether copper and manganese had precipitated out in the same ratios, the Au/hopcalite catalysts were also analysed for copper and manganese. The analysed copper and manganese concentrations and calculated Cu/Mn ratios for CPHop 1-4 (Table 22), showed a good correlation between the Cu/Mn ratios in the starting solution and final product.

Table 22. Cu/Mn molar ratios for co-precipitated Au/hopcalite catalysts

Catalyst	wt % Cu	wt % Mn	Cu/Mn (molar ratio)
CPHop 1	23.3	35.5	0.57
CPHop 2	23.4	36.9	0.55
CPHop 3	22.5	36.5	0.53
CPHop 4	20.7	35.4	0.50

Li_2CO_3 was used in the making of CPHop 1 and Na_2CO_3 was used for CPHop 2-4. As with the CPMn- catalysts made using Li_2CO_3 as a base, excess Li_2CO_3 had to be added in. With CPHop 1 and CPHop 2, the mixed metal salt solution was pumped into the base at a flowrate

of 5.9 ml/min. CPHop 3 was made by adding the mixed metal salt solution in instantaneously – the same method as CPMn 24 was used.

With CPHop 4, the optimised conditions reported by Hutchings *et al.*[11, 46] for co-precipitated hopcalite catalysts were used for making this Au/hopcalite catalyst. So inverse co-precipitation, with an end pH of 8.9 was employed. The optimum ageing time was reported to be 12 h[11]. However, only ageing times of 0-12 h and 24 h were tested. Since no ageing times between 12 h and 24 h were examined, it cannot be known for certain that 12 h was the optimum ageing time. So a strict ageing time of 12 h was not kept. Rather, CPHop 4 was left to age overnight, which turned out to be 13 h ageing. The optimum calcination conditions were reported to be 500°C for 17 h. It was felt that these conditions would be too extreme for Au/hopcalite catalysts. Therefore the calcination conditions were kept at 400°C for 4 h, as with the CPMn- catalysts.

The activities of the CPHop catalysts are shown below in Table 23 and Figure 51.

Table 23. Calculated μmol CO/g Au/s for co-precipitated Au/hopcalite catalysts (CPHop 1-4, calcined at 400°C,)

Catalyst	μmol CO/g Au/s
CPHop 1	7.3
CPHop 2	11
CPHop 3	10
CPHop 4	3.6

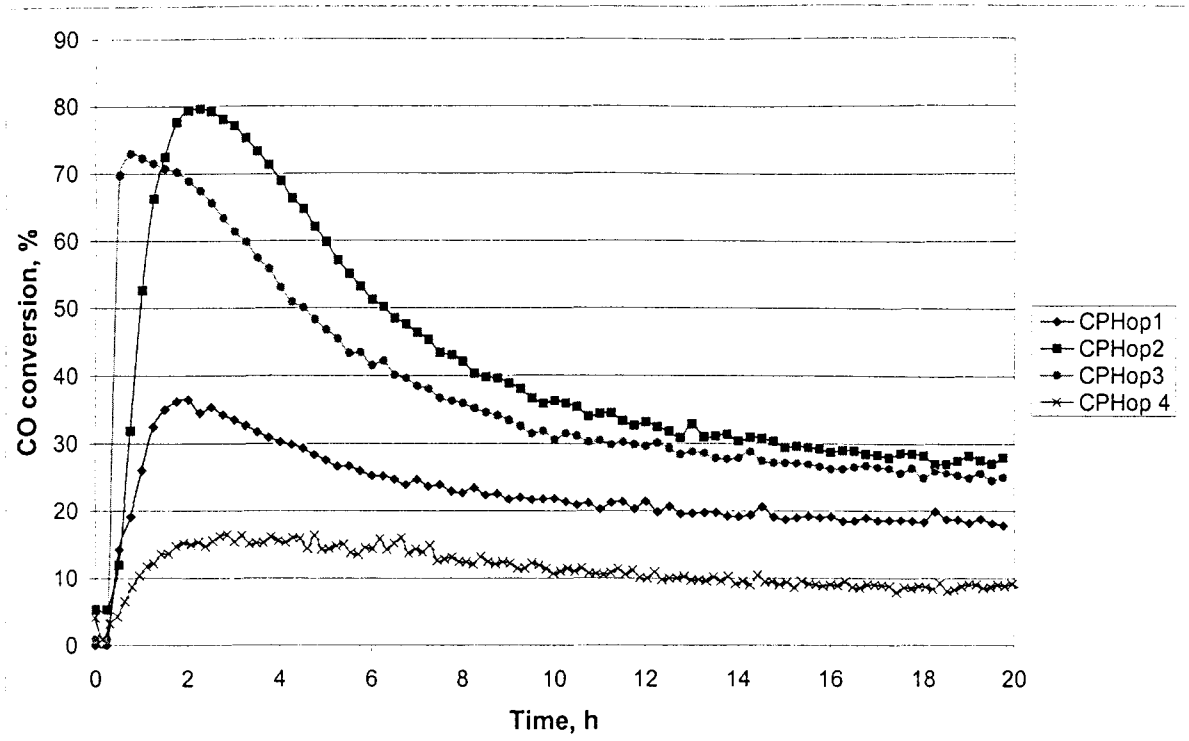


Figure 51. Comparison of activities of CPHop 1-4; 0.50 g catalyst, 60 ml/min; room temperature

Disappointingly, none of the co-precipitated Au/hopcalite catalysts had high activities. CPHop 2 (made with Na_2CO_3) had a higher activity than CPHop 1 (made with Li_2CO_3). Surprisingly, whether the mixed metal salt solution was added in over time (CPHop 2) or added in instantaneously (CPHop 3), did not make a difference to the activities of these catalysts. The catalyst made using the method by Hutchings *et al.*[11] fared the worst. So although these conditions were ideal for co-precipitated hopcalite catalysts, the addition of gold obviously requires very different preparation conditions.

The CPHop catalysts were seen to have the same initial exothermic reaction as the deposition-precipitation Au/hopcalite catalysts. Their activities were also seen to decrease over time, like the deposition-precipitation catalysts. It has been claimed by Mirzaei *et al.* [27] that the problem of deactivation of hopcalite catalysts over time (caused by blocking of surface active sites by alkali metal ions), can be resolved by ageing the catalyst for 12 h. They found that with increasing ageing time, manganese gets more incorporated into the hopcalite structure, thus changing the surface charge on the catalyst. Thus less Na^+ was retained on the surface and was easily removed.

CPHop 4 definitely did not show the same level of deactivation as the other catalysts. But it also did not have a huge exothermic reaction like the other catalysts. So whether it's observed lack of deactivation is actually due to it being aged for 12 h, or whether the deactivation is merely not as noticeable as the others (due to its very slight exothermic reaction), is debatable. However what can definitely be concluded is that this catalyst had the lowest activity of all the CPHop- catalysts. So the optimum preparation method specified by Hutchings *et al* [11]. for making hopcalite, is definitely not optimum for the preparation of Au/hopcalite catalysts.

So far, none of the preparation methods have led to very active Au/hopcalite catalysts. Even though it was expected that optimising preparation conditions on the Au/Mn_xO_y catalysts would make it easier to optimise the Au/hopcalite catalysts, this did not occur.

HRSEM analysis was carried out on the CPHop- catalysts to determine if the different preparation conditions had an effect on support morphology, as was the case with the CPMn- catalysts. CPHop 1, made with Li_2CO_3 as the base, was similar to the CPMn- catalysts made with Li_2CO_3, in numerous ways. CPHop 1 support particles also consisted of both large, uniformly-shaped particles and small, feathery particles (Figure 52).

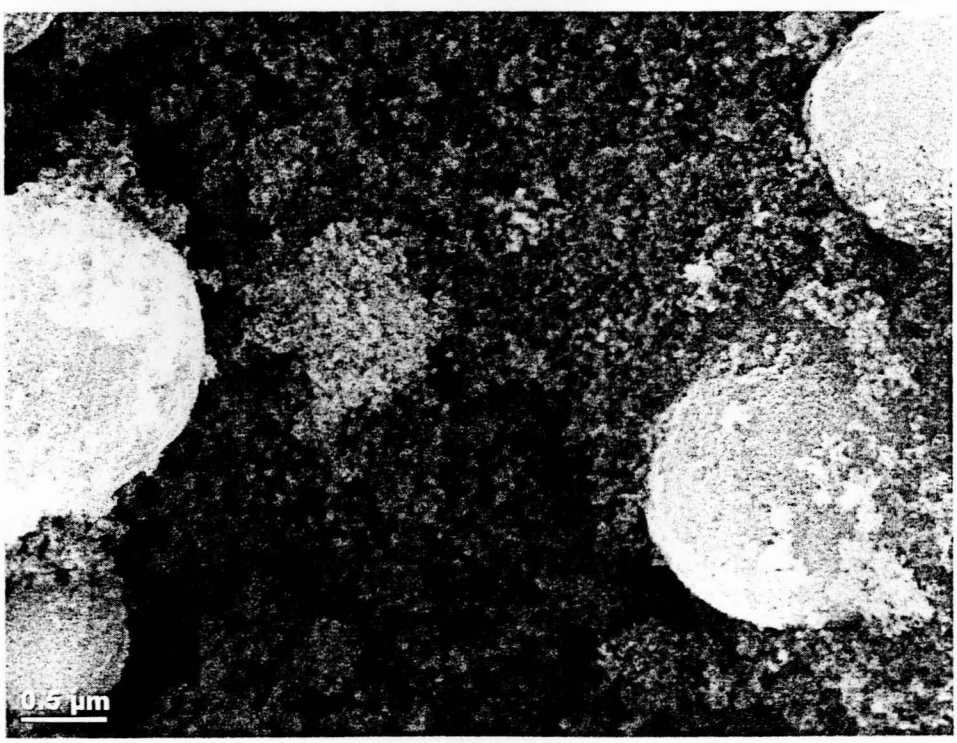


Figure 52. Secondary electron image of CPHop 1

As with the CPMn- catalysts, gold was only present on the small, feathery particles. Although the gold loading on CPHop 1 was similar to the other CPHop- catalysts (Table 20), it was very difficult to find gold on this catalyst. It is possible that most of the gold was deeply embedded in the support, and therefore could not be seen on the HRSEM backscattered mode. The images obtained were not very clear, and the gold particles that were seen, were large (> 50 nm). The secondary- and backscattered- electron images of CPHop 1, showing the presence of gold on the small, loosely coagulated support particles, are shown in Figure 53.

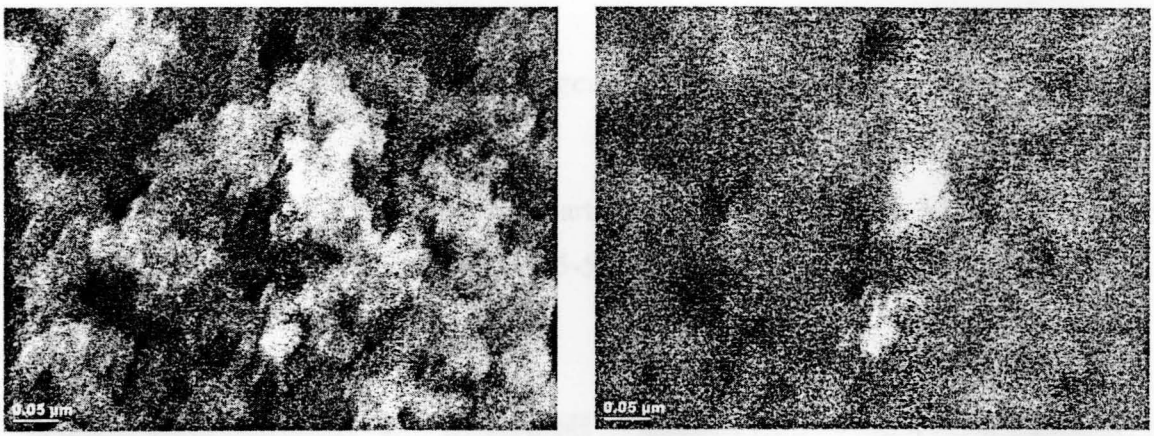


Figure 53. Secondary electron image and backscattered electron image of CPHop 1

CPHop 2 and CPHop 3, both made with Na_2CO_3, did not look very different structurally. Unlike the CPMn- catalysts, the rate of addition of the mixed metal salts to the base, did not yield strikingly different catalyst activities (Figure 51), or support particle sizes and structure (Figure 54).

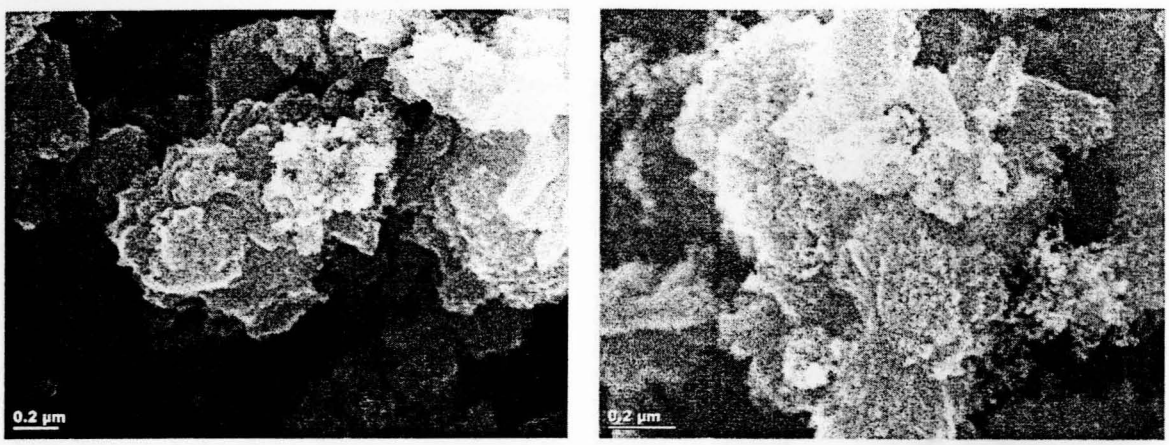


Figure 54. Secondary electron images of CPHop 2 (left) and CPHop 3 (right)

Both CPHop 2 and CPHop 3 had gold particle sizes ranging from 30-200 nm. However, CPHop 2 had gold mostly in the range of 35-50 nm, whereas CPHop 3 had gold mainly in the range of 100-150 nm (Figure 55).

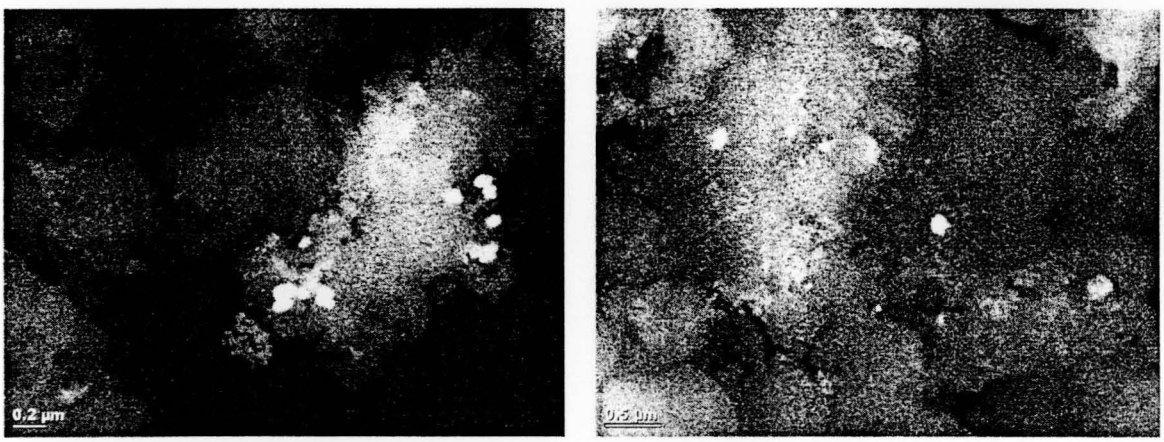


Figure 55. Backscattered electron images of CPHop 2 (left) and CPHop 3(right)

Considering that the instantaneous-precipitation method yielded much smaller gold- and support- particles with the CPMn- catalysts, it is surprising that the CPHop- catalysts yielded such different results. Possibly the 3 h ageing time, while not a problem for CPMn- catalysts, resulted in gold- and support- particle agglomeration on CPHop 3.

CPHop 4 was distinctly different to the other catalysts, in that it was very crystalline (Figure 56). The gold particles on CPHop 4 ranged from 85-215 nm.

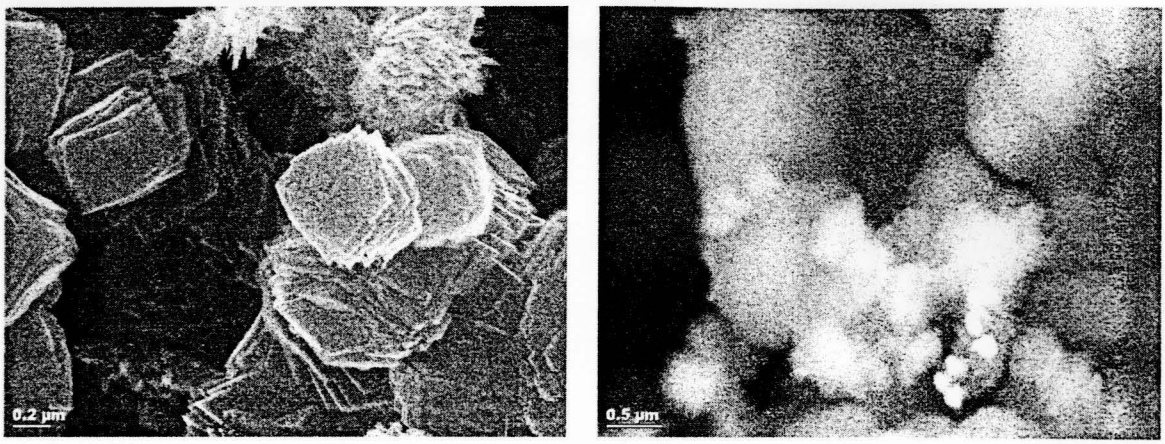


Figure 56. Secondary electron image and backscattered electron image of CPHop 4

An XRD comparison of CPHop 3 and CPHop 4, is shown in Figure 57.

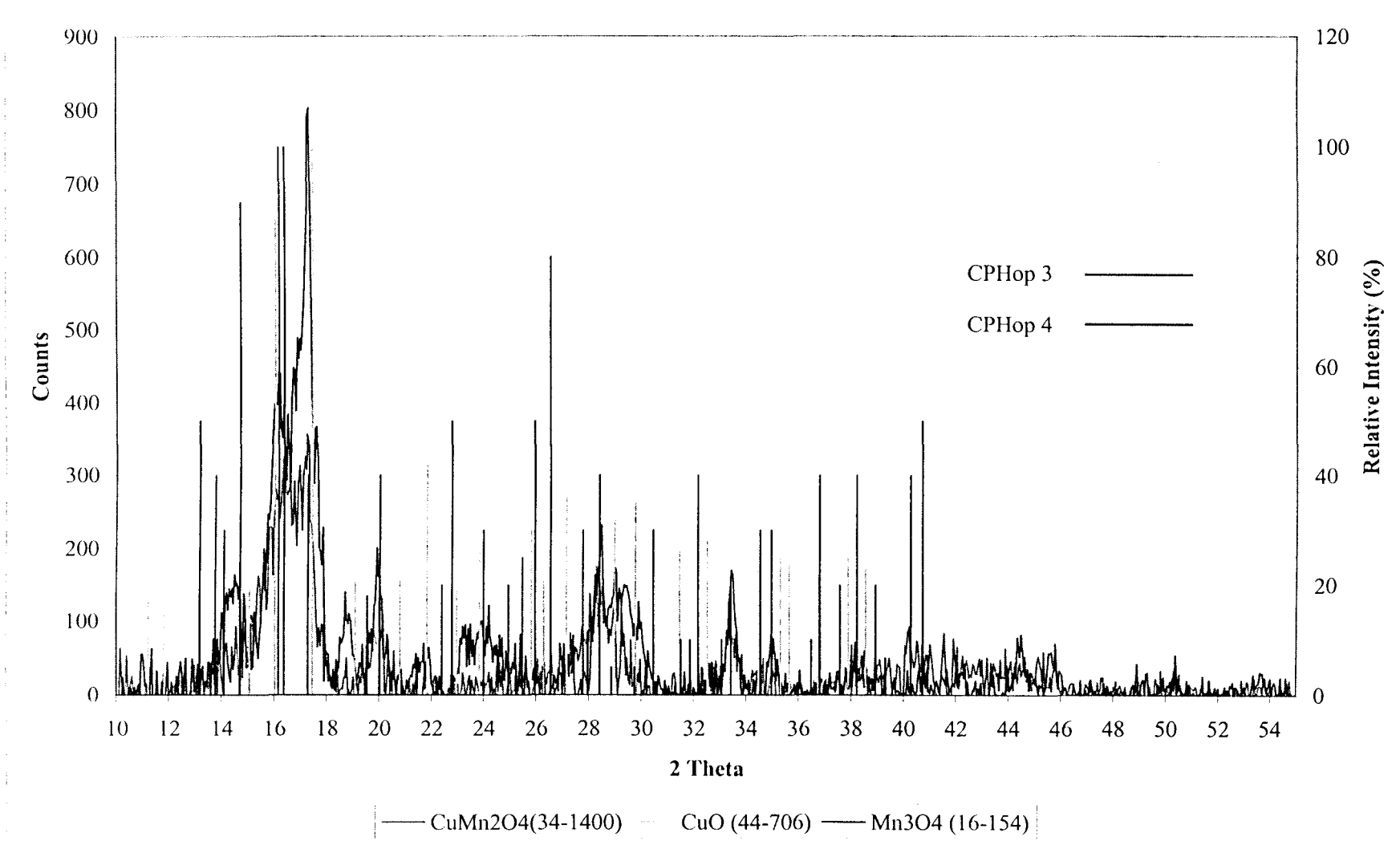


Figure 57. XRD spectra of CPHop 3 and CPHop 4

(Background correction, Kα lines stripped)

XRD studies by Hutchings *et al.*[46] on co-precipitated hopcalite catalysts, showed the presence of CuO, $Cu_{1.4}Mn_{1.6}O_4$ and Mn_2O_3 from 0 h ageing, right up to 5 h. After 5 h, the species present were $Cu_{1.2}Mn_{1.8}O_4$, Cu_2O and Mn_2O_3. The intensity of the Mn_2O_3 peaks decreased with ageing time until, after 12 h ageing, they could no longer detect Mn_2O_3 by X-ray diffraction. So after 12 h, only $CuMn_2O_4$ and CuO were seen, and the ratio of Cu/Mn of 0.5 was reached. It was also stated that the catalyst aged for 12 h was less crystalline than those aged for shorter times.

Very different results were obtained on the co-precipitated Au/hopcalite catalysts. The spectra of both catalysts are very similar, the only difference being that CPHop 4 was more crystalline than CPHop 3. This can be seen in the higher, sharper peaks of CPHop 4. That the 12 h aged catalyst was more crystalline, contradicts the result by Hutchings *et al* [46]. Also, both catalysts appear to contain $CuMn_2O_4$, CuO and Mn_3O_4. Mn_2O_3 did not provide as good a fit in the diffraction patterns of CPHop 3 and CPHop 4, as Mn_3O_4 did.

7. CATALYST PARTICLE SIZE OPTIMISATION

Since it is not viable to have the catalysts in powder-form in industry, an attempt was made to form large granules from CPMn2_200 powder. The powder was compacted at high pressure into a hard disc. The disc was then crushed with a mortar and pestle to yield catalyst particles between 710 and 1400 μm. The granules were tested on the CO rig to determine if the activity had been compromised. As can be seen in Figure 58, the activity was not affected by compacting the catalyst.

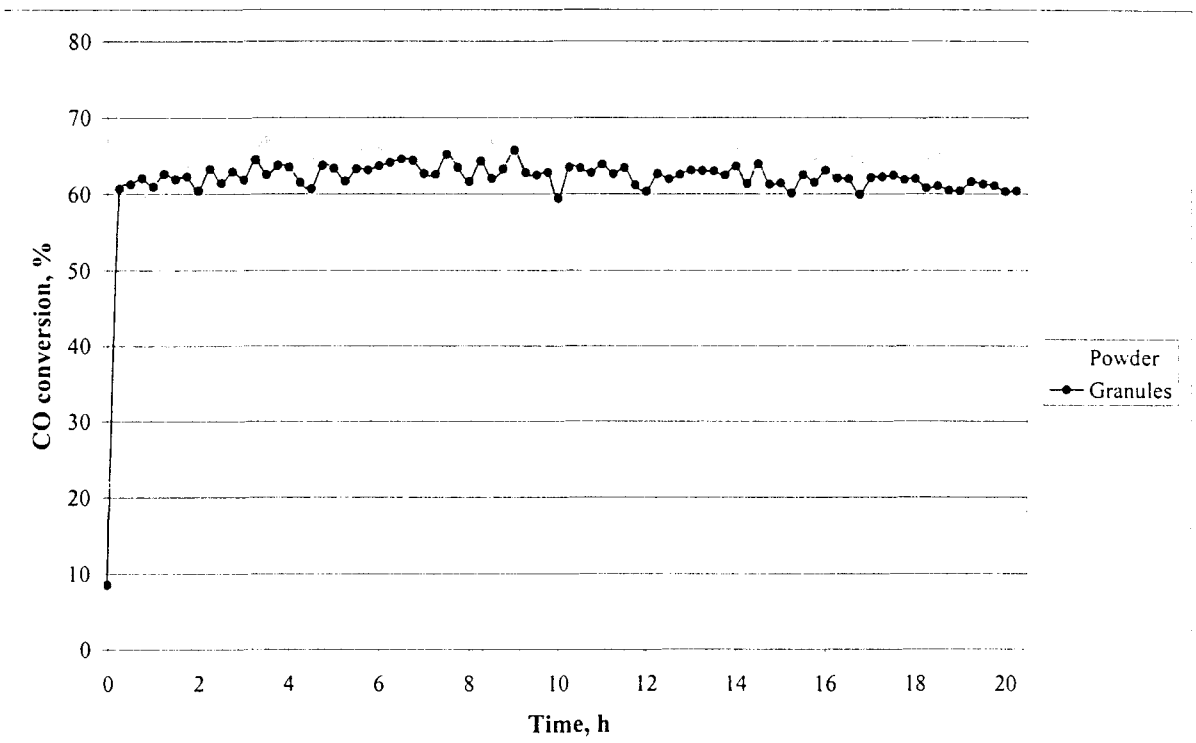


Figure 58. Comparison of activity of CPMn2_200 in powder and granular form; 0.5 g catalyst, 60 ml/min, room temperature

The surface areas of the powder and granules were compared, and were found to be very similar. The powder had a surface area of 100 m^2/g and the granules of 90 m^2/g. The fact that increasing the catalyst's particle size by means of compaction, did not adversely affect the catalyst's activity, is promising for industrial applications.

8. CONCLUSION

The deposition-precipitation and colloidal gold methods did not yield active Au/MnO_2 or Au/hopcalite catalysts. Co-precipitated Au/hopcalite catalysts were also inactive. None of the catalysts made with the above methods had activities higher than 20 μmol CO/g Au/s. In the case of the Au/hopcalite catalysts, the catalysts were always seen to deactivate over time - regardless of the preparation method employed. The Au/MnO_2 catalysts did not exhibit this deactivation. The activities either were stable or increased with time – but they were still always low. The gold particles on these catalysts were all very large – sometimes even in the μm range.

Co-precipitated Au/Mn_xO_y catalysts were highly active, reaching the maximum activity in a very short space of time. Their activities were also very stable, and they did not deactivate over time. The highest activities were found on those catalysts where the mixed metal salt solution ($HAuCl_4$ + $Mn(NO_3)_2.xH_2O$) was added into the base in one aliquot. This instantaneous precipitation yielded smaller support and smaller gold particles, than when the metal salts were pumped in over a period of time. The most active catalysts had activities of just under 385 μmol CO/g Au/s. Gold particles on the active co-precipitated catalysts were mainly around 20 nm in diameter, although there were also particles as small as 7 nm and as large as 40 nm. XRD analysis showed multiple Mn_xO_y phases present in these co-precipitated catalysts.

The most active CPMn- catalysts (made by means of instantaneous precipitation) performed far better than those made by Hoflund *et al*[5]. These CPMn- catalysts were more active when made with Na_2CO_3 than with Li_2CO_3. This contradicts the results obtained by Hoflund *et al.* They had stated that co-precipitated Au/Mn_xO_y catalysts made with Li_2CO_3 performed better. However, their method appeared to involve dropwise addition, which would confirm the results obtained for CPMn 5 (the lithium-'promoted' catalyst made by means of dropwise addition). Attempts to reproduce CPMn 5 were unsuccessful, so no definite conclusions could be drawn about which base provided the more active catalysts with the dropwise addition method. The surface area of the best-performing catalyst (CPMn 25) was double that of the catalysts made by Hoflund *et al.* (reported to be around 60 m^2/g).

The addition of cerium to Au/Mn_xO_y co-precipitated catalysts did not promote these catalysts, as it was hoped it would. Even minor amounts of cerium affected the activity of these catalysts. It is speculated that the cerium is over-oxygenating the Mn_xO_y support – which then results in lower activity.

The gold-phosphine method, reported to yield highly active catalysts[24], was not investigated in this study, as it had already been attempted at Mintek on hopcalite (SG-2157 and N-140) and freshly-precipitated manganese hydroxides[47]. Although these phosphine-derived catalysts were more active than the Au/hopcalite, deposition-precipitation Au/MnO_2 and colloidal Au/MnO_2 catalysts made in this study, they were not as active as the co-precipitated Au/Mn_xO_y catalysts.

Compacting and crushing a catalyst powder to obtain larger granules was also attempted. The activities and surface areas of the powders and granules were very similar. This bodes well for industrial purposes, where powders are not ideal due to the large pressure drops obtained over the catalyst bed.

Recommendations for future testwork:

- Investigate ageing times for co-precipitated Au/Mn_xO_y catalysts. Whether the optimum ageing time varies depending on the initial base concentration, is also an avenue that should be explored.
- Au/hopcalite co-precipitated catalysts still have to be optimised. The preparation conditions ideal for co-precipitated Au/Mn_xO_y catalysts cannot be applied to Au/hopcalite. This system will have to be investigated independently. It is possible that the optimum Cu/Mn ratio of hopcalite alone is not the optimum for Au/hopcalite. Different Cu/Mn ratios should be investigated.
- The Au/Mn_xO_y system should be further characterised. Techniques such as TPR and XPS should be used to attempt to obtain a better understanding of this system.
- Since manganese oxides reportedly have potential for NO_x applications, the co-precipitated Au/Mn_xO_y catalysts should be tested for NO_x reduction.

9. REFERENCES

1. R. Lin, W.P. Liu, Y.J. Zhong, M.F. Luo, *Catalyst characterisation and activity of Ag-Mn complex oxides*, Appl. Catal. A: General, **220**, pp 165-171, 2001

2. I. Spassova, M. Khristova, D. Panayotov, D. Mehandjiev, *Coprecipitated CuO-MnO_x catalysts for low-temperature CO-NO and CO-NO-O_2 reactions*, J. Catal., **185**, 43-57, 1999

3. H.Y. Chen, J. Lin, K.L. Tan, J. Li, *Comparative studies of manganese-doped copper-based catalysts: the promoter effect of Mn on methanol synthesis*, Appl. Surf. Sc., **126**, 323-331, 1998

4. J.F. Trillat, J. Massardier, B. Moraweck, H. Praliaud, A.J. Renouprez, *Reduction of NO by CO on manganese promoted palladium catalysts*, Stud. Surf. Sci. Catal., **116**, 103-112, 1998

5. G.B.Hoflund, S.D. Gardner, D.R. Schryer, B.T. Upchurch, E.J. Kielin, *Au/MnO_x catalytic performance characteristics for low-temperature carbon monoxide oxidation*, Appl. Cat. B: Environ., **6**, 117-126, 1995

6. S.D. Gardner *et al.*, *Catalytic behaviour of noble metal/reducible oxide materials for low-temperature CO oxidation. 2. Surface characterisation of Au/MnO_x*, Langmuir, **7**, 2140-2145, 1991

7. S.D. Gardner et al., *Catalytic behaviour of noble metal/reducible oxide materials for low-temperature CO oxidation. 1.Comparison of catalyst performance*, Langmuir, **7**, 2135-2139, 1991

8. A. Ueda, M. Haruta, *Reduction of nitrogen monoxide with propene over Au/Al_2O_3 mixed mechanically with Mn_2O_3, Appl. Cat. B: Environ.*, **18**, 115-121, 1998

9. D. Thompson, *New advances in gold catalysis part I*, Gold Bull., **31** (4), 1998

10. M. Haruta, T. Kobayashi, H. Sano, N. Yamada, *Novel gold catalysts for the oxidation of carbon monoxide at a temperature far below 0°C*, Chem. Lett., 405-408, 1987

11. G.J. Hutchings, A.A. Mirzaei, R.W. Joyner, M.R.H. Siddiqui, S.H. Taylor, *Effect of preparation conditions on the catalytic performance of copper manganese oxide catalysts for CO oxidation*, Appl. Catal. A: General **166**, 143-152, 1998

12. S. Taylor, et al., *The beneficial effect of gold additions on the activity of hopcalite catalyst used for the low temperature oxidation of carbon monoxide*, Int. Cat. Gold Conf., Cape Town, South Africa, April 2001

13. Y. Zhang-Steenwinkel, J. Beckers, A. Bliek, *Surface properties and catalytic performance in CO oxidation of cerium substituted lanthanum-manganese oxides*, Appl. Catal. A: General, **235**, 79-92, 2002

14. H. Chen, A. Sayari, A. Adnot, F. Larachi, *Composition-activity effects of Mn-Ce-O composites on phenol catalytic wet oxidation*, Appl. Catal. B: Environmental, **32**, 195-204, 2001

15. M. Machida, D. Kurogi and T. Kijima, *MnO_x-CeO_2 binary oxides for catalytic NO_x-sorption at low temperatures. Selective reduction of sorbed NO_x*, Chem. Mater. **12**, 3165-3170, 2000

16. Report of the National Research Institute, Osaka, *The abilities and potential of gold as a catalyst*, 1999

17. Q. Fu, A. Weber, M. Flytzani-Stephanopoulos, *Nanostructured Au-CeO_2 catalysts for low-temperature water-gas shift*, Catal. Letters, **77** (1-3), 87-95, 2001

18. M. Haruta, *Size- and support- dependency in the catalysis of gold*, Catal. Today, 36, 153-166, 1997

19. G.C. Bond and D.T. Thompson, *Gold-catalysed oxidation of carbon monoxide*, Gold Bull., **33** (2), 41-51, 2000

20. M.M. Schubert et al., *CO oxidation over supported gold catalysts – "inert" and "active" support materials and their role for the oxygen supply during reaction*, J. Catal., **197**, 113-122, 2001

21. D. Thompson, *New advances in gold catalysis*, Precious Metals, International Precious Metals Institute, 269-301, 1998

22. M. Campanati, G. Fornasari, A. Vaccari, *Fundamentals in the preparation of heterogeneous catalysts*, Catalysis Today, **77**, 299-314, 2003

23. M. Haruta et al., *Low-temperature oxidation of CO over gold supported on TiO_2, Fe_2O_3, and Co_3O_4*, J. Catal., **144**, 175-192, 1993

24. A.I. Kozlov, A.P. Kozlova, H. Liu, Y. Iwasawa, *A new approach to active supported Au catalysts*, Appl. Catal. A: General, **182**, 9-28, 1999

25. A. Wolf, F. Schüth, *A systematic study of the synthesis conditions for the preparation of highly active gold catalysts*, Appl. Catal. A: General, **226**, 1-13, 2002

26. S. Vepřek, D.L. Cocke, S. Kehl, H.R. Oswald, *Mechanism of the deactivation of hopcalite catalysts studied by XPS, ISS and other techniques*, J. Catal., **100**, 250-263, 1986

27. A.A. Mirzaei, et al., *Ambient temperature carbon monoxide oxidation using copper manganese oxide catalysts: effect of residual Na^+ acting as catalyst poison*, Catal. Comm., **4**, 17-20, 2003

28. M.A.P. Dekkers, M.J. Lippits, B. E. Niewenhuys, *Supported gold/MO_x catalysts for NO/H_2 and CO/O_2 reactions*, Catalysis Today, **54**, 381-390, 1999

29. D.E. O' Reilly, E.M. Peterson, C.E. Scheie, J.M. Williams, *Nuclear magnetic resonance of the aquated proton. II. Chloroauric acid tetrahydrate. Phase transitions and molecular motion*, J. Chem. Phy., **55**, 5629-5635, 1971

30. M. Haruta and T. Kobayashi, *Method for the production of ultra-fine gold particles immobilized on a metal oxide*, U.S. Patent **4839327**, 1989

31. M.C. Kung, J.H. Lee, A. Chu-Kung, H.H. Kung, *Selective reduction of NO_x by propene over Au/ γ-Al_2O_3 catalysts*, Stud. Surf. Sci. Catal., **101**, 701-710, 1996

32. F.C. Buciuman, F. Patcas, T. Hahn, *A spillover approach to oxidation catalysis over copper and manganese mixed oxides*, Chemical Engineering and Processing, **38**, 563-569, 1999

33. G. G. Xia, Y.G. Yin, W.S. Willis, J.Y. Wang, S.L. Suib, *Efficient stable catalysts for low temperature carbon monoxide oxidation*, J. Catal., **185**, 91-105, 1999

34. S. Bakardjieva, P. Bezdička, T. Grygar, P. Vorm, *Reductive dissolution of microparticulate manganese oxides*, J. Solid State Electrochem., **4**, 306-313, 2000

35. J.B. Chung, R.J. Zazoski, *Oxidation of Cr (III) to Cr (VI) by pyrolusite*, Agric. Chem. Biotechnol., **45** (3), 125-130, 2002

36. M. Haruta, *Novel catalysis of gold deposited on metal oxides*, Catal. Surv. Jpn., **1**, 61-73, 1997.

37. H. G. Raubenheimer and S. Cronje, *Gold progress in chemistry, biochemistry and technology*, (H. Schmidbaur ed.), John Wiley & Sons, England, 575, 1999

38. D.G. Duff, A. Baiker, *A new hydrosol of gold clusters. 1. Formation and particle size variation*, Langmuir, 2301-2309, 1993

39. J.D. Grunwaldt, C. Kiener, C. Wögerbauer, A. Baiker, *Preparation of supported gold catalysts for low-temperature CO oxidation via "size-controlled" gold colloids*, J. Catal. **181**, 223-232, 1999

40. S. Imamura, M. Shono, N. Okamoto, A.Hamada, S. Ishida, *Effect of cerium on the mobility of oxygen on manganese oxides*, Appl. Catal. A: General, **142**, 279-288, 1996.

41. M. Haruta, T. Kobayashi, S. Tsubota, Y. Nakahara, *Method for production of ultra-fine gold particle-immobilised oxides*, U.S. Patent **5051394**, 1991

42. M. Haruta, M. Daté, *Advances in the catalysis of Au nanoparticles,* Appl. Catal. A: General, **222**, 427-437, 2001.

43. S. Ivanova, C. Petit, V. Pitchon, *Gold catalyst: From the solution to the application*, presented at Mintek by V. Pitchon, 14 Feb. 2003

44. H. -S. Oh *et al.*, *Selective catalytic oxidation of CO: Effect of chloride on supported Au catalysts*, J. Catal. **210**, 375-386, 2002

45. Q. Xu, K.C.C. Kharas, A.K. Datye, *The preparation of highly dispersed Au/Al_2O_3 by aqueous impregnation*, Catal. Lett., **85** (3-4), 229-235, 2003

46. G.J. Hutchings, A.A. Mirzaei, R.W. Joyner, M.R.H. Siddiqui, S.H. Taylor, *Ambient temperature CO oxidation using copper manganese oxide catalysts prepared by coprecipitation: effect of ageing on catalyst performance*, Catal. Lett., **42**, 21-24, 1996

47. T.R. Tshikhudo, *Private communication*, Mintek, 2002

APPENDIX A

*Oxidation Catalyst
Envicat® SG 2157

Size and shape:	Ø 3.5 X 10 mm extrudates
Colour:	black
Active components:	CuO and MnO_x (hopcalite)
Bulk density:	0.8 kg/l
Mechanical stability:	waterproof and sufficient mechanical steadiness
Surface area:	80 - 130m^2/g
Application area:	Ozone decomposition in general and in water purification plants in particular
Performance: (e.g.)	SV = 2.500 ^{1}/h, 25° 18 g ozone/m^3 => complete conversion

*The original datasheet provided was of poor quality. This is therefore a re-typed copy of the original.

N-140

for Oxidation/Adsorption

I. Chemical Composition, (nominal)

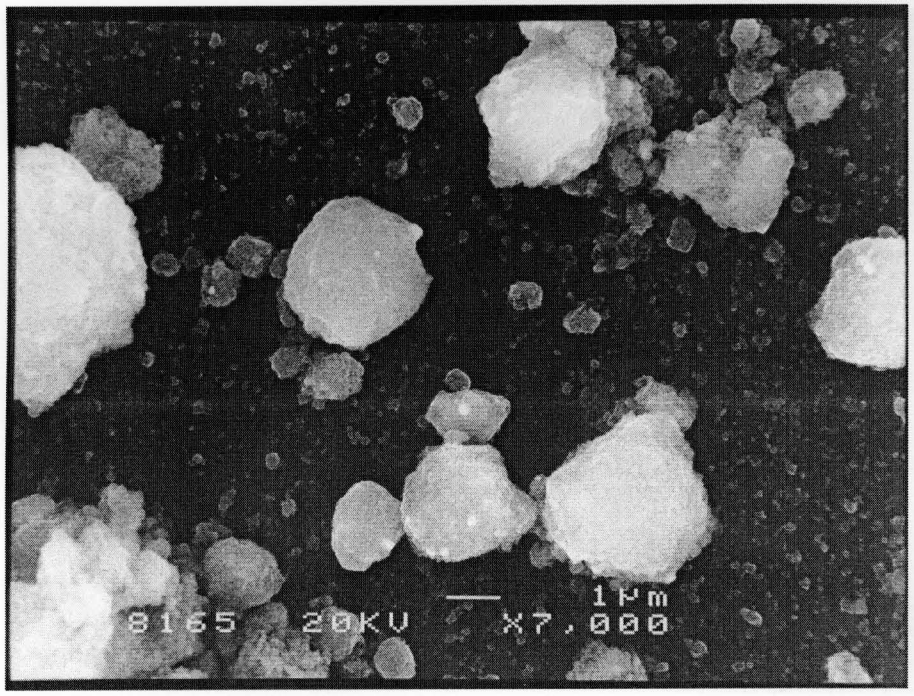
CuO	22	wt%
MnO2	50	wt%
Water H2O	28	wt%

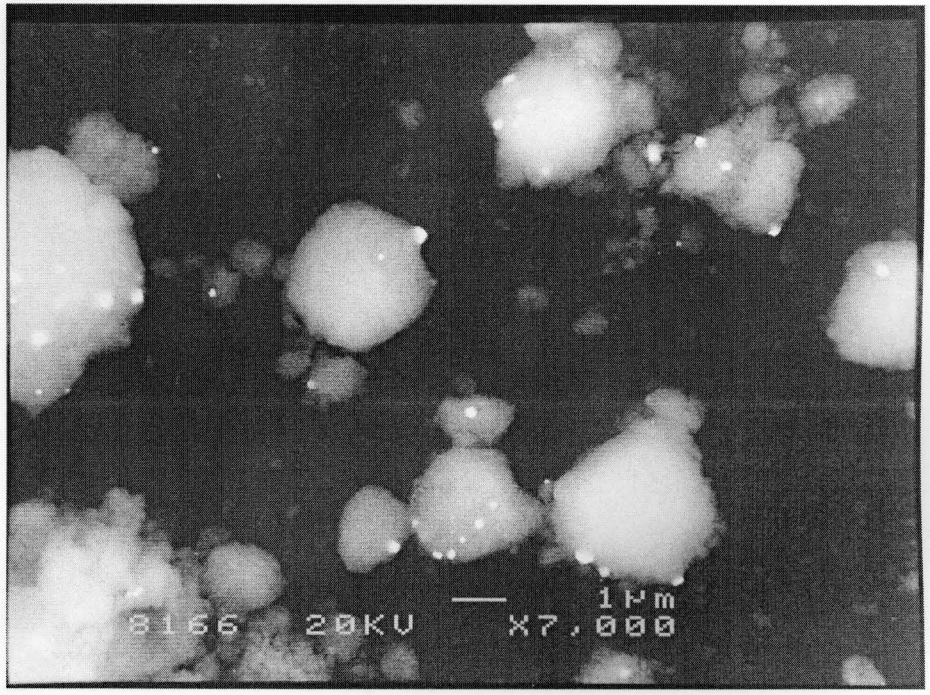
II. Physical Properties (typical)

Particle Shape	Tablets
Catalyst Size	4.5 x 4.5 mm
Bulk Density	0.9 kg/l
Side Crush Strength	6 kg
Surface Area	200 m^2/g
Temperature	max 350° C

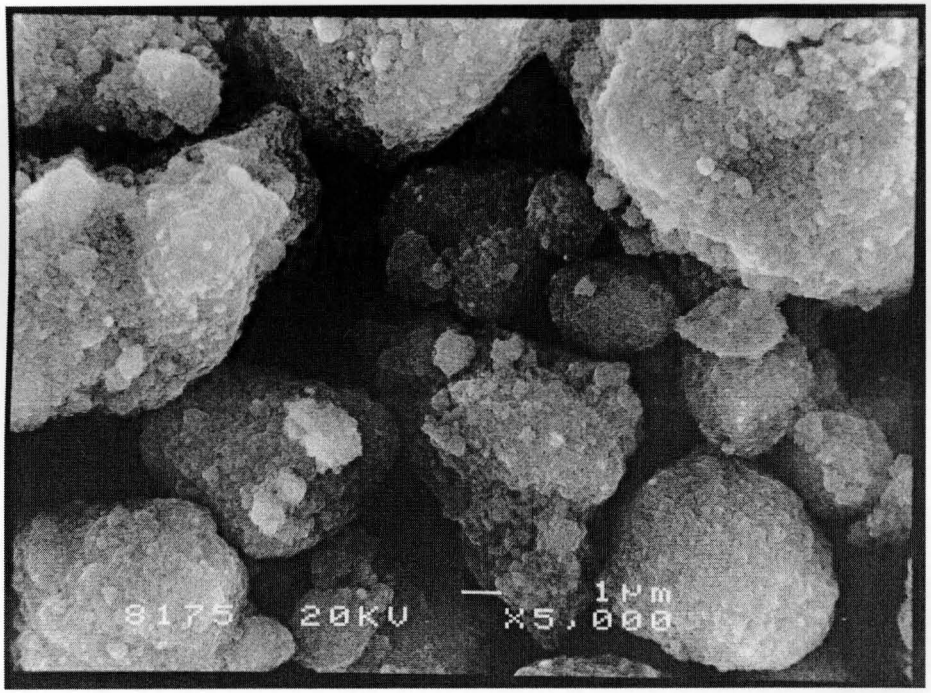
APPENDIX B

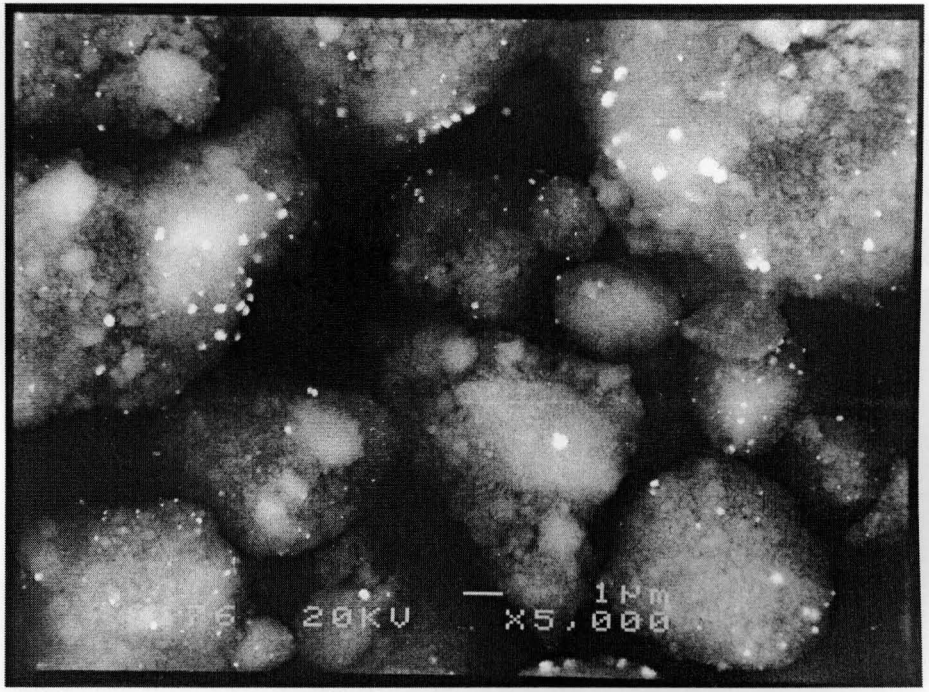
Secondary- and backscattered- electron images of Hop 0



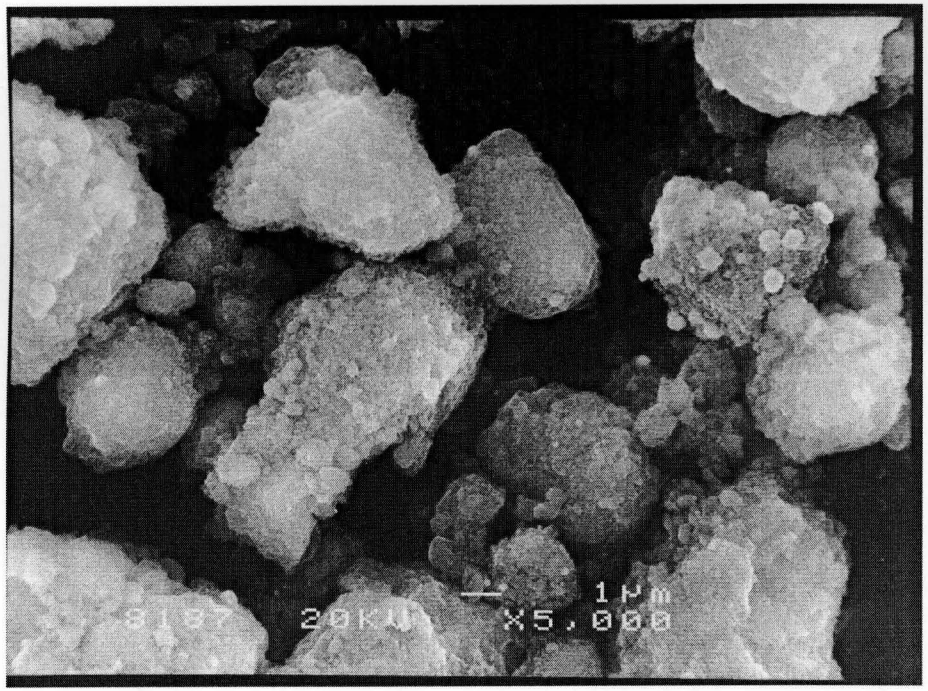


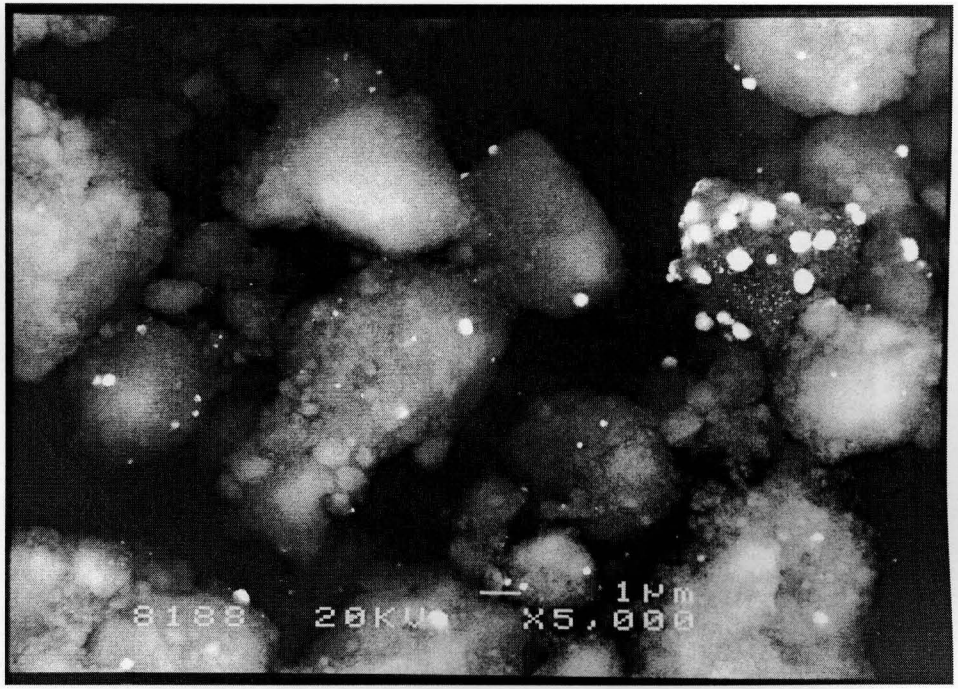
Secondary- and backscattered- electron images of Hop 1



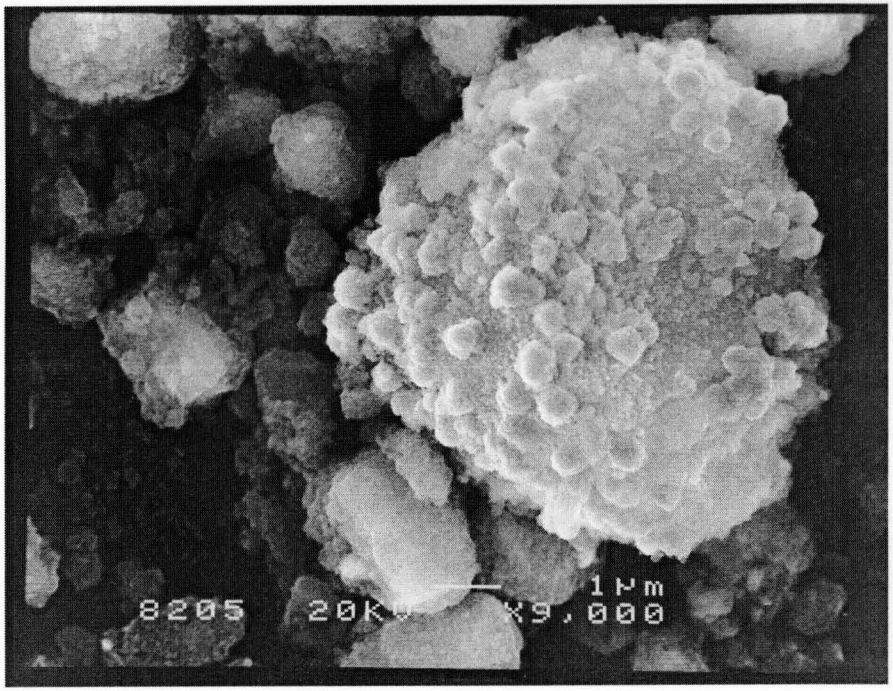


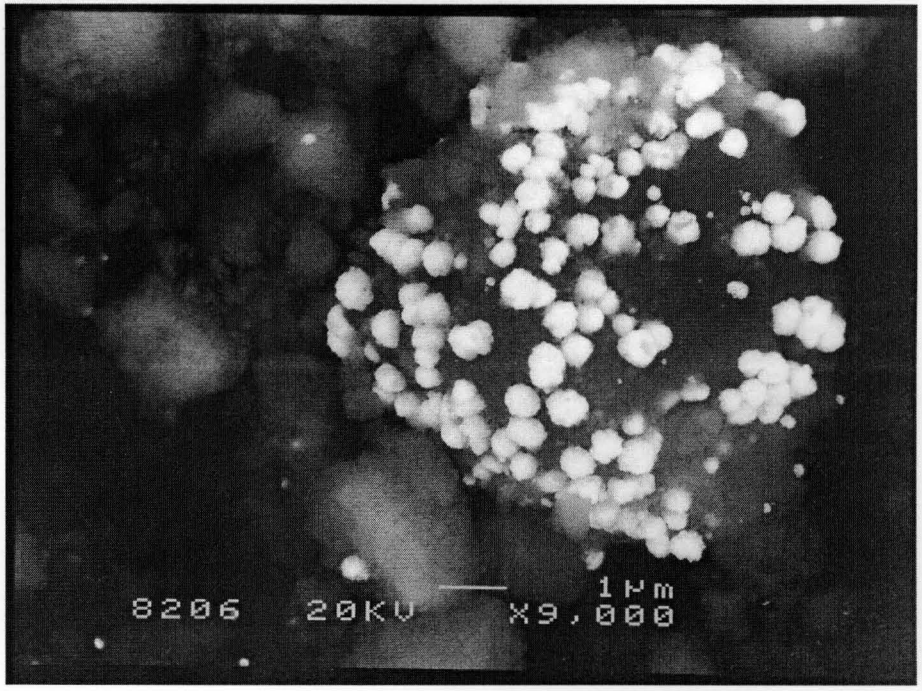
Secondary- and backscattered- electron images of Hop 3



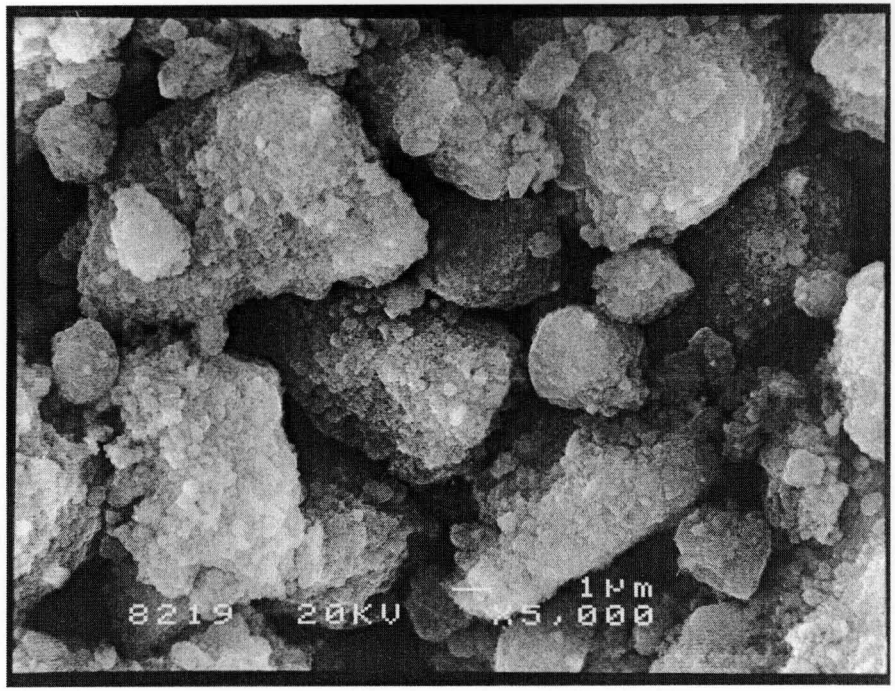


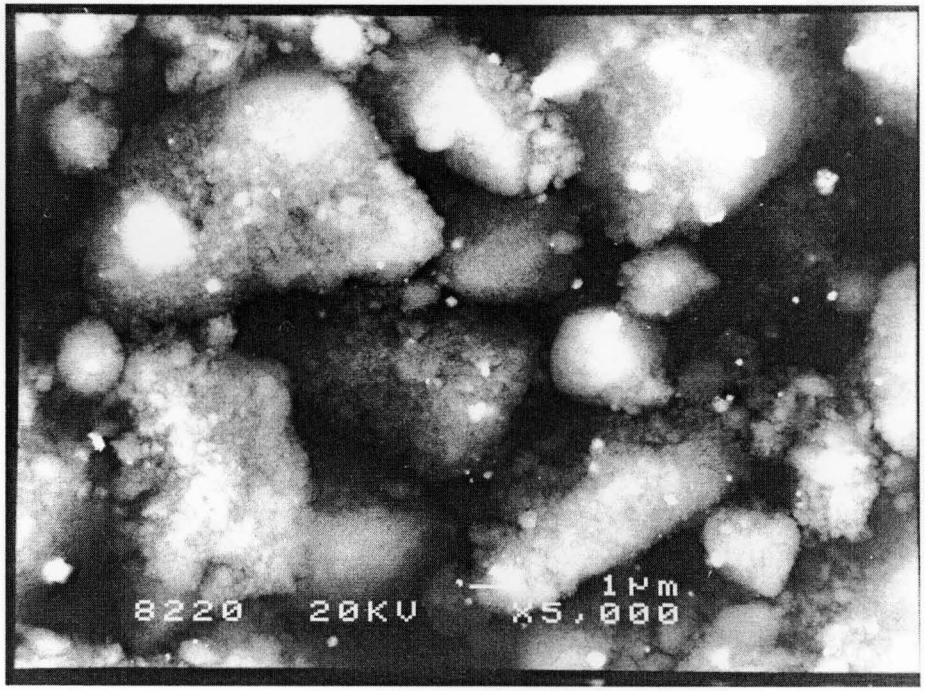
Secondary- and backscattered- electron images of Hop 5





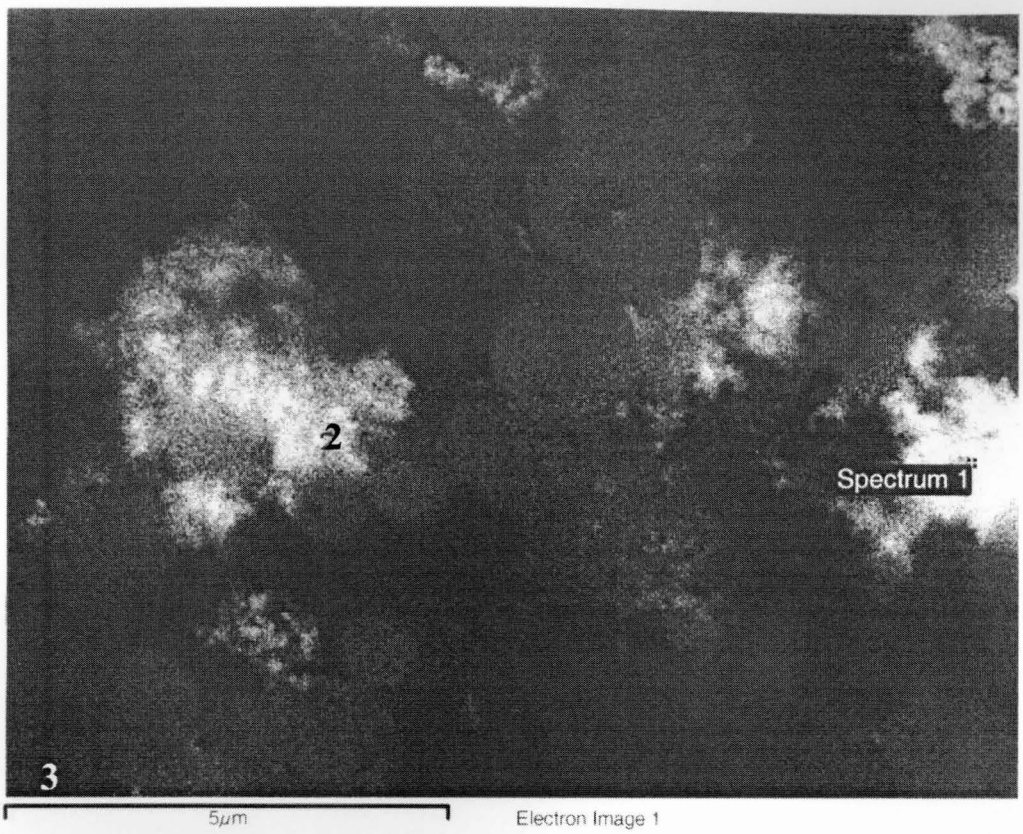
Secondary- and backscattered- electron images of Hop 8





APPENDIX C

HRSEM/EDS of CPMn 10

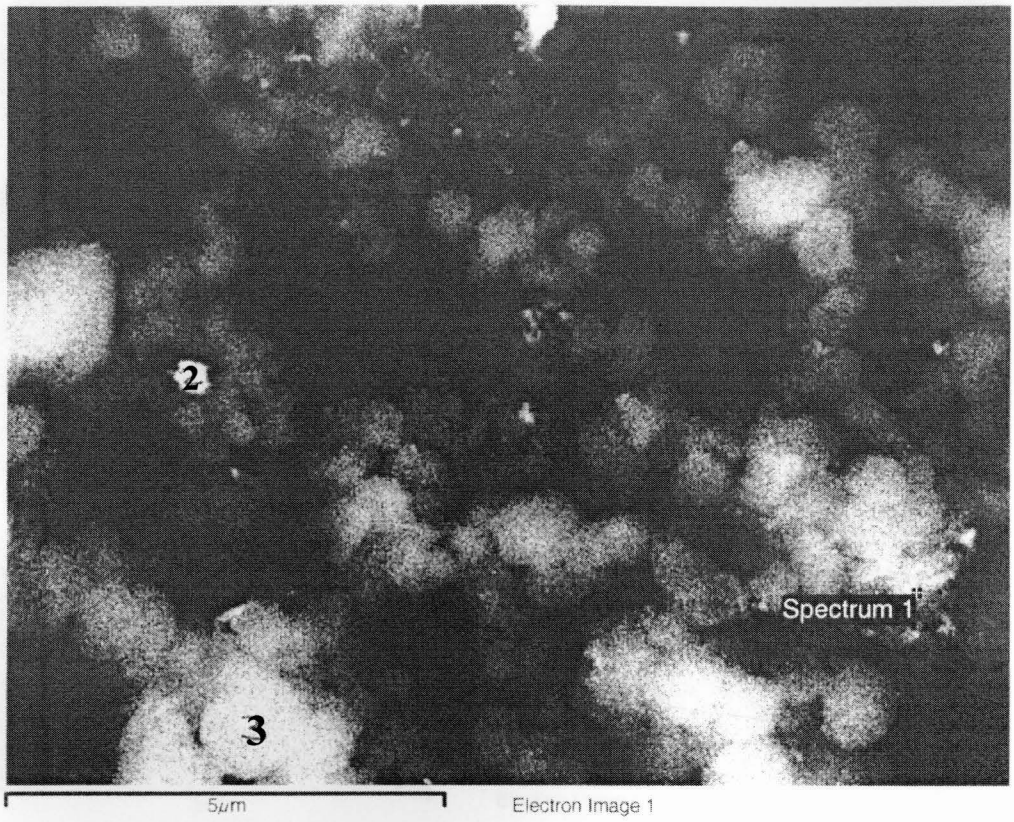


Processing option : All elements analyzed (Normalised)

Spectrum	C	O	Mn	Au	Total
Spectrum 1	3.22	28.08	39.87	28.83	100.00
Spectrum 2	4.47	31.18	40.94	23.41	100.00
Spectrum 3	9.79	46.46	39.12	4.62	100.00
Max.	9.79	46.46	40.94	28.83	
Min.	3.22	28.08	39.12	4.62	

All results in Weight Percent

HRSEM/EDS of CPMn 24 A



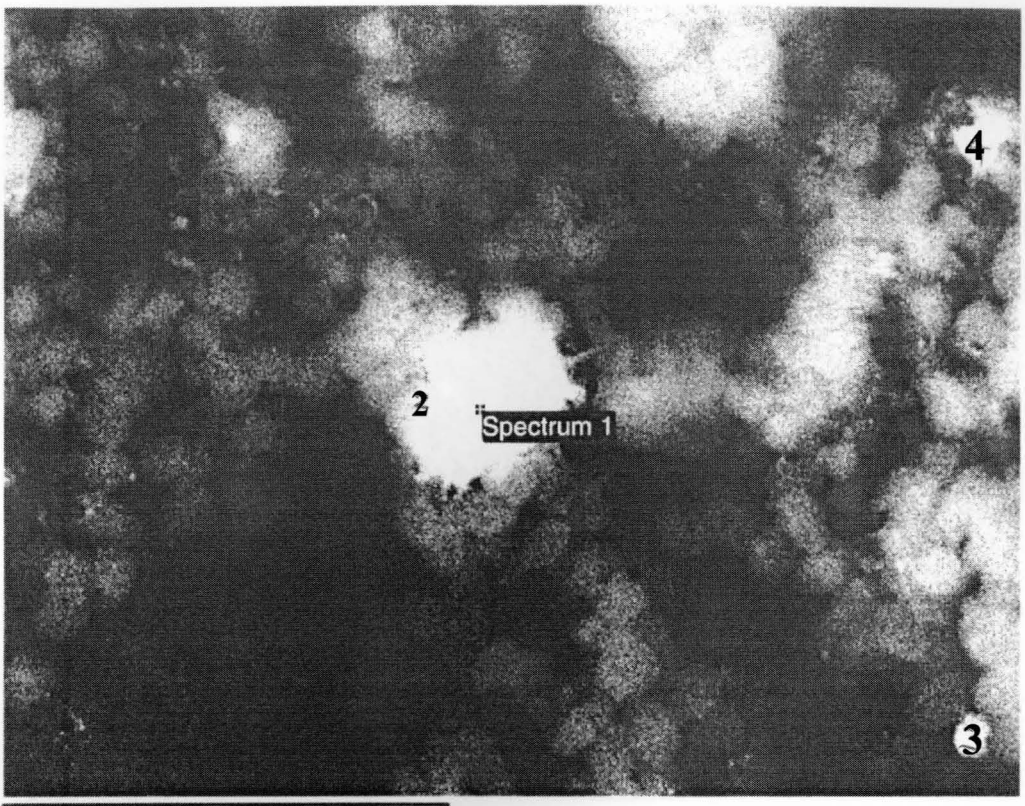
Processing option : All elements analyzed (Normalised)

Spectrum	C	O	Al*	Mn	Au	Total
Spectrum 1	9.69	20.57	52.57	12.30	4.86	100.00
Spectrum 2	12.23	22.44	38.74	9.97	16.63	100.00
Spectrum 3	14.07	38.44	26.07	21.43		100.00
Max.	14.07	38.44	52.57	21.43	16.63	
Min.	9.69	20.57	26.07	9.97	4.86	

All results in Weight Percent

* Catalyst mounted on Al for HRSEM analysis - correction for Al mounting was not done on this picture

HRSEM/EDS of CPMn 24 B



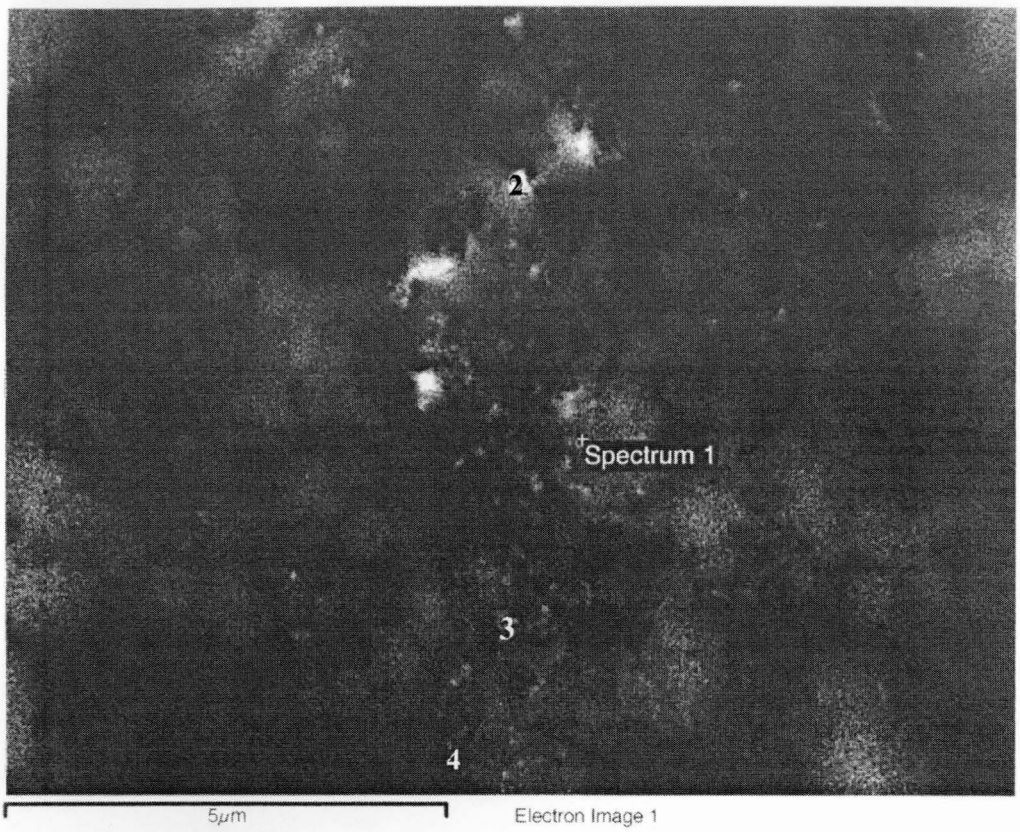
Electron Image 1

Processing option : All elements analyzed (Normalised)

Spectrum	C	O	Mn	Au	Total
Spectrum 1	10.58	40.09	34.18	15.15	100.00
Spectrum 2	10.44	40.60	36.10	12.85	100.00
Spectrum 3	9.55	38.62	21.69	30.14	100.00
Spectrum 4	10.69	40.70	22.52	26.09	100.00
Max.	10.69	40.70	36.10	30.14	
Min.	9.55	38.62	21.69	12.85	

All results in Weight Percent

HRSEM/EDS of CPMn 24 C

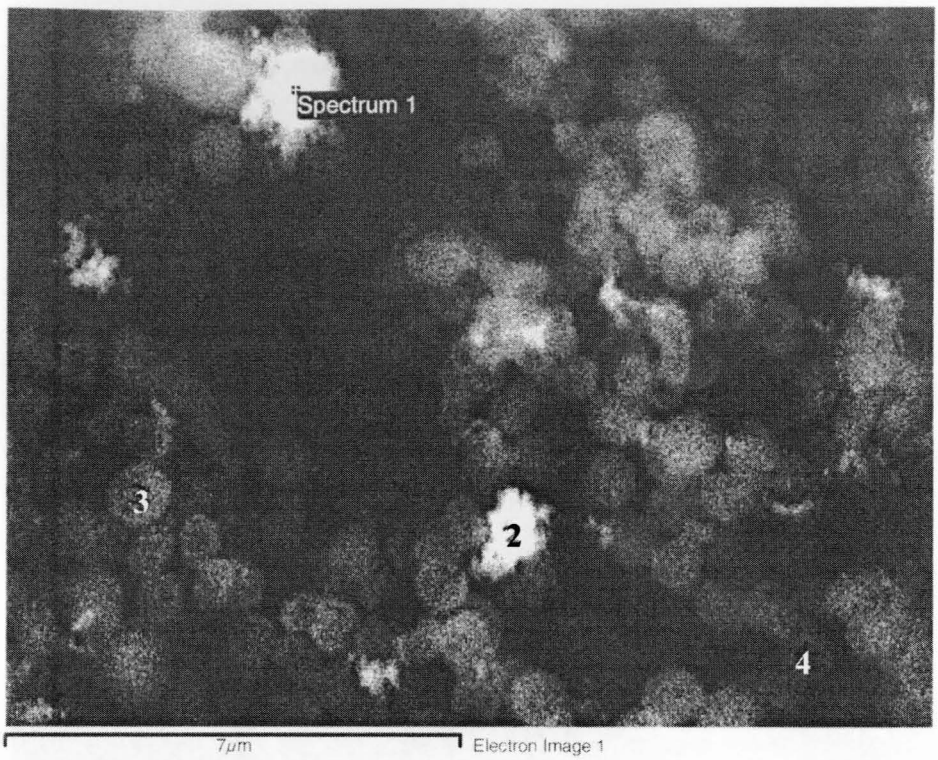


Processing option : All elements analyzed (Normalised)

Spectrum	C	O	Mn	Au	Total
Spectrum 1	11.31	45.47	33.90	9.33	100.00
Spectrum 2	9.91	41.57	28.11	20.41	100.00
Spectrum 3	8.10	39.55	46.99	5.35	100.00
Spectrum 4	12.23	43.38	35.35	9.03	100.00
Max	12.23	45.47	46.99	20.41	
Min	8.10	39.55	28.11	5.35	

All results in Weight Percent

HRSEM/EDS of CPMn 27



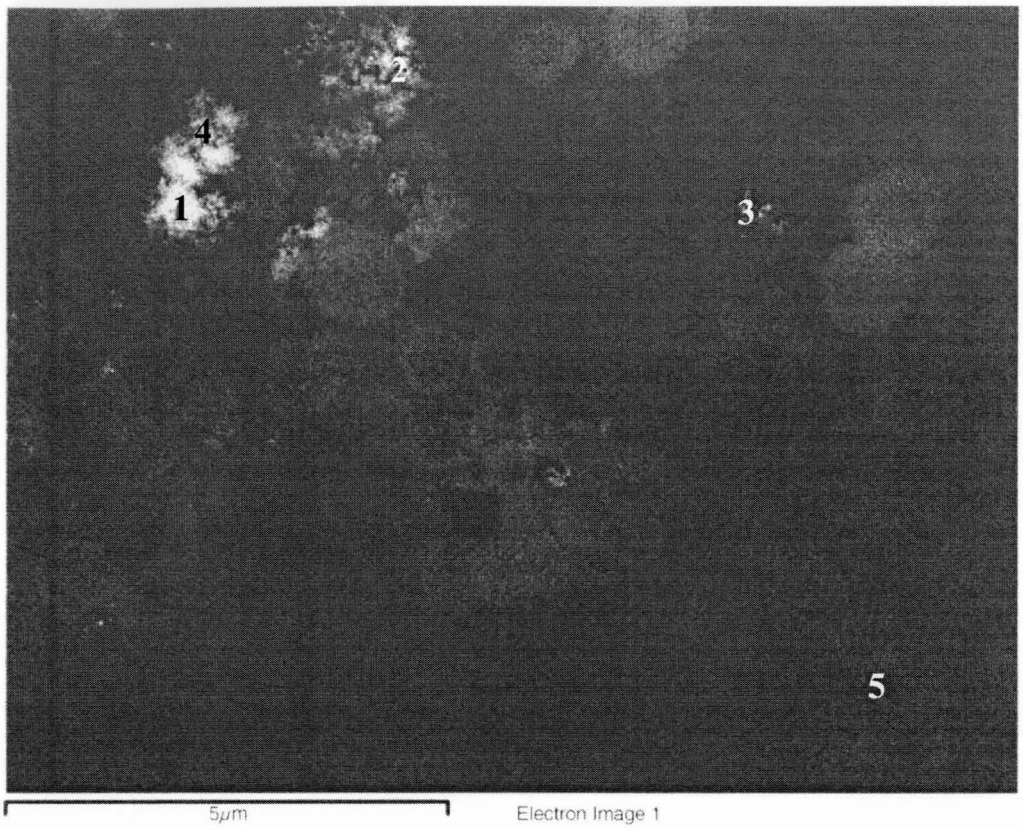
Processing option : All elements analyzed (Normalised)

Spectrum	C	O	Al *	Mn	Cu	Au	Total
Spectrum 1	7.91	33.69	8.84	27.79		21.78	100.00
Spectrum 2	7.28	37.56	12.42	35.28		7.46	100.00
Spectrum 3	11.02	40.94	16.77	30.11	1.15		100.00
Spectrum 4	7.61	37.39	14.56	38.73		1.70	100.00
Max	11.02	40.94	16.77	38.73	1.15	21.78	
Min	7.28	33.69	8.84	27.79	1.15	1.70	

All results in Weight Percent

* Catalyst mounted on Al for HRSEM analysis - correction for Al mounting was not done on this picture

HRSEM/EDS of CPMn 27_u

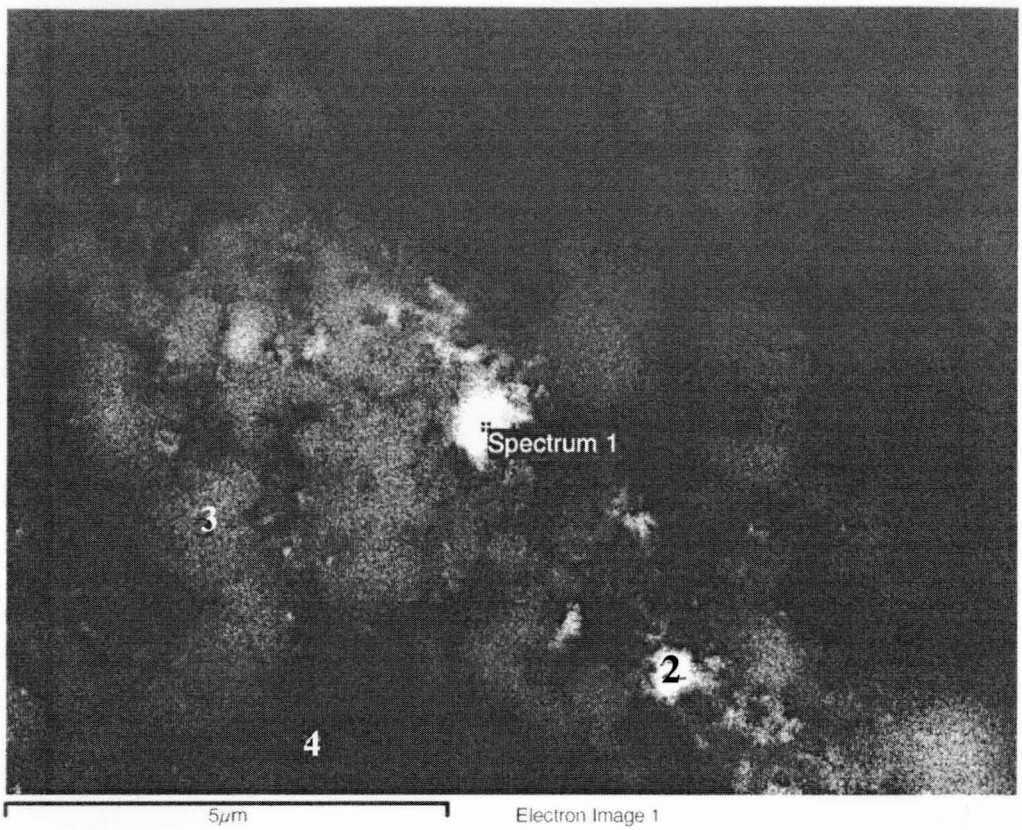


Processing option : All elements analyzed (Normalised)

Spectrum	C	O	Mn	Au	Total
Spectrum 1	12.53	46.14	28.46	12.86	100.00
Spectrum 2	10.29	40.73	38.21	10.76	100.00
Spectrum 3	13.13	46.41	32.49	7.97	100.00
Spectrum 4	12.73	44.09	31.96	11.22	100.00
Spectrum 5	17.40	54.64	27.97		100.00
Max.	17.40	54.64	38.21	12.86	
Min.	10.29	40.73	27.97	7.97	

All results in Weight Percent

HRSEM/EDS of CPMn 28



Processing option : All elements analyzed (Normalised)

Spectrum	C	O	Mn	Au	Total
Spectrum 1	11.21	37.30	31.51	19.98	100.00
Spectrum 2	10.06	32.31	35.39	22.24	100.00
Spectrum 3	13.10	44.44	42.46		100.00
Spectrum 4		37.17	26.96	35.87	100.00
Max.	13.10	44.44	42.46	35.87	
Min.	10.06	32.31	26.96	19.98	

All results in Weight Percent